

A study on hull shape optimization for TLP by
using optimization algorithm

(最適化アルゴリズムを用いた TLP 浮体形状最適化に関する研究)

杉田 年男

Contents

1	Background	9
1.1.	Floating Offshore Production Facilities	9
1.2.	History and trend of TLPs	14
1.3.	TLP hull shape	17
1.3.1.	Conventional TLP (CTLP)	18
1.3.2.	MOSES TLP.....	19
1.3.3.	SeaStar TLP.....	20
1.3.4.	Extended TLP (ETLP)	21
1.4.	TLP hull design and sizing	22
1.1.1	Global Performance	22
1.1.2	Structural Integrity.....	23
1.1.1	Transportation and installation.....	24
1.1.2	Topside Support and Integration Method.....	24
1.1.3	Drilling Operation	24
1.1.4	Riser and well bay layout.....	24
1.1.5	Constructability	24
2	Purpose of this Study.....	25
3	Methodology – Sizing Strategy.....	27
3.1	Conventional Hull Sizing Method	27
3.2	Sizing Strategy	28
3.3	Criteria	28
3.4	Optimization Algorithm	30
3.4.1	Adaptive Simulated Annealing Method.....	31
3.4.2	Real-coded Genetic Algorithm.....	32
3.4.3	Steepest Gradient Method	33
3.4.4	Program Test.....	33
4	Methodology - Calculation Mesh	39
4.1	Conventional TLP – Circular Column.....	40
4.2	Conventional TLP – Rectangular Column	43
4.3	MOSES SSIP TLP –Rectangular Column.....	46
4.4	MOSES SSIP TLP – Circular Column	49
4.5	Classic MOSES TLP.....	52
5	Methodology - Hydrodynamic Calculation.....	55
5.1	Flow Field around a Floating Body	55
5.2	Integral Equation for the velocity potential.....	57

5.3	Numerical solution of Integral equation	58
5.4	Free-Surface Green Function	59
5.5	Hydrodynamic force	63
5.6	Kochin Function and Wave Drift Forces	64
5.7	Motion Equation for TLP	65
5.7.1	Motion Equation for TLP	65
5.7.2	Mass matrix	66
5.7.3	Damping matrix	67
5.7.4	Restoring Matrix	67
5.7.5	External force	72
5.8	Maximum Response Calculation	72
5.9	Program Verification	75
6	Methodology - Global Performance Calculation	80
6.1	Global Parameters	80
6.2	Mean Condition Calculation	81
6.2.1	Restoring Forces	82
6.2.1.1	Tendon and TTR Restoring Forces	82
6.2.1.2	SCR Restoring Forces	83
6.2.1.3	Hydrostatic Forces	85
6.2.2	Environmental Forces	86
6.2.2.1	Drag Force Coefficient	86
6.2.2.2	Current Coefficient Calculation	88
6.2.2.3	Wind Coefficient Calculation	89
6.3	Wave-frequency Motion Calculation	89
6.4	Low-frequency Motion Calculation	89
6.4.1	Wind Induced Motion	89
6.4.2	Wind Spectrum	90
6.4.3	Variable Wave Drift Force Induced Motion	91
6.5	Maximum/Minimum Value Calculation	91
6.6	Program Verification	92
7	Methodology - Global Structure Calculation	97
7.1	Section Properties	98
7.2	Correspondence	98
7.3	Spring Boundary corresponding Tendon stiffness	99
7.4	Matrix Method	100
7.4.1	Element Stiffness Matrix	101

7.4.2	Coordinate Conversion and Global Stiffness Matrix	102
7.4.3	Calculation of Section Forces	105
7.4.4	Distributed Load.....	106
7.5	Load Cases.....	107
7.5.1	Static Loads	107
7.5.2	Wave Loads	107
8	Methodology - Weight Calculation	109
8.1	Scantling Calculation.....	109
8.1.1	Plating.....	109
8.1.2	Stiffener	110
8.2	Weight estimation	111
9	Calculation Result.....	113
9.1	Calculation Condition	113
9.2	GoM Pre-2005 condition (Case 1)	115
9.3	GoM Post-2005 condition (Case 2).....	116
9.4	GoM Post-2005 condition (Case 3).....	117
10	Discussion.....	118
10.1	Comparison with an existing TLP hull shape.....	118
10.2	Pre v.s. Post Hurricane Condition	119
10.3	Hash v.s. Mild Environment	120
10.4	Comparison with hydrodynamic optimization result	121
10.5	Optimization process for GoM pre-2005.....	122
10.6	Optimization process for GoM post-2005	126
10.7	Optimization process for Southeast Asian Condition	129
10.8	Study on Criteria – Pre-2005 condition.....	132
11	Conclusion	140
12	Acknowledgement	141
	Reference	142

Figures

Figure 1-1 Components of a TLP [1-1]	10
Figure 1-2 Production Semi [1-2]	11
Figure 1-3 Truss SPAR [1-3]	11
Figure 1-4 Ship-shaped FPSO [1-4]	12
Figure 1-5 TLP and water depth [1-7].....	14
Figure 1-6 Distribution of TLPs [1-7].....	16
Figure 1-7 TLP Hull configurations [1-1].....	17
Figure 1-8 Brutus TLP [1-8]	18
Figure 1-9 Brutus TLP System Schematic [1-8].....	18
Figure 1-10 Classic MOSES TLP [1-4].....	19
Figure 1-11 MOSES SSIP TLP [1-4]	20
Figure 1-12 SeaStar Platform [1-11]	20
Figure 1-13 Bigfoot E-TLP model [1-12]	21
Figure 1-14 Global Performance Parameters	23
Figure 3-1 Conventional Sizing Method	27
Figure 3-2 Flow Chart of Hull Optimization Program	28
Figure 3-3 Simulated annealing Method 1 (Left; $f(x,y)$, Right; $g(x,y)$)	32
Figure 3-4 Simulated annealing Method 1 (Left; $f(x,y)$, Right; $g(x,y)$)	35
Figure 3-5 Simulated annealing Method 2 $g(x,y)$	35
Figure 3-6 Genetic Algorithm 1 (Left; $f(x,y)$, Right; $g(x,y)$)	36
Figure 3-7 Genetic Algorithm 2 $g(x,y)$	36
Figure 3-8 Steepest Gradient Method 1 (Left; $f(x,y)$, Right; $g(x,y)$)	37
Figure 3-9 Steepest Gradient Method 2 $g(x,y)$	38
Figure 4-1 Main dimensions of Conventional TLP – Circular Column	40
Figure 4-2 Quarter Panel Model for CTLP	41
Figure 4-3 Full Panel Model for CTLP.....	41
Figure 4-4 Structural Beam Model for CTLP	42
Figure 4-5 Main dimensions of Conventional TLP – Rectangular Column.....	43
Figure 4-6 Quarter Panel Model for CTLP (Rectangular Column).....	44
Figure 4-7 Full Panel Model for CTLP (Rectangular Column)	44
Figure 4-8 Structural Beam Model for CTLP (Rectangular Column).....	45
Figure 4-9 Main dimensions of MOSES SSIP TLP –Rectangular Column	46
Figure 4-10 Quarter Panel Model for MOSES SSIP	47
Figure 4-11 Full Panel Model for MOSES SSIP	47
Figure 4-12 Structural Beam Model for MOSES SSIP	48

Figure 4-13 Main dimensions of MOSES SSIP TLP –Circular Column.....	49
Figure 4-14 Quarter Panel Model for MOSES SSIP (Circular Column)	50
Figure 4-15 Full Panel Model for MOSES SSIP (Circular Column).....	50
Figure 4-16 Structural Beam Model for MOSES SSIP (Circular Column)	51
Figure 4-17 Main dimensions of Classic MOSES TLP	52
Figure 4-18 Quarter Panel Model for Classic MOSES	53
Figure 4-19 Full Panel Model for Classic MOSES	53
Figure 4-20 Structural Beam Model for Classic MOSES	54
Figure 5-1 Flow Field around a Floating Body [5-1]	55
Figure 5-2 Method used for Green Function [5-1]	60
Figure 5-3 TLP element coordinate [5-5]	70
Figure 5-4 Catenary line coordinate [5-5]	72
Figure 5-5 Wadam Calculation model.....	75
Figure 5-6 Surge motion RAO (Upright).....	76
Figure 5-7 Surge motion RAO (Offset).....	76
Figure 5-8 Sway motion RAO (Upright)	76
Figure 5-9 Sway motion RAO (Offset).....	76
Figure 5-10 Heave motion RAO (Upright).....	76
Figure 5-11 Heave motion RAO (Offset)	76
Figure 5-12 Roll motion RAO (Upright).....	76
Figure 5-13 Roll motion RAO (Offset)	76
Figure 5-14 Pitch motion RAO (Upright).....	77
Figure 5-15 Pitch motion RAO (Offset).....	77
Figure 5-16 Yaw motion RAO (Upright).....	77
Figure 5-17 Yaw motion RAO (Offset)	77
Figure 5-18 Tendon tension RAO (Upright).....	77
Figure 5-19 Tendon tension RAO (Offset).....	77
Figure 5-20 Tendon tension RAO (Upright).....	77
Figure 5-21 Tendon tension RAO (Offset).....	77
Figure 5-22 Tendon tension RAO (Upright).....	78
Figure 5-23 Tendon tension RAO (Offset)	78
Figure 5-24 Wave drift force Fx (Upright)	78
Figure 5-25 Wave drift force Fx (Offset)	78
Figure 5-26 Wave drift force Fy (Upright)	78
Figure 5-27 Wave drift force Fy (Offset)	78
Figure 5-28 Wave drift force Mz (Upright).....	78

Figure 5-29 Wave drift force M_z (Offset).....	78
Figure 6-1 Schematic of Catenary Line Shape	83
Figure 6-2 Wind and current loading on the platform	86
Figure 6-3 Drag force on rectangular cross section (DNV-RP-C205).....	87
Figure 6-4 DeepC analysis model.....	92
Figure 6-5 Offset value comparison	93
Figure 6-6 Setdown value comparison	93
Figure 6-7 DeepC time history of up-wave tendon tension.....	94
Figure 6-8 DeepC spectrum of up-wave tendon tension.....	94
Figure 6-9 DeepC time history of down-wave tendon tension	95
Figure 6-10 DeepC spectrum of down-wave tendon tension	95
Figure 7-1 Beam Structural Model and Hydrodynamic Panel Model	97
Figure 7-2 Section view of Pontoon and Column	98
Figure 7-3 Correspondence between panels and beams.....	99
Figure 7-4 Spring Boundary corresponding to Tendons.....	100
Figure 7-5 Coordinate Conversion [7-1]	103
Figure 8-1 Compartment assumption for CTLP.....	111
Figure 8-2 Weight Calculation Method	112
Figure 9-1 Topside Model.....	114
Figure 10-1 Comparison with an existing TLP.....	118
Figure 10-2 Comparison between Pre- and Post-Hurricane Hull Shape.....	119
Figure 10-3 Comparison of Hull Shape for harsh and mild environment.....	120
Figure 10-4 Comparison with hydrodynamic optimization result	121
Figure 10-5 Column diameter v.s. Hull total weight (Case 1).....	122
Figure 10-6 Column distance v.s. Hull total weight (Case 1).....	123
Figure 10-7 Pontoon breadth v.s. Hull weight (Case 1).....	123
Figure 10-8 Pontoon height v.s. Hull weight (Case 1)	124
Figure 10-9 Draft v.s. Hull weight (Case 1).....	124
Figure 10-10 Column Height v.s. Hull weight (Case 1).....	125
Figure 10-11 Column diameter v.s. Hull weight (Case 2).....	126
Figure 10-12 Column distance v.s. Hull weight (Case 2)	126
Figure 10-13 Pontoon width v.s. Hull weight (Case 2)	127
Figure 10-14 Pontoon Height v.s. Hull weight (Case 2)	127
Figure 10-15 Draft v.s. Hull weight (Case 2)	128
Figure 10-16 Column Height v.s. Hull weight (Case 2).....	128
Figure 10-17 Column diameter v.s. Hull weight (Case 3)	129

Figure 10-18 Column distance v.s. Hull weight (Case 3)	129
Figure 10-19 Pontoon width v.s. Hull weight (Case 3)	130
Figure 10-20 Pontoon Height v.s. Hull weight (Case 3)	130
Figure 10-21 Draft v.s. Hull weight (Case 3)	131
Figure 10-22 Column Height v.s. Hull weight (Case 3).....	131
Figure 10-23 Criteria 1, 2, & 3 (Case 1)	132
Figure 10-24 Ballast Amount Condition (Case 1).....	133
Figure 10-25 Installation Stability Condition (Case 1)	133
Figure 10-26 Quayside stability Condition (Case 1).....	134
Figure 10-27 Deck post location Condition (Case 1).....	134
Figure 10-28 Airgap Condition (Case 1).....	135
Figure 10-29 Tendon Pretension Condition (Case 1).....	135
Figure 10-30 Natural Period Condition (Case 1)	136
Figure 10-31 Max Offset Condition (Case 1).....	137
Figure 10-32 Minimum Tendon Tension Condition (Case 1).....	137
Figure 10-33 Airgap Condition (Case 1).....	138
Figure 10-34 Tendon Strength Condition (Case 1)	138
Figure 10-35 Hull strength Condition (Case 1)	139

Tables

Table 1-1 Comparison of Floating Production Unit.....	13
Table 1-2 TLP Technology evolution [1-1]	15
Table 3-1 Geometry criteria (criteria 1)	29
Table 3-2 Hull Sizing criteria (criteria 2).....	29
Table 3-3 Design criteria (criteria 3)	30
Table 3-4 Variable, objective function and constraint condition	30
Table 3-5 Optimization result (ASA)	34
Table 3-6 Optimization result (GA)	35
Table 3-7 Optimization result (SGM).....	37
Table 5-1 Nondimensionalization of Mass Matrix.....	66
Table 5-2 Nondimensionalization of Damping Matrix	67
Table 5-3 Nondimensionalization of Restoring Matrix.....	67
Table 5-4 Nondimensionalization of External Force	72
Table 6-1 Effective shape coefficient (DNV-RP-C205)	88
Table 6-2 Reduction Factor for finite length (DNV-RP-C205).....	88
Table 6-3 Global performance comparison.....	96
Table 7-1 Section Properties	98
Table 7-2 Member ID definition	99
Table 7-3 Symbols for matrix method formulation.....	100
Table 7-4 Load Cases	107
Table 8-1 Structural Members for Conventional TLP.....	111
Table 9-1 Environmental Condition	113
Table 9-2 Topside Condition.....	113
Table 9-3 Riser Condition	114
Table 9-4 Calculation result for GoM pre-2005 (Case1)	115
Table 9-5 Calculation result for GoM post-2005 (Case 2).....	116
Table 9-6 Calculation Result for Southeast Asian Condition (Case 3)	117
Table 10-1 Comparison with an existing TLP	118
Table 10-2 Comparison between Pre- and Post-Hurricane Hull Shape	119
Table 10-3 Comparison between Pre- and Post-Hurricane Hull Shape	120
Table 10-4 Comparison with hydrodynamic optimization result.....	121

1 Background

Tension leg platform (TLP) is an offshore platform, which is tethered by tendon pipes and has small heave, roll and pitch motions. Currently more than twenty TLPs have been installed and most of them are operated as oil production, drilling or wellhead platforms. Originally, TLPs are installed mainly at Gulf of Mexico and North Sea, but now their installation locations are becoming more global, such as West Africa, South America, and Southeast Asia, due to recent oil discoveries in these areas. To design the hull shape, usually past design experience or some of empirical factors are utilized, but now it is becoming more important to find optimized hull shape suitable for each environment condition, which any past designed TLP hasn't experienced. This study proposes practical system to design hull shape at initial stage by utilizing optimization algorithms and shows it has better performance than previous studies, wide range of application, and practical calculation efficiencies.

1.1. Floating Offshore Production Facilities

Offshore production facilities for oil production have two major types: fixed and floating type. Most of the offshore facilities are categorized in the following categories:

- Fixed Type
 - Jacket Structure
 - MOPU
 - GBS
 - Compliant Tower
- Floating Type
 - FPSO, FSO
 - Semi-Submersible
 - TLP
 - SPAR

Jacket structures, Mobile Offshore Production Unit (MODU), Gravity Base Structure (GBS), and Compliant Tower belong to the fixed type. These structures have less motion than floating types, but these facilities are subject to the restriction of water depth. TLP, Semi-Submersible, SPAR and F(P)SO are categorized as floating type. Characteristics of these floating structures are explained in the following pages. Comparison of each floating type is shown in Table 1-1.

[Tension Leg Platforms]

TLP consist of hull, Topsides, tendons, risers, pile and foundation (See Figure 1-1). Typically the hull of TLP consists of columns and pontoons. Because TLP has very small heave, roll and pitch motion, dry completion, drilling operation and workover from the platform are applicable. Normally, top tension risers (TTR) are used as production, drilling or workover risers and Steel catenary risers (SCR) are used as oil/gas export risers. Because of the difficulty to design tendons for deep water, the applicable water depth is limited. The current deepest record is 1,425m (Magnolia TLP).

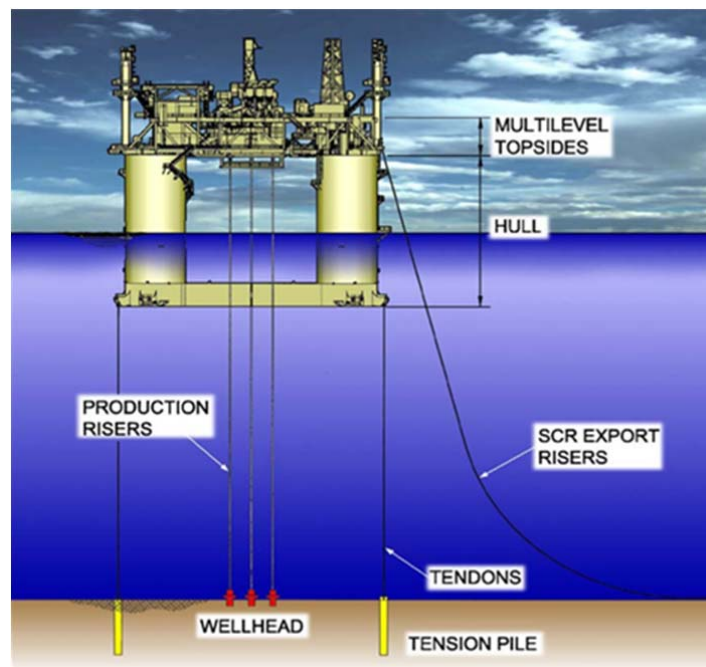


Figure 1-1 Components of a TLP [1-1]

[Semi-Submersibles]

Semi-Submersibles are used for oil production platform, as well as drilling rig, crane vessel and offshore support vessel (OSV). Semi-submersibles consist of columns and pontoons (Figure 1-2). Typically production semi-submersibles tend to have ring pontoon, while others (drilling, crane vessel and OSV) have twin pontoons. Columns provide sufficient hydrostatic stability. Sometimes production Semi-submersible platforms are converted from drilling semi-submersible rigs. Semisubmersibles are moored by conventional mooring legs, which consist chain, wire rope or polyester rope and can operate in wide range of water depth. The motions of Semisubmersibles are relatively small, but not as small as TLP or SPAR. Typically dry completion is not applicable at this moment.



Figure 1-2 Production Semi [1-2]

[SPAR]

Single Point Anchor Reservoir (SPAR) has small motion and dry completion is applicable. SPAR has variations: Classic SPAR, Truss SPAR (Figure 1-3) and Cell SPAR. Unlike TLPs, SPAR is hydrostatically stable and has conventional catenary or taut mooring legs. Topside of SPAR has to be integrated at offshore, after launching hull into water and making it vertical. Motion of SPAR is small because its natural period is longer than wave period to avoid resonance, but consideration is needed when it's installed in swell dominant area.

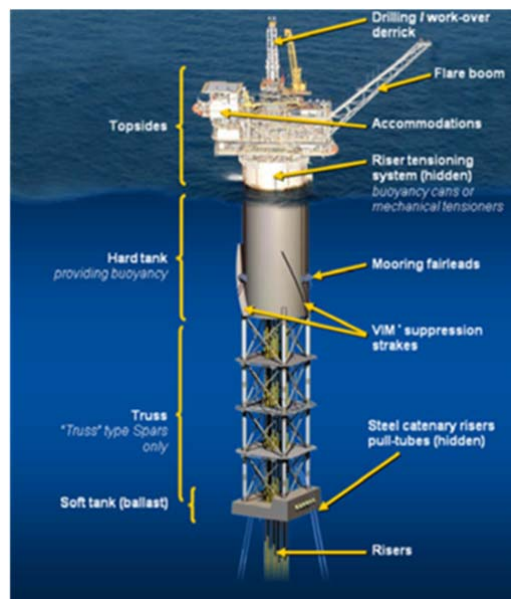


Figure 1-3 Truss SPAR [1-3]

[FPSO,FSO]

F(P)SO stands for Floating (Production) Storage Offloading unit. FPSO has storage tanks and offloading system (Figure 1-4). Sales oil is exported by shuttle tankers. Most of the FPSOs are ship shaped, and can be converted from used tankers. Mooring systems are either single point mooring (SPM) or spread mooring. For single point mooring, turret system is used and it allows vessel to weathervane. Mooring legs are conventional catenary lines or taut lines. FPSO has relatively large motion and basically it's not suitable for harsh environment. Some of FPSO has disconnectable turret mooring system to evacuate from heavy weather. Normally flexible risers are used for FPSOs. Seven FPSOs [1-5] have cylindrical hull and don't need turret system.

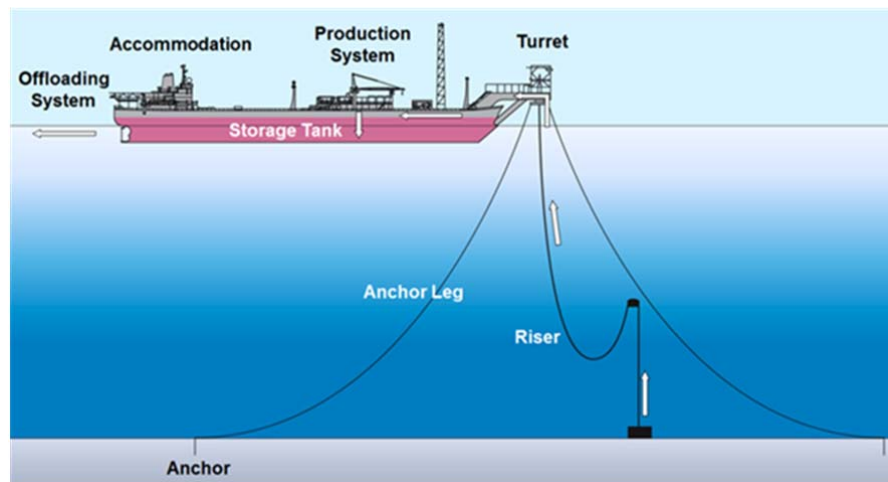


Figure 1-4 Ship-shaped FPSO [1-4]

Table 1-1 Comparison of Floating Production Unit

	FPSO, FSO	Semi	TLP	SPAR
Number of units in Service*	FPSO 164 FSO 93	41	24	20
Motion	Large	Small	Small (Heave, Roll, Pitch)	Small (Heave, Roll, Pitch)
Storage	O	N/A	N/A	N/A*
Export	Shuttle Tanker/ Pipeline	Pipeline/ Connected to nearby unit	Pipeline/ Connected to nearby unit	Pipeline/ Connected to nearby unit
Topside integration	Yard	Yard	Yard/Offshore*	Offshore
Construction	New built/ Conversion	New built/ Conversion	New built	New built
Completion	Wet Tree	Wet Tree*	Wet/Dry Tree	Wet/Dry Tree
Drilling/ Workover	N/A	O	O	O
Hull Type	Ship-Shaped, Sevan,		CTLP, MOSES, SeaStar, ETLP	Classic SPAR, Truss SPAR, Cell SPAR,

* As of 2014 [1-6]

* AASTA Spar (under construction) will have storage capacity.

* Topsides of Mini-tlp is integrated at offshore

1.2. History and trend of TLPs

First TLP is Hutton TLP which is installed at Hutton field in North Sea in 1984. After that, more than twenty TLPs have been fabricated and installed, and they have been updating the deepest records (Figure 1-5). R. D'Souza and Rajiv Aggarwal [1-1] categorized history of TLP construction into the following three phases:

- | | | |
|-----------|----------------|-----------------------------------|
| Phase I | 1984 - 1995 | Pioneering |
| Phase II | 1996 - 2001 | Innovation and Standardization |
| Phase III | 2002 - Present | Commoditization and Globalization |

Now we are in Phase III and the technology for TLP is well matured and proven.

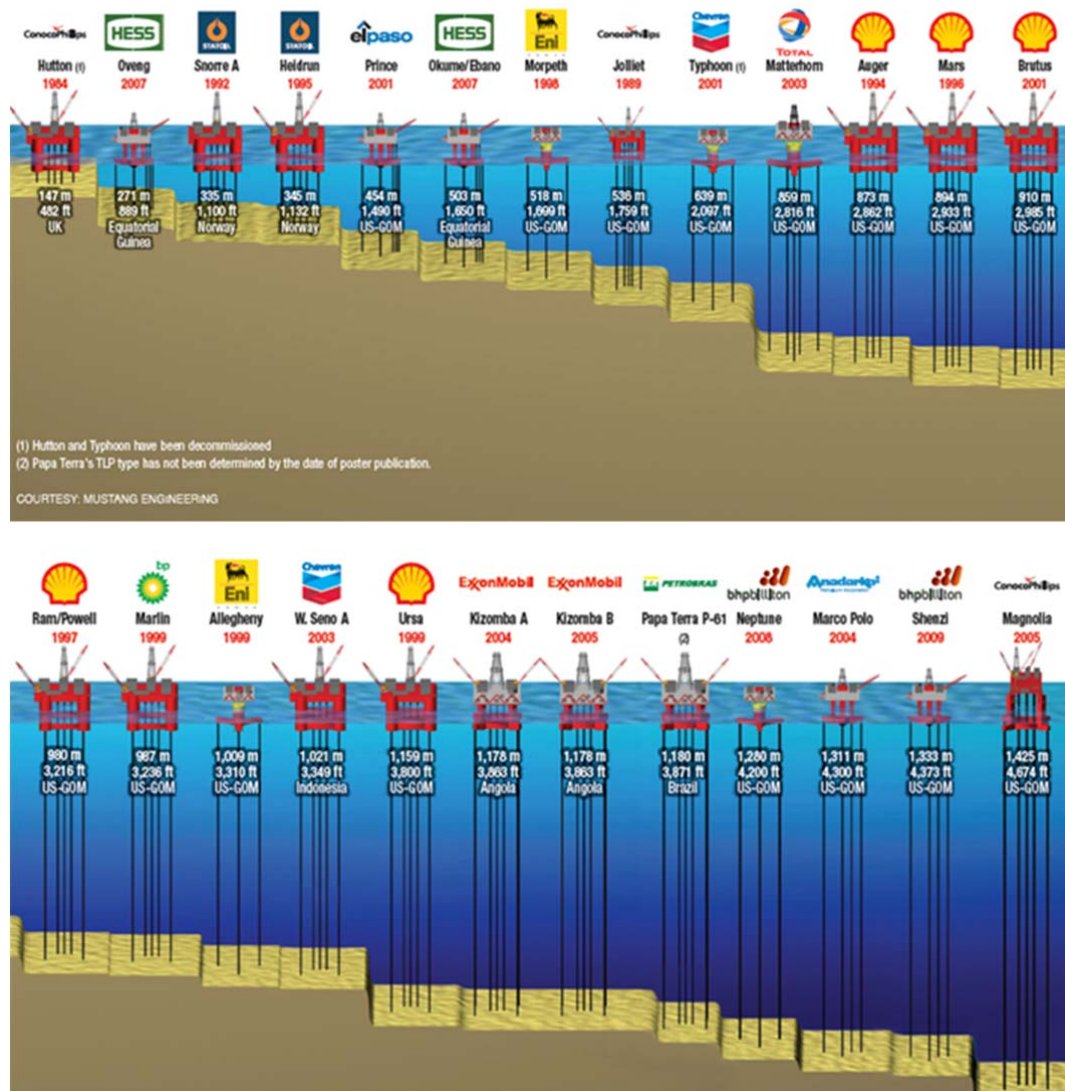


Figure 1-5 TLP and water depth [1-7]

Table 1-2 TLP Technology evolution [1-1]

Phase	No.	Field	Operator	Year Installed	Location	Water Depth (ft)	Contracting Strategy	Contractor	Installation Type	Installation Contractor
Phase I - Pioneering	1	Hutton	Conoco	1984	North Sea	486	OM	Conoco	Floatover	Heerema
	2	Joliet	Conoco	1989	GOM	1,760	OM	Conoco	Offshore Lift	Multiple
	3	Snorre	Saga	1992	North Sea	1,050	OM	Saga	Floatover	Multiple
	4	Auger	Shell	1994	GOM	2,860	OM	Shell	Floatover	Heerema
	5	Heidrun	Conoco	1995	North Sea	1,134	OM	Conoco	Floatover	Multiple
Phase II - Innovation and Standardization	6	Mars	Shell	1996	GOM	2,940	OM	Shell	Quayside	Heerema
	7	RamPowell	Shell	1997	GOM	3,214	OM	Shell	Quayside	Heerema
	8	Morpeth	British Borneo	1998	GOM	1,670	EPCM	Atlantia	Offshore Lift	JRM
	9	Marlin	BP	1999	GOM	3,240	TEPC	ABB	Quayside	Heerema
	10	Allegheny	British Borneo	1999	GOM	3,294	EPCM	Atlantia	Offshore Lift	JRM
	11	Ursa	Shell	1999	GOM	3,950	OM	Shell	Offshore Lift	Heerema
	12	Typhoon	Chevron	2001	GOM	2,097	EPCM	Atlantia	Offshore Lift	JRM
	13	Brutus	Shell	2001	GOM	2,985	OM	Shell	Quayside	Heerema
	14	Prince	El Paso	2001	GOM	1,450	TEPC	MODEC	Offshore Lift	Heerema
Phase III - Commoditization and Globalization	15	Matterhorn	Total	2003	GOM	2,850	TEPC	Atlantia	Offshore Lift	Heerema
	16	West Seno A	Unocal	2003	Indonesia	3,200	TEPCI	HHI	Dry Dock	Clough
	17	Marco Polo	Anadarko	2004	GOM	4,300	TEPC	MODEC	Offshore Lift	Heerema
	18	Kizomba A	Exxon-Mobil	2004	Angola	3,937	TEPCI	ABB	Quayside	ABB-LG
	19	Magnolia	Conoco	2004	GOM	4,674	OM	Conoco	Quayside	Saipem
	20	Kizomba B	Exxon-Mobil	2005	Angola	3,330	TEPCI	DSME	Quayside	DSME
	21	Okume	Hess	2006	Equ. Guinea	1,640	TEPC	MODEC	Dry Dock	Heerema
	22	Oveng	Hess	2006	Equ. Guinea	918	TEPC	MODEC	Dry Dock	Heerema
	23	Neptune	BHP	2007	GOM	4,250	EPCM	SBM	Offshore Lift	Heerema
	24	Shenzi	BHP	2009	GOM	4,373	TEPC	MODEC	Offshore Lift	Heerema
	25	Papa Terra	Petrobras	2013	Brazil	3,871	TEPCI	FloaTEC	Floatover	JRM
	26	Olympus	Shell	2013	GOM	3,016	OM	Shell	Quayside	Heerema
	27	Big Foot	Chevron	2014	GOM	5,200	OM	Chevron	Quayside	Heerema
	28	Malikai	Shell	2015	Malaysia	1,640	TEPC	Technip-MMHE	Quayside	Heerema
	29	Moho Nord	Total	2015	Congo	2,559	TEPC	HHI	Quayside	NA

Notes:		Rows Color indicates:
ABB-LG	ABB Lummus Global	Early TLPs w/varying hull, tendon, foundation designs
DSME	Daewoo Shipbuilding & Marine Engineering	CTLP or ETLT hull design
EPCM	Engineering, Procurement, Construction and Management	Concrete hull design
HHI	Hyundai Heavy Industries	SeaStar hull design
JRM	J. Ray McDermott	Moses hull design
OM	Operator Managed	SSIP hull design
SBM	Single Buoy Moorings	
TEPC	Turnkey EPC	
TEPCI	Turnkey EPCI (EPC and Installation)	

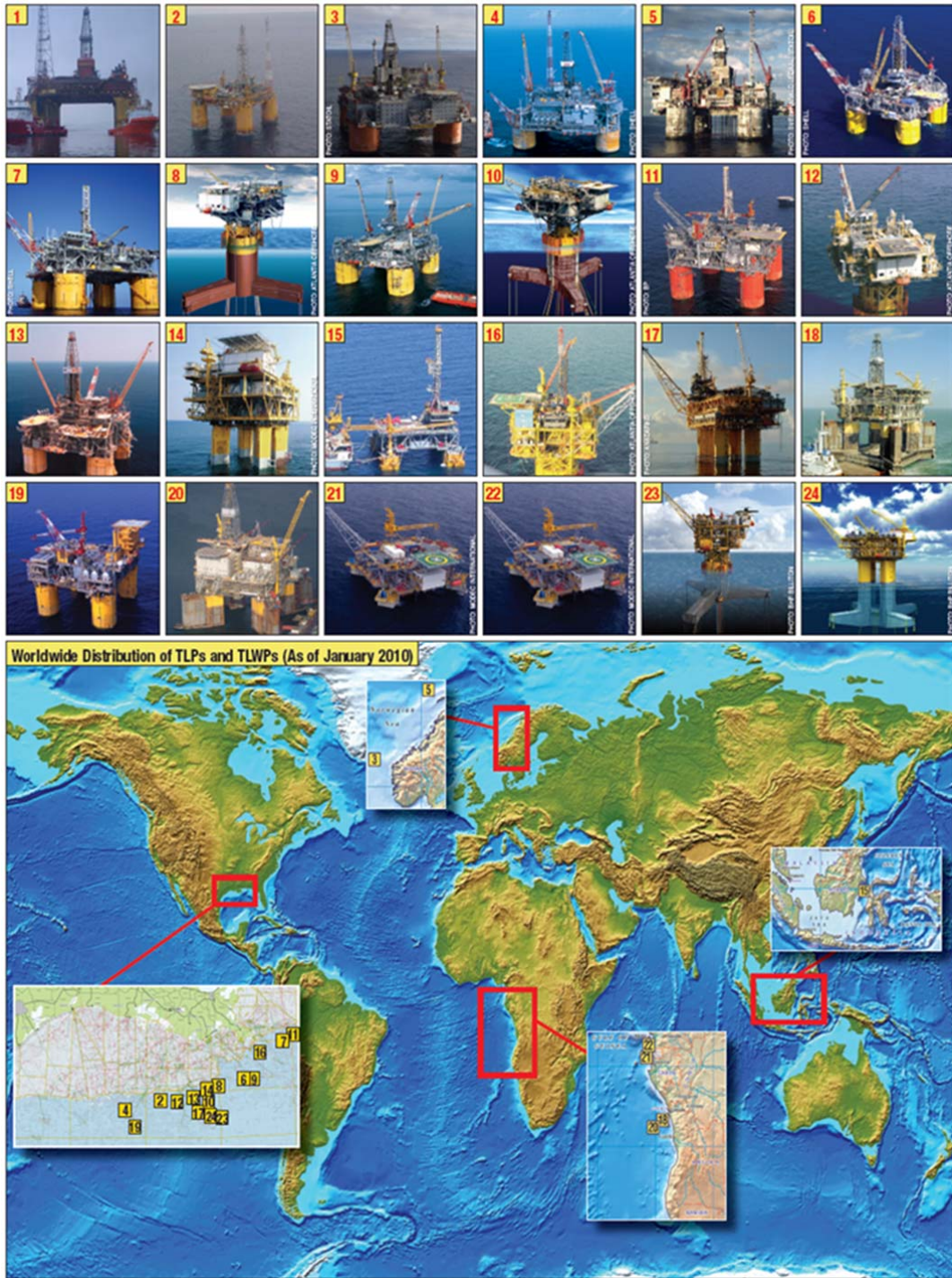


Figure 1-6 Distribution of TLPs [1-7]

1.3. TLP hull shape

TLP hull shapes are categorized into the following four types;

- Conventional TLP (C-TLP)
- MOSES TLP
- SeaStar TLP
- Extended TLP (E-TLP)

These TLPs are all field proven. The plan view of each type is shown in Figure 1-7.

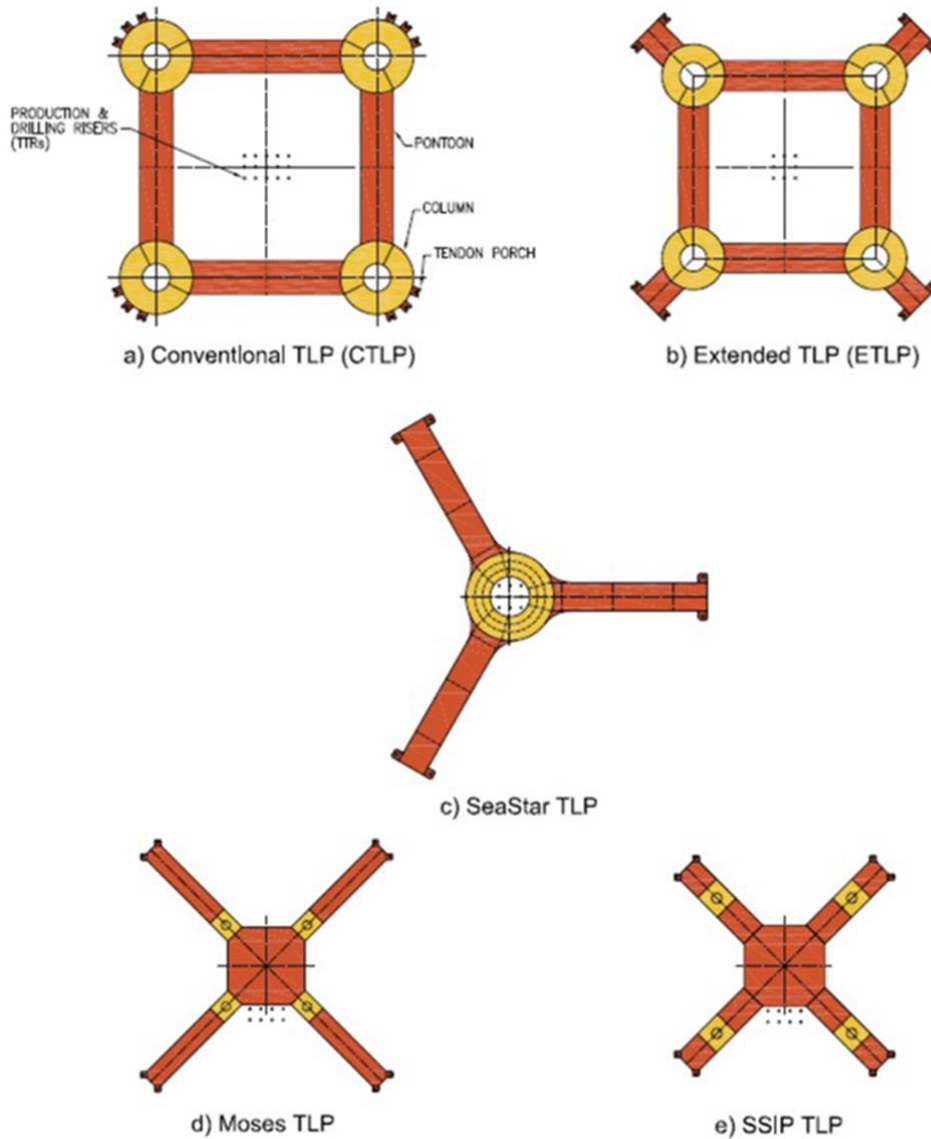


Figure 1-7 TLP Hull configurations [1-1]

1.3.1. Conventional TLP (CTLP)

Conventional TLP is the most common type of TLP hull shape. Usually it consists of four columns connected by four pontoons. Figure 1-8 and Figure 1-9 shows configuration of Brutus TLP as a typical example of CTLP. Column is not necessarily circular, so West Seno TLP has squared column [1-9].



Figure 1-8 Brutus TLP [1-8]

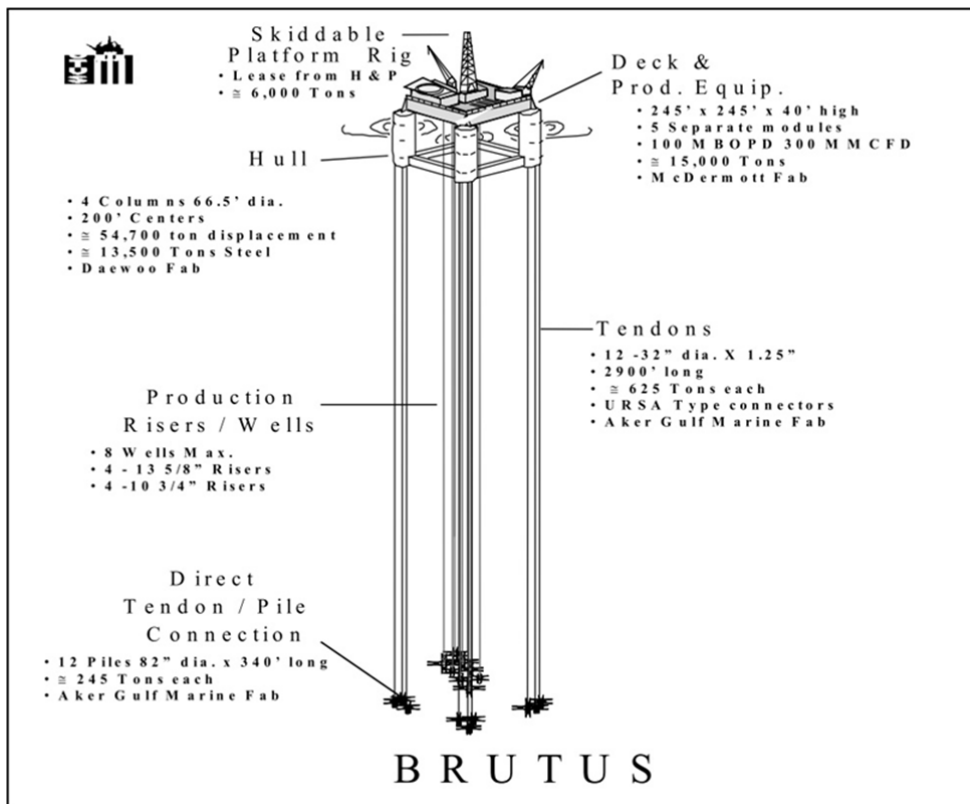


Figure 1-9 Brutus TLP System Schematic [1-8]

1.3.2. MOSES TLP

MOSES stands for Minimum Offshore Surface Equipment System. Classic MOSES TLP and MOSES SSIP TLP fall into this category. Unlike conventional TLPs, MOSES has cross-shaped pontoon, not ring pontoon.

Classic MOSES TLP is regarded as mini-TLP, which doesn't have hydrostatic stability for wet-tow or installation to minimize the hull steel structure. Classic MOSES TLP is suitable for relatively small oil fields. Prince TLP, MarcoPolo TLP, and Shenzi TLP belong to Classic MOSES TLP.

Oveng/Okume and Ebano belong to MOSES SSIP. MOSES SSIP TLP has hydrostatic stability for wet-tow and installation, and enables us to reduce offshore integration cost.

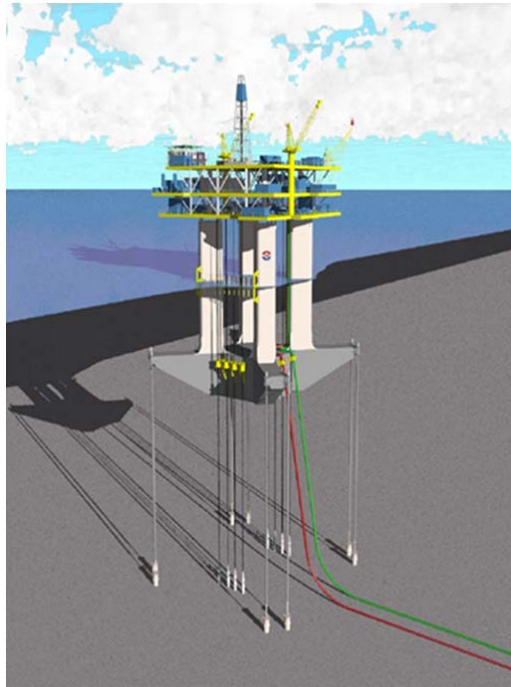


Figure 1-10 Classic MOSES TLP [1-4]

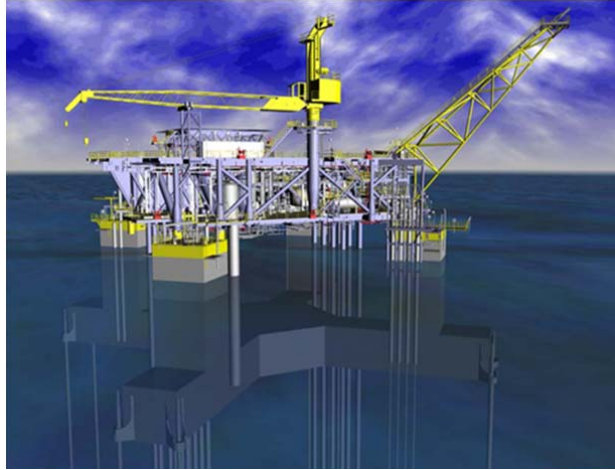


Figure 1-11 MOSES SSIP TLP [1-4]

1.3.3. SeaStar TLP

SeaStar has single column with three pontoons. Tendons are connected at the end of pontoon. Production risers are located at the center of the column. SeaStar is also categorized as mini-tlp, and Topsides is integrated at offshore using floating crane. Morpheth, Allegheny, Typhoon, Matterhorn, Neptune [1-10] are categorized as SeaStar TLP.



Figure 1-12 SeaStar Platform [1-11]

1.3.4. Extended TLP (ETLP)

Extended TLP (ETLP) has similar hull shape as conventional TLP, but there are extended structure on each column and tendon porches are connected to the structure. This makes roll and pitch motion performance better. Kizomba A, Kizomba B, Magnolia, Papa Terra, and Bigfoot (Figure 1-13) belong to ETLP.

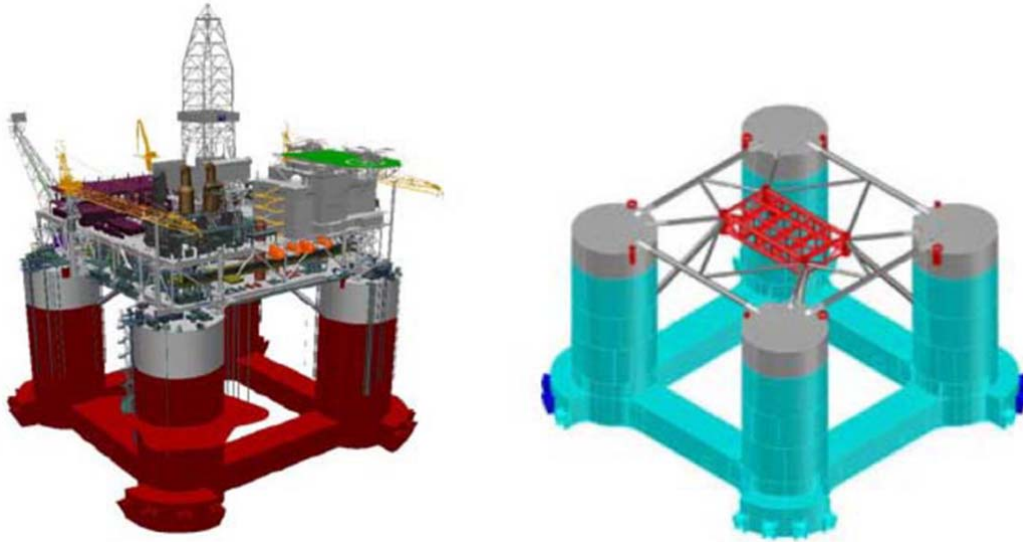


Figure 1-13 Bigfoot E-TLP model [1-12]

1.4. TLP hull design and sizing

This subsection summarizes the key point to decide hull dimensions from a design point of view. Typical hull sizing method is described in the reference [1-13][1-14]. Typically offshore platform project has the following phases;

1. Conceptual Study Phase
2. FEED (Front End Engineering Design) Phase
3. Fabrication and Installation Phase
4. Operation Phase

Major design works are mainly done at Phase 1-3, and are categorized into the following three stages;

1. Conceptual Design
2. Basic Design
3. Detail Design

Main purpose of conceptual study is concept selection and feasibility study. The basic study gives main design parameters and cost estimation. The detail design is mainly for fabrication. This study focus on the conceptual design and basic design.

At the beginning stage of designing TLPs, hull main dimension should be decided. This hull main dimension has a large impact on the later works. If good optimized hull design is carried out at initial stage, less design changes and reworks will happen through project. The following subsection explains what is needed to consider when designing TLPs.

1.1.1 Global Performance

Global performance shows statics and dynamics of the platform under the site environment conditions. Criteria of global performance parameters (Such as Min/Max Tendon tension, Airgap, Offset/Set-down) (Figure 1-14) are defined in API RP 2T. Heave, roll and pitch natural period should be smaller than 4.5 sec in order to avoid resonance with waves. The tendon pretension ratio is calculated dividing total tendon pretension by hull displacement. Pretension provides horizontal restoring force of the platform and avoids too much horizontal offset. For Gulf of Mexico, pretension ratio varies from 15% to 35%.

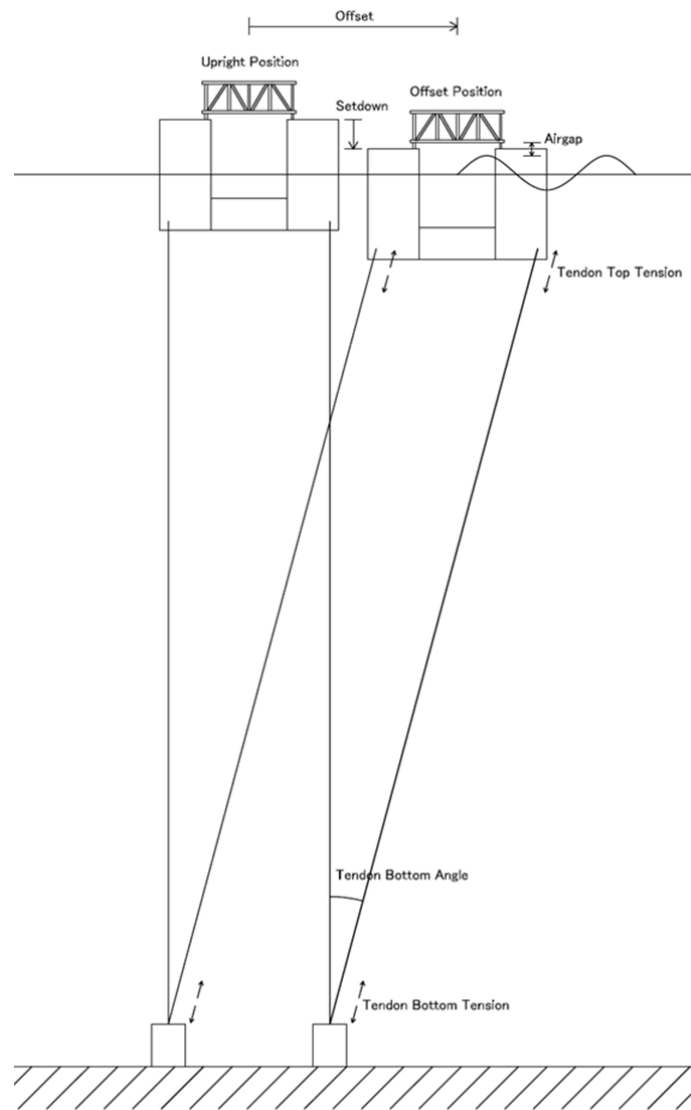


Figure 1-14 Global Performance Parameters

1.1.2 Structural Integrity

The structural strength is required as per class requirement. Global strength is the strength of platform main members like columns and pontoons. Normally global finite element analysis (FEA) with hydrodynamic loads is carried out to evaluate global strength. Local strength is defined in equations specified in classification society rules. Buckling strength and fatigue life are also evaluated as per class requirement.

1.1.1 Transportation and installation

Depending on the situation, TLP is transported either by dry-tow or wet-tow, and installed at site. Proper hydrostatic stability should be kept during wet-tow, installation or quay-side condition. Normally, the draft is restricted at quayside and during inshore tow.

1.1.2 Topside Support and Integration Method

Typically, Topsides are integrated at offshore for mini-TLPs and at fabrication yard for other TLPs. At offshore, Topside is lifted by offshore crane vessel and mated with hull. At fabrication yard, Topside is mated with hull at quayside or floating dock. Depending of the sizes, sometimes Topside is separated into several modules and integrated to hull.

1.1.3 Drilling Operation

Drilling facilities are installed either permanently or temporarily. If the temporarily method, like Tender Assist Drilling (TAD) or modular platform drilling is applied, total platform weight during severe environment conditions is reduced and this makes platform performance better because TLP can maintain high pretension. For TAD operation, deck height is limited for operability and tender assist vessel is moored to TLP with proper clearance with TLP.

1.1.4 Riser and well bay layout

Hull should provide proper space for riser arrangement so that the hull, mooring leg and riser will not clash each other. Conventional TLP has relatively large spaces for riser arrangement. Mini TLPs has smaller space for risers and need keel guide to avoid clash of riser and hull.

1.1.5 Constructability

Some TLPs have squared column for constructability, although square column has larger wind and current drag force than circular column. All MOSES TLPs and West Seno TLP have squared column. Column shell does not need to be formed to circular and connection between column and pontoon become simple. It also gives better equipment and piping arrangement.

2 Purpose of this Study

As explained in previous section, now TLPs technologies are matured and proven, and they are being installed globally and subject to various environments. When the hulls of TLPs are designed for these environments, engineers face the following problems:

1. It takes lots of time and effort to find optimized hull shape within limited amount of time and resources.
2. Normally past project data is utilized to find the good starting point, but it is not always applicable because design condition is not always similar.
3. Empirical factors such as pretension ratio, pontoon/column ratio, and volumetric weight factor is utilized to extrapolate hull shape from past experience, but this is also not useful when there is not enough supporting data.
4. The design process can be simplified by focusing on one governing criteria, but only if governing criteria is obvious.

Clauss, and Birk carried out hull shape optimization with utilizing optimization algorithm [2-1]. They optimized TLP hull shape by minimizing tendon tension response. Birk et al. carried out optimization of TLP hull by maximizing tendon fatigue life [2-2]. Lee and Lim also carried out hull shape optimization by maximizing tendon fatigue life with considering second order forces [2-3, 2-4].

1. These preceding works are focusing on hydrodynamic response or tendon fatigue life and set these to objective function. However, these are not always governing criteria for TLP hull shape.
2. In these preceding studies, initial hull shape must be input and the objectives of these optimizations are to improve hull shape.
3. Only in-place conditions are considered in these preceding studies, but hull shape is also governed by construction, transportation, and installation criteria.

Based on the above issues, the purpose of this study is as follows:

- Develop hull optimization system that can find the optimized TLP hull shape. This system has more practical approach than preceding works: The platform weight and tendon weight are objective function to be minimized and design criteria are constraint condition.
- Compare the result with existing units for verification

- Compare with the result of hydrodynamic optimization
- Study application of TLPs to several environment condition

3 Methodology – Sizing Strategy

3.1 Conventional Hull Sizing Method

The conventional hull sizing is carried out by engineers in several disciplines as follows.

- Naval Architects
- Structural Engineers
- Mooring Engineers
- Outfitting Engineers
- Hull System Engineers
- Electrical & Instrument Engineers

Naval architects take care of weight control, hydrostatic stability, hydrodynamic and global performance analysis. Structural engineer check the structural integrity of the hull. Mooring engineer check the strength of the tendons. Hull system and E&I engineer check if there is enough space to arrange the piping and equipment. First initial hull shape and tendon size are estimated by past project data or engineer's experience. Then, weight and center of gravity information is passed to naval architect who carries out hydrodynamic analysis. Hydrodynamic coefficients are passed to naval architect who is in charge of global performance. Hydrodynamic loads and inertia loads are passed to structural engineers. Then tendon tension data is handed over to mooring engineers. Each engineer checks the criteria in charge and if there is problem, hull shape is revised and they do the same process again.

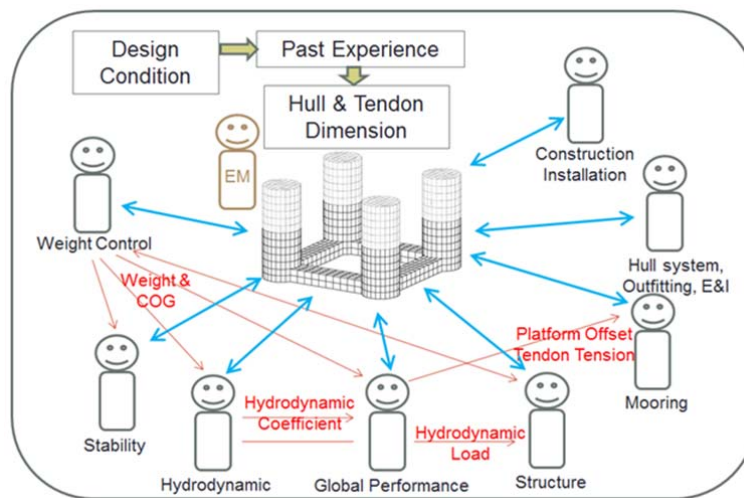


Figure 3-1 Conventional Sizing Method

3.2 Sizing Strategy

The flow chart in Figure 3-2 shows the framework of the hull sizing program. The hull sizing work is modeled as multivariable minimization problem with multiple constraint conditions. The program finds an optimized solution that meets the criteria at basic design stage, and then generates necessary design data for further design development.

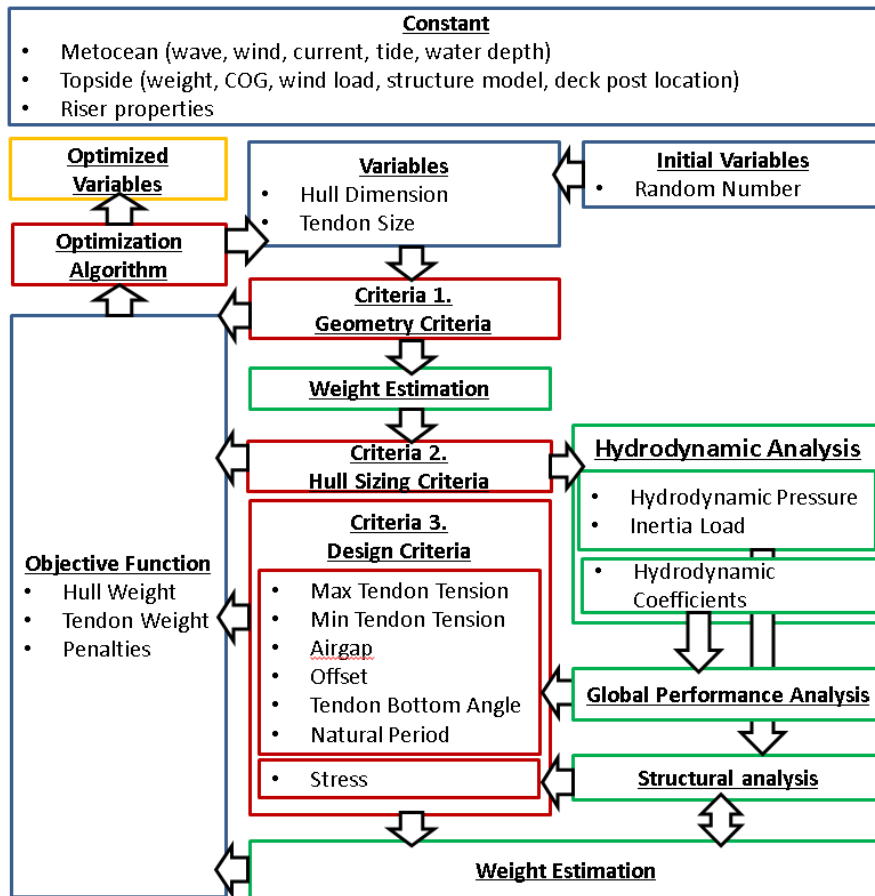


Figure 3-2 Flow Chart of Hull Optimization Program

3.3 Criteria

There are three types of criteria in the program;

- Geometry criteria (criteria 1)
- Hull sizing criteria (criteria 2)
- design criteria (criteria 3)

As hydrodynamic and structure analyses consume a large amount of computation time, geometry criteria and hull sizing criteria are checked prior to the analysis so as to

improve the efficiency of the optimization process. Geometry criteria (criteria 1) are summarized in the table 2.

Table 3-1 Geometry criteria (criteria 1)

Geometry Criteria	Column dia.<Column distance
Geometry Criteria	Column dia.>Pontoon width
Geometry Criteria	Draft>Pontoon height
Geometry Criteria	Column height>Draft

Hull sizing criteria (criteria 2) are summarized in the table 3. Deck support locations have to be consistent with column locations. Column height has to meet minimum air gap criteria set. The metacentric height (GM) for the installation condition must remain positive and adequate. If the hull shape does not meet these criteria at any step, the program will skip the hydrodynamic and structure analysis and put a penalty in the extended objective function.

Table 3-2 Hull Sizing criteria (criteria 2)

Ballast Amount	>5% of displacement
GM for installation	>2.0m
GM for quayside draft	>2.0m
Deck post location	On column
Airgap estimation	>1.5m
Tendon pretension ratio	5% - 50%

The following Table 4 shows design criteria (criteria 3), which include global performance criteria and strength criteria. Global performance criteria are in line with API RP 2T. Strength criteria are in accordance with ABS MODU rule [8-1].

Table 3-3 Design criteria (criteria 3)

	Operating	Extreme	Survival
[Global performance]			
Max. Offset (% Water Depth)	< 10%	<12%	<14%
Airgap	>1.5 m		> 0 m
Min. Tendon Tension	>0 N		
Max. Tendon Tension	API 2T 9.6.2.3 Pipe Strength [6-1]		
[Structural strength]			
Axial Stress	$0.6\sigma_y$	$0.8\sigma_y$	$1.0\sigma_y$
Shear Stress	$0.4\sigma_y$	$0.53\sigma_y$	$0.67\sigma_y$

3.4 Optimization Algorithm

Table 1 shows variable, objective function and constraint condition in the sizing system. The hull dimension (column and pontoon size) and tendon size are defined as variables. Design conditions such as metocean data, topside and riser properties are constant parameters. The objective function is the sum of hull and tendon weight. The constraint conditions are design criteria such as global performance and strength.

Table 3-4 Variable, objective function and constraint condition

x	Variables	Hull Dimension Tendon Size
$f(x)$	Objective function	Hull and Tendon Weight
$g_i(x) \leq 0$	Constraint condition	Initial Criteria Global Performance Criteria Strength Criteria

The criteria are incorporated into objective function using penalty function method [3-1] and the extended objective function is expressed in Eq. (3-1). μ_i is the penalty coefficient of constraint condition i. Starting from an initial value, μ_i is increased successively until the variables meet all the criteria and optimized solution converges.

$$f'(x) = f(x) + \sum_i \mu_i \text{Max}\{g_i(x), 0\} \quad (\text{Eq. 3-1})$$

3.4.1 Adaptive Simulated Annealing Method

One of the optimization method used in this study is Simulated Annealing Method (SA)[3-2]. This method is applicable for multi-variable and non-linear global optimization problem. This optimization method mimics the physical process of annealing in metallurgy. The minimum energy state can be found by cooling down the temperature slowly. In this program, extended objective function at step k is defined as energy E_k .

$$E_k = f'(x_k) \quad (\text{Eq. 3-2})$$

At the initial step, x_k is generated from uniform random number. Then variables x_{k+1} are generated from random numbers which follow the normal distribution expressed in Eq. (3-3). (Adaptive Simulated Annealing (ASA)[3-2]). u^i is the uniform random number.

$$x_{k+1}^i = x_k^i + y^i(UB_i, LB_i) \quad (\text{Eq. 3-3})$$

$$y^i = \text{sign}\left(u^i - \frac{1}{2}\right) T_k^i \left[\left(1 + \frac{1}{T_k^i}\right)^{|2u^i-1|} - 1 \right] \quad (\text{Eq. 3-4})$$

$$x_k^i \in [UB_i, LB_i] \quad (\text{Eq. 3-5})$$

The Eq. (3-6) shows the probability of acceptance of x_{k+1} . If E_{k+1} is smaller than or equal to E_k , x_k is always replaced by x_{k+1} . In the other case, x_k is replaced by x_{k+1} depending on the probability shown in Eq. (3-6).

$$h_k(x_k) = \begin{cases} 1 & E_{k+1} \leq E_k \\ \exp\left(-\frac{E_{k+1} - E_k}{T_k}\right) & E_{k+1} > E_k \end{cases} \quad (\text{Eq. 3-6})$$

This generation of x_{k+1} , judgment of the acceptance and replacement of x_k are repeated enough times until E_k reaches equilibrium at temperature T_k . The Eq. (3-7) shows cooling schedule. After the E_k reaches equilibrium at temperature T_k , the temperature for the next step T_{k+1} is calculated from the following equation. D is the dimension of variable.

$$T_k^i = T_0^i \exp(-c_i k^{1/D}) \quad (\text{Eq. 3-7})$$

Then new equilibrium E_{k+1} will be searched at temperature T_{k+1} . This process is repeated until temperature became cool enough and variable x_k converges.

3.4.2 Real-coded Genetic Algorithm

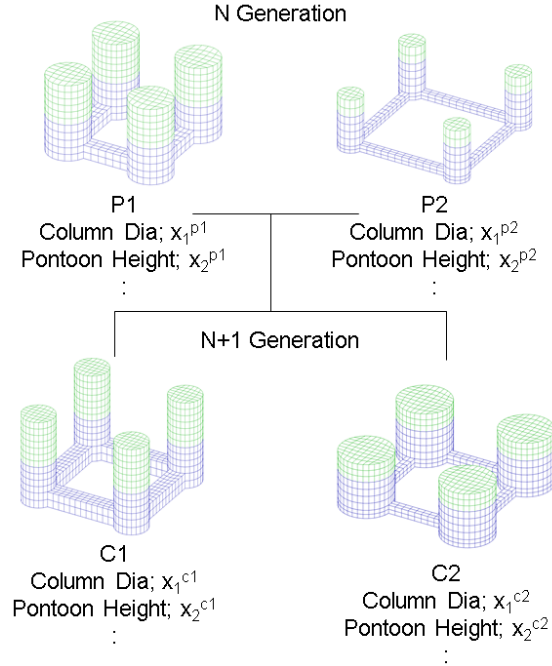


Figure 3-3 Simulated annealing Method 1 (Left: $f(x,y)$, Right: $g(x,y)$)

Genetic Algorithm (GA) [3-3][3-4] is also popular method for optimization of non-linear and multi-variable problem. This method mimics natural selection process. In this study, real coded genetic algorithm is adopted. Figure 3-3 shows the concept of genetic algorithm. Genetic operator is expressed as follows:

$$[x_1, x_2, x_3, \dots, x_n]_k^j \quad (\text{Eq. 3-8})$$

$$x_i \in [UB_i, LB_i] \quad (\text{Eq. 3-9})$$

Each individual has a genetic operator and are evaluated based on objective function value. Every generation has a certain number of individuals. Couples of individuals are selected based on the objective value number. Better objective function value means higher probability to be selected. Then, couples are crossed over. If couple has value a

and b in genetic operator, the genetic operators of the next generation are decided by the following equations, using normal random number N .

$$c = m + \xi d \quad (\text{Eq. 3-10})$$

$$m = \frac{a + b}{2} \quad (\text{Eq. 3-11})$$

$$d = (a - b) \quad (\text{Eq. 3-12})$$

$$\xi = N(0, \sigma^2) \quad (\text{Eq. 3-13})$$

The generated new individuals are mutated by certain probability. Using normal random number, mutation is operated as follows:

$$c = N(a, \sigma^2) \quad (\text{Eq. 3-14})$$

The genetic operators of best few individuals are preserved to the next generation as elites. These operations are done by generation and the best individual at the last generation is the optimized solution.

3.4.3 Steepest Gradient Method

Steepest Gradient Method (SGM) [3-5][3-6] is a simple algorithm. At every step, objective function and its gradient are calculated, and the search is always going to steepest directions. α is step size.

$$x_{i,k+1} = x_{i,k} + \alpha d_{i,k} \quad (\text{Eq. 3-15})$$

$$d_{i,k} = -\frac{\partial f_k}{\partial x_{i,k}} \quad (\text{Eq. 3-16})$$

This step size, should be selected properly, otherwise program cannot find minimum value. This method tends to converge to local extremal values.

3.4.4 Program Test

To study the performance of optimization program, minimum values of the following functions are calculated by ASA, GA and SGM. This function f is simple, but g has lots of local extremals.

$$f(x, y) = x^2 + y^2 - 10 \quad (\text{Eq. 3-17})$$

$$g(x, y) = x^2 + y^2 - 5(\cos 5x + \cos 5y) \quad (\text{Eq. 3-18})$$

The minimum value of this function is as follows.

$$f_m(0, 0) = -10 \quad (\text{Eq. 3-19})$$

$$g_m(0, 0) = -10 \quad (\text{Eq. 3-20})$$

The convergence condition is shown in the following equation;

$$\frac{f - f_m}{f_m} < 10^{-6} \quad (\text{Eq. 3-21})$$

$$\frac{g - g_m}{g_m} < 10^{-6} \quad (\text{Eq. 3-22})$$

[ASA]

The Table 3-5 shows the program test result. Figure 3-4 and Figure 3-5 show the optimization route.

Table 3-5 Optimization result (ASA)

function	run	x	y	f	Calculation Time (sec)
f	Run1	0.0002330	0.0024870	-9.9999938	0.078
f	Run2	0.0004813	-0.0007605	-9.9999992	0.093
f	Run3	-0.0005818	-0.0013593	-9.9999978	0.078
g	Run1	0.0001260	0.0000473	-9.9999988	0.076
g	Run2	-0.0001402	0.0003340	-9.9999917	0.071
g	Run3	0.0000699	0.0001404	-9.9999984	0.085

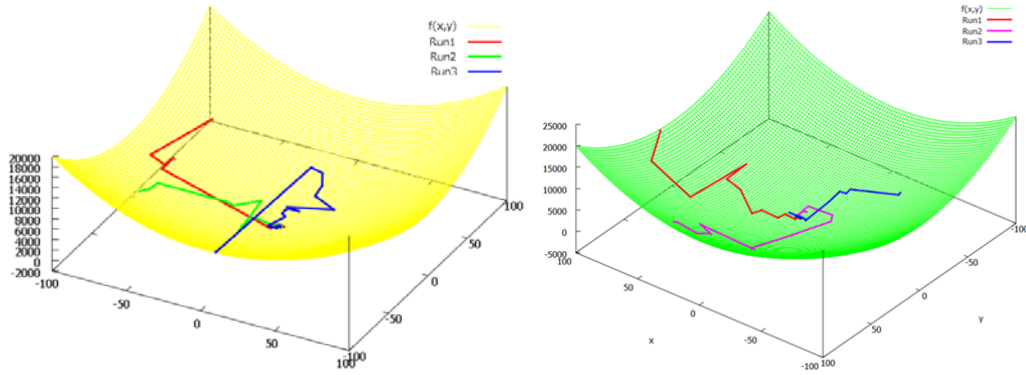


Figure 3-4 Simulated annealing Method 1 (Left: $f(x,y)$, Right: $g(x,y)$)

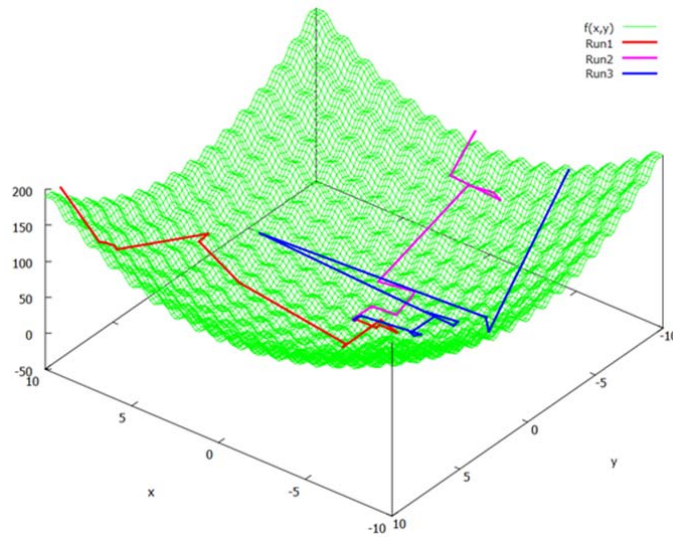


Figure 3-5 Simulated annealing Method 2 $g(x,y)$

[GA]

The Table 3-6 shows the program test result. Figure 3-6 and Figure 3-7 show the optimization route. The points shows the generated all the individuals for each run.

Table 3-6 Optimization result (GA)

function	run	x	y	f	Calculation Time (sec)
f	Run1	0.0001154	-0.0003790	-9.9999998	0.046
f	Run2	0.0010711	-0.0020444	-9.9999947	0.047
f	Run3	-0.0000290	-0.0026327	-9.9999931	0.023

g	Run1	-0.0001913	-0.0003227	-9.9999911	0.068
g	Run2	-0.0003235	0.0001053	-9.9999927	0.071
g	Run3	-0.0001101	0.0001312	-9.9999981	0.097

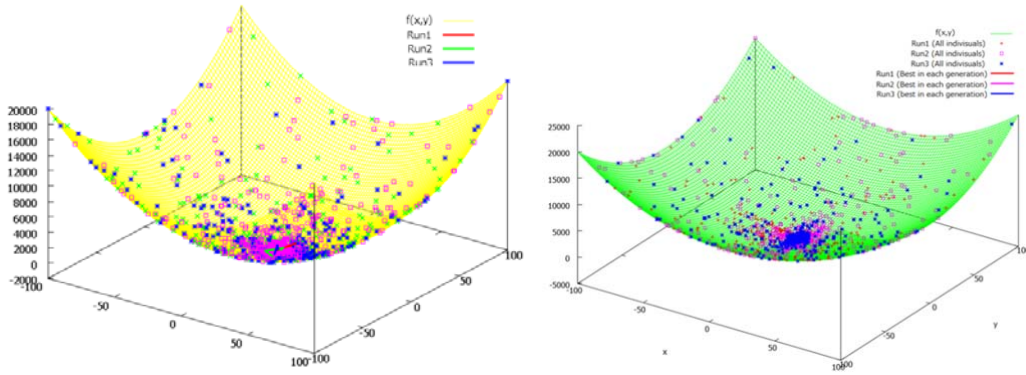


Figure 3-6 Genetic Algorithm 1 (Left; $f(x,y)$, Right; $g(x,y)$)

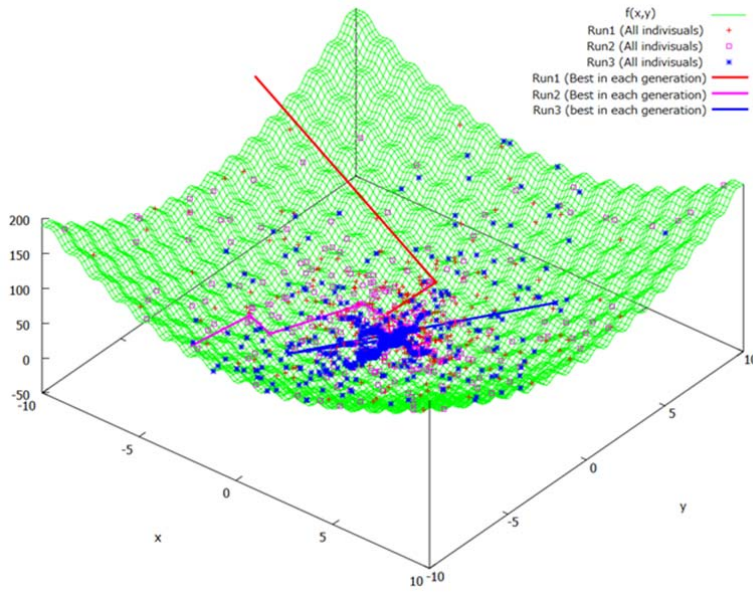


Figure 3-7 Genetic Algorithm 2 $g(x,y)$

[SGM]

The Table 3-7 shows the program test result. Figure 3-8 and Figure 3-9 show the optimization route. Program was kept running until it converges to the solution by changing initial values for each run. For simple function, SGM can calculate solution very quickly, but when the function has lots of local extremes, SGM cannot calculate the solution.

Table 3-7 Optimization result (SGM)

function	run	x	y	f	Calculation Time (sec)
f	Run1	0.0000134	-0.0001275	-10.0000000	0.013
f	Run2	-0.0000012	0.0000004	-10.0000000	0.013
f	Run3	-0.0000000	0.0000000	-10.0000000	0.013
g	Run1	0.0000009	-0.0000009	-10.0000000	0.111
g	Run2	0.0001295	-0.0000000	-9.9999989	0.096
g	Run3	0.0000012	0.0000005	-10.0000000	0.136

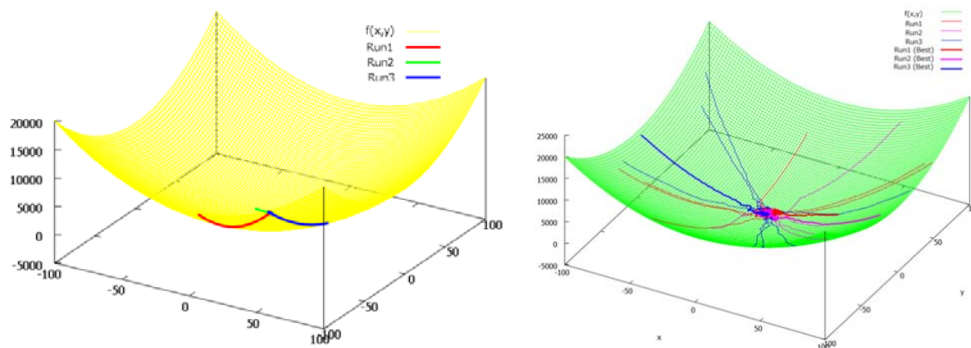


Figure 3-8 Steepest Gradient Method 1 (Left: $f(x,y)$, Right: $g(x,y)$)

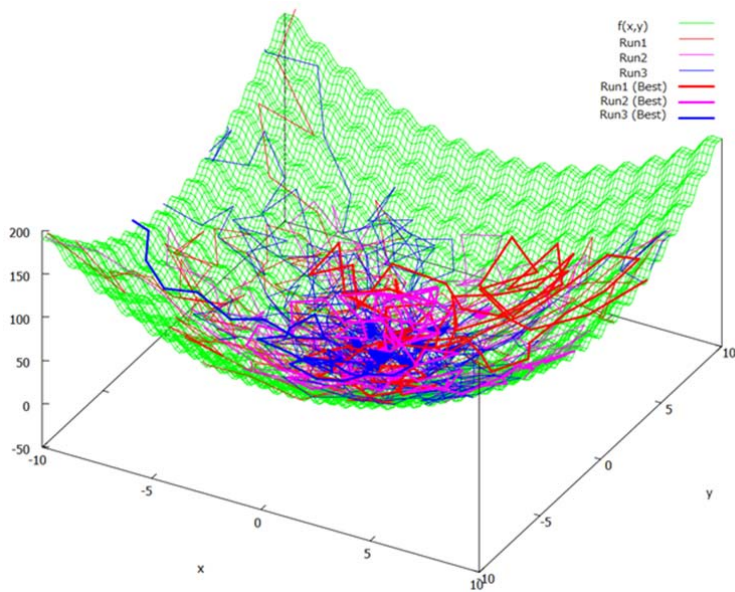


Figure 3-9 Steepest Gradient Method 2 $g(x,y)$

4 Methodology - Calculation Mesh

The auto-meshing program for the followings hull types are prepared for this study.

- Conventional TLP – Circular Column
- Conventional TLP – Rectangular Column
- MOSES SSIP TLP – Circular Column
- MOSES SSIP TLP – Rectangular Column
- Classic MOSES TLP

Each hull type has the following calculation mesh.

- Quarter Panel model
This is used for hydrodynamic calculation.
- Full panel model
This is used for mapping of hydrodynamic pressure load.
- Structural Beam model
This is used for strength calculation.

4.1 Conventional TLP – Circular Column

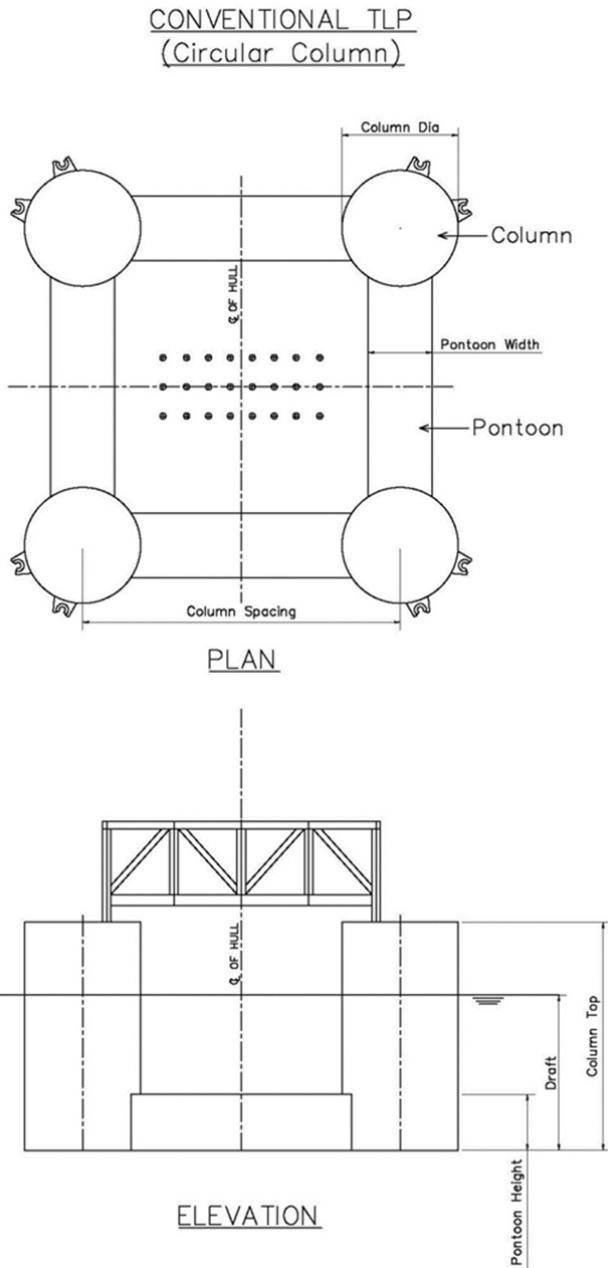


Figure 4-1 Main dimensions of Conventional TLP – Circular Column

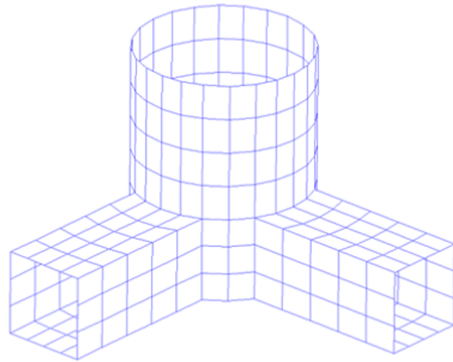


Figure 4-2 Quarter Panel Model for CTLP

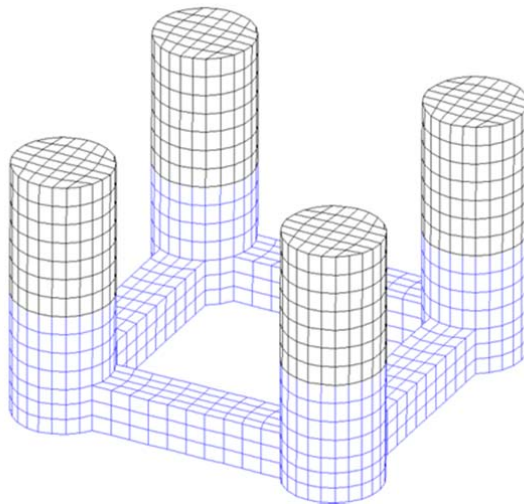


Figure 4-3 Full Panel Model for CTLP

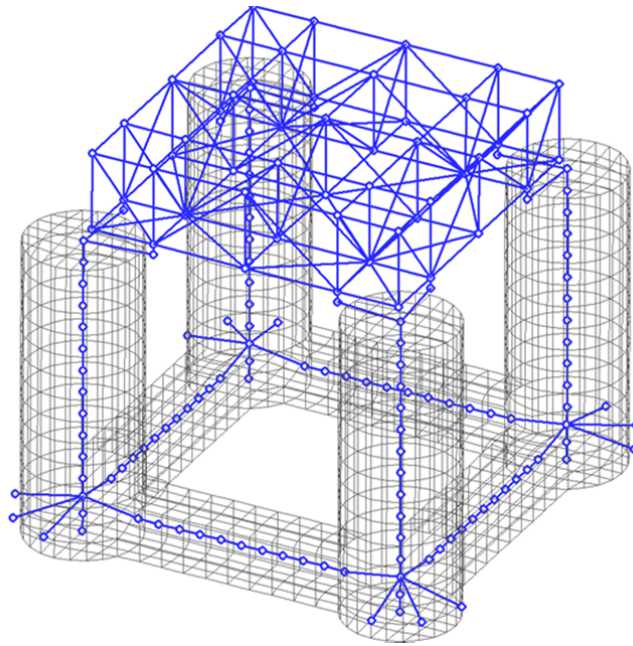


Figure 4-4 Structural Beam Model for CTLP

4.2 Conventional TLP – Rectangular Column

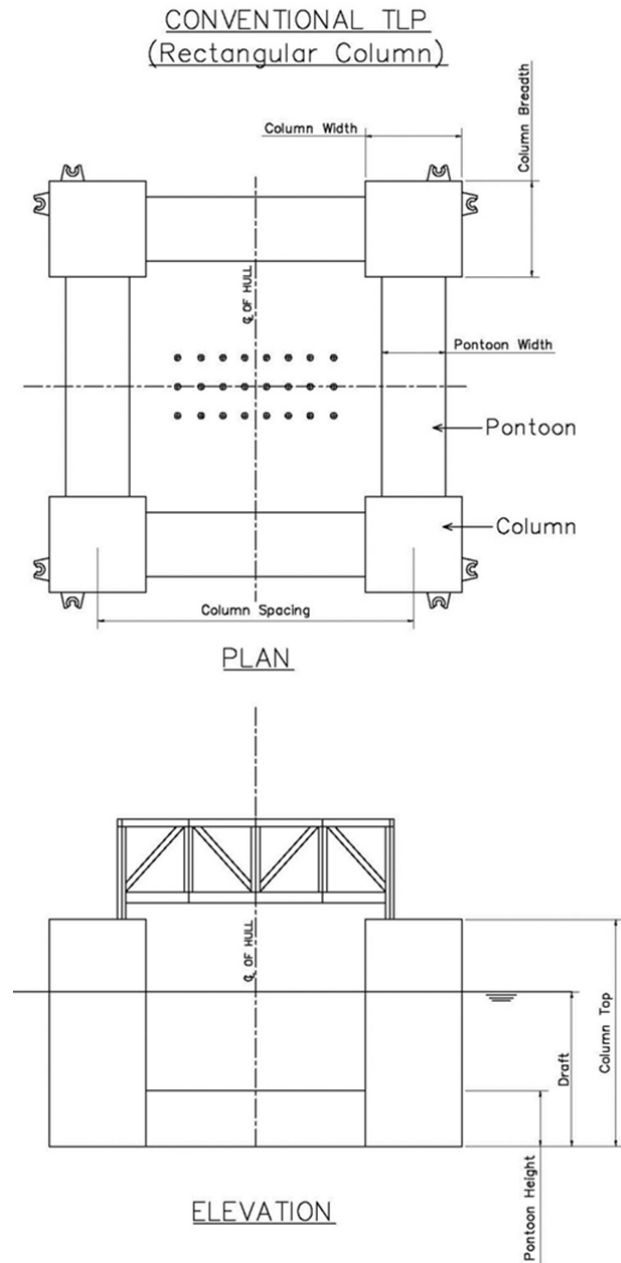


Figure 4-5 Main dimensions of Conventional TLP – Rectangular Column

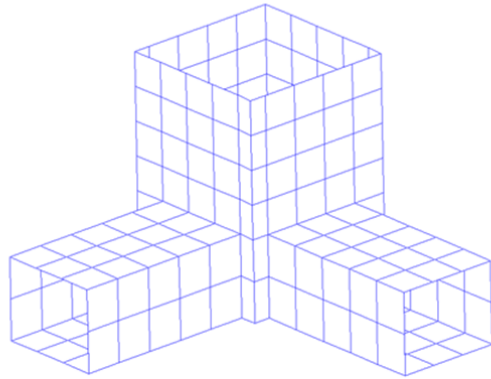


Figure 4-6 Quarter Panel Model for CTLP (Rectangular Column)

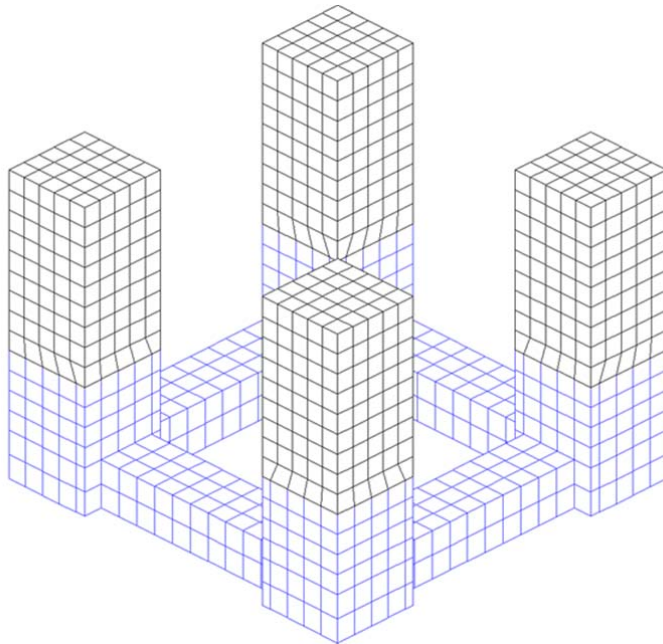


Figure 4-7 Full Panel Model for CTLP (Rectangular Column)

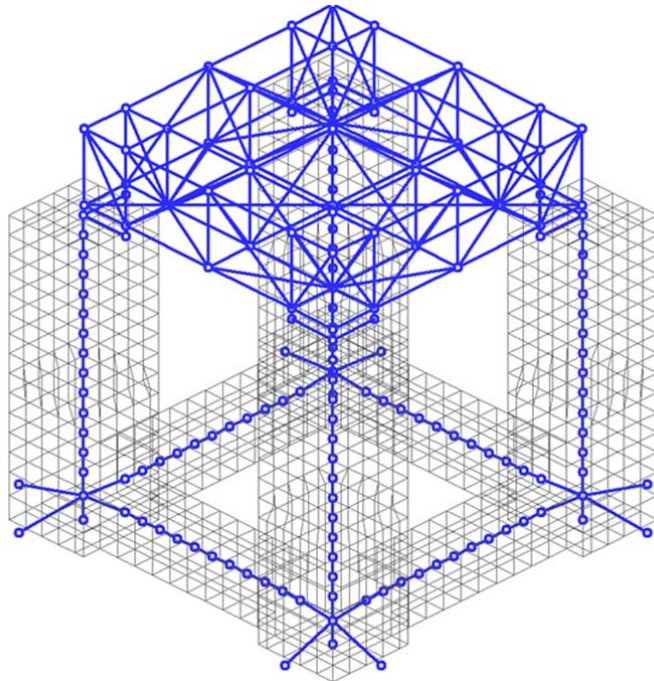


Figure 4-8 Structural Beam Model for CTLP (Rectangular Column)

4.3 MOSES SSIP TLP –Rectangular Column

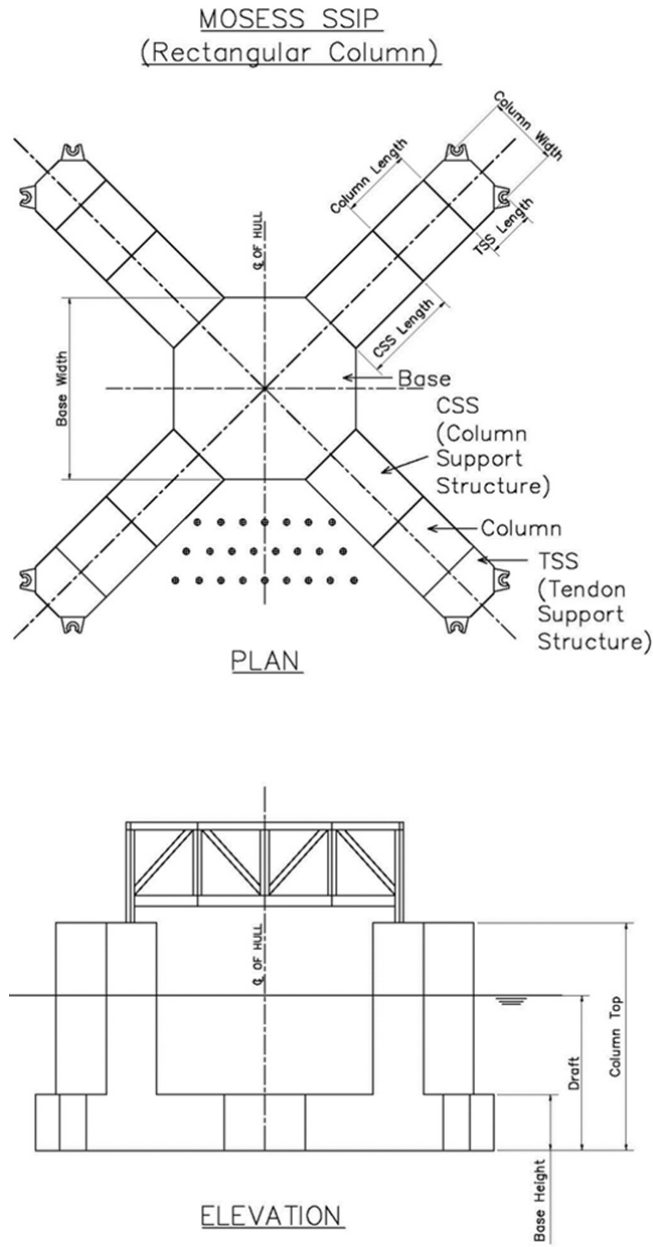


Figure 4-9 Main dimensions of MOSES SSIP TLP –Rectangular Column

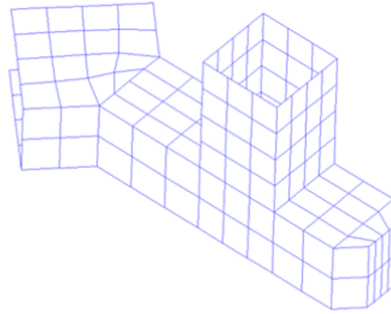


Figure 4-10 Quarter Panel Model for MOSES SSIP

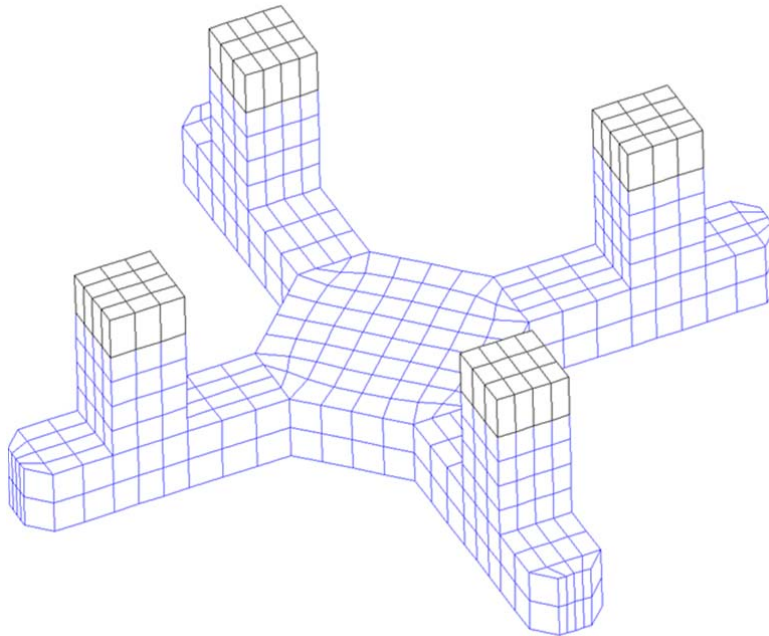


Figure 4-11 Full Panel Model for MOSES SSIP

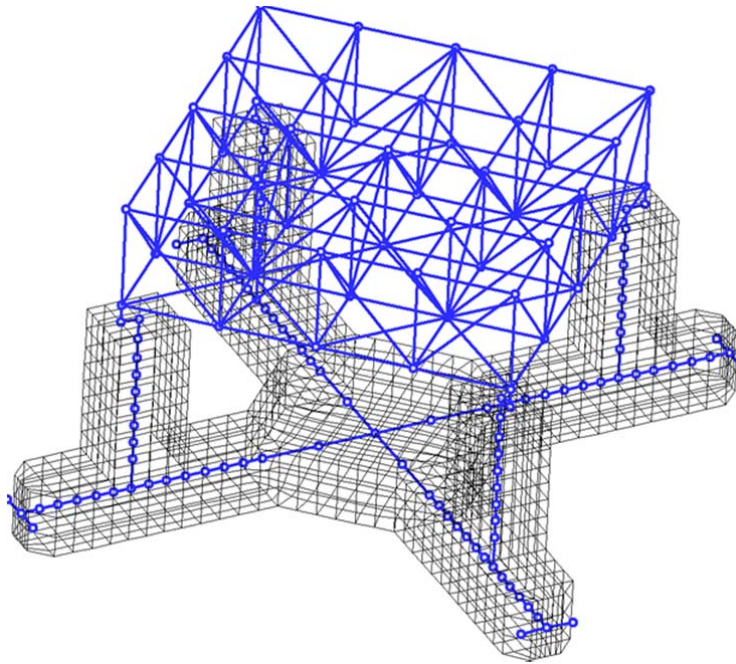


Figure 4-12 Structural Beam Model for MOSES SSIP

4.4 MOSES SSIP TLP – Circular Column

MOSESS SSIP
(Circular Column)

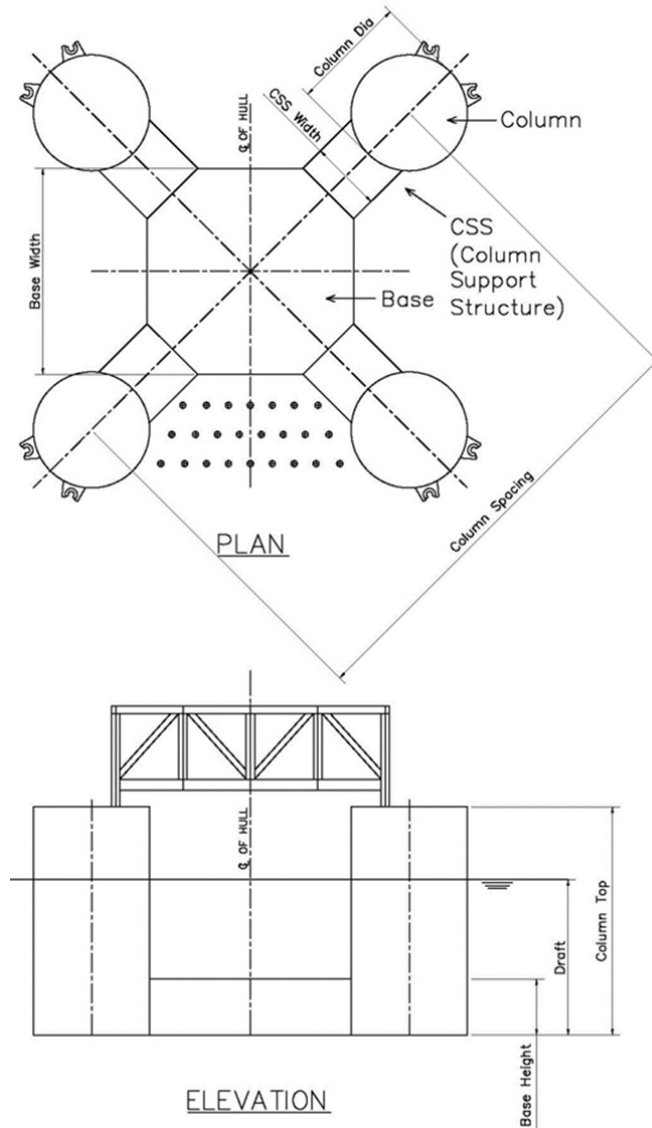


Figure 4-13 Main dimensions of MOSES SSIP TLP –Circular Column

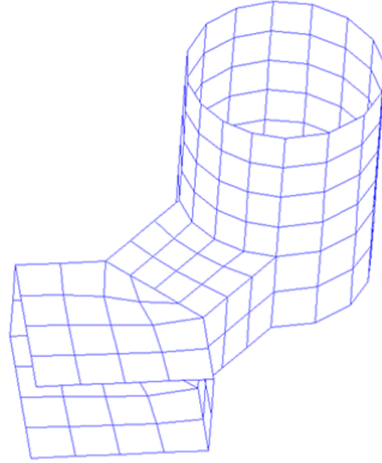


Figure 4-14 Quarter Panel Model for MOSES SSIP (Circular Column)

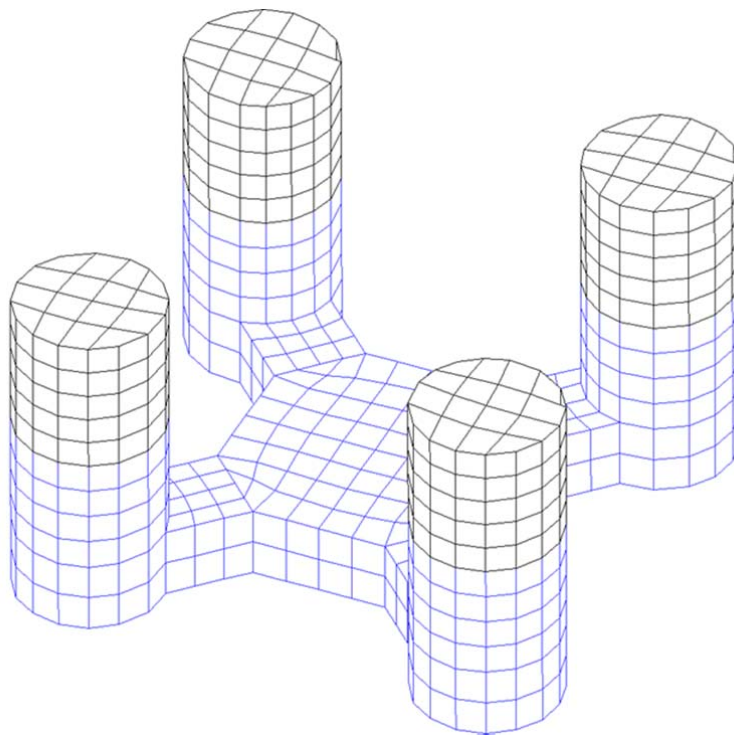


Figure 4-15 Full Panel Model for MOSES SSIP (Circular Column)

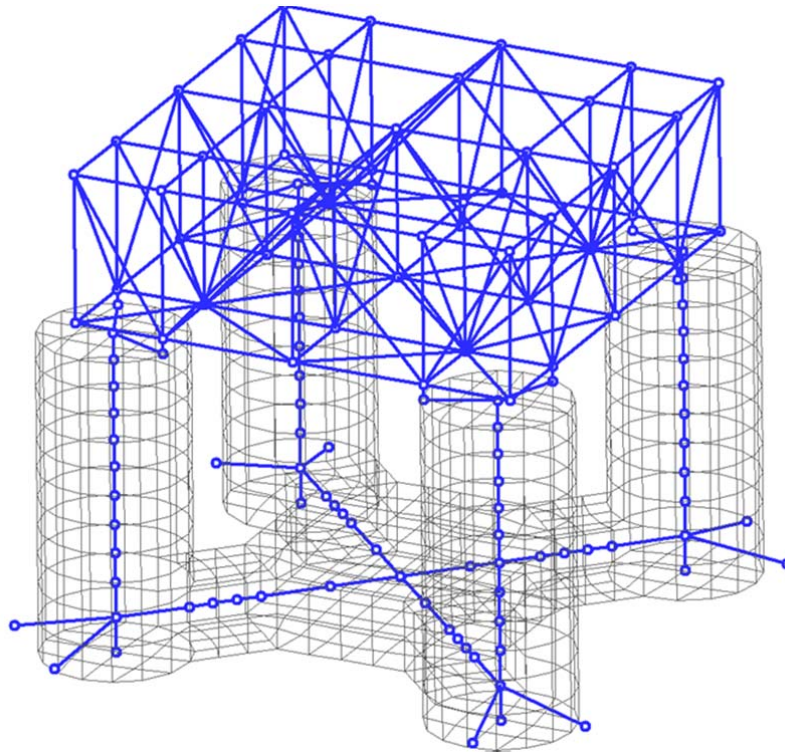


Figure 4-16 Structural Beam Model for MOSES SSIP (Circular Column)

4.5 Classic MOSES TLP

Classic MOSESS

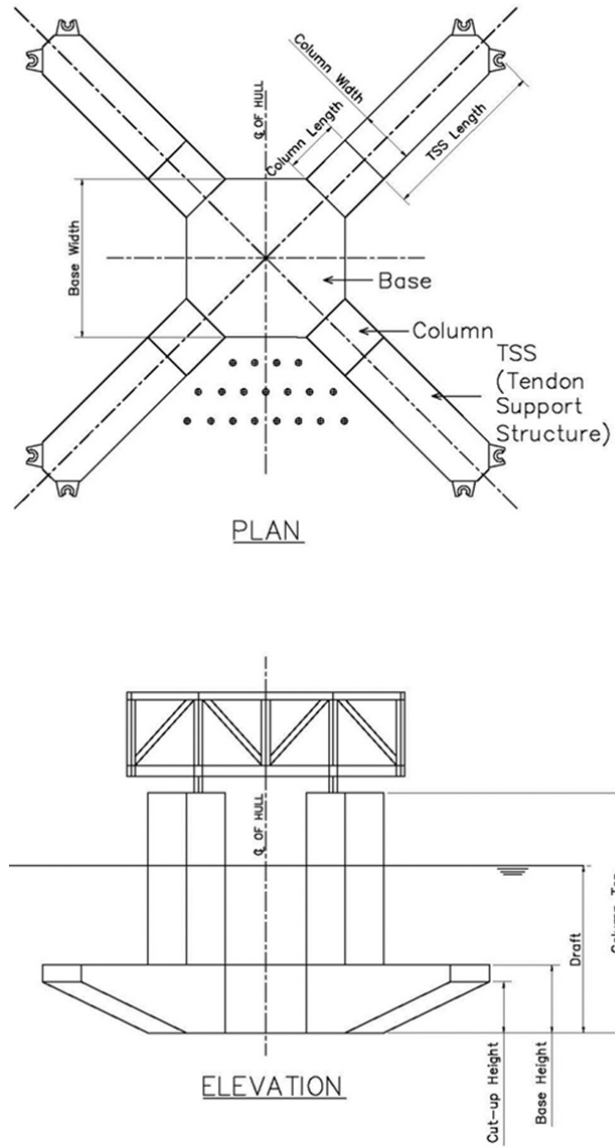


Figure 4-17 Main dimensions of Classic MOSES TLP

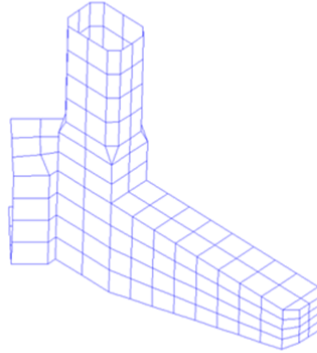


Figure 4-18 Quarter Panel Model for Classic MOSES

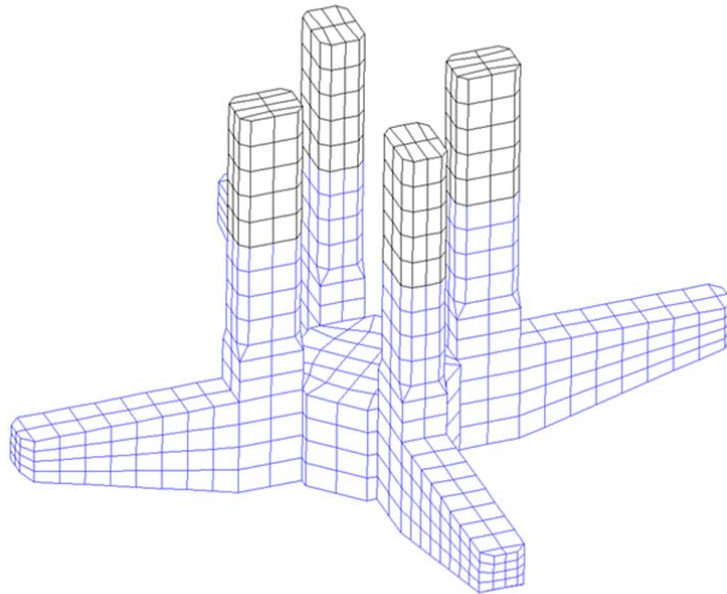


Figure 4-19 Full Panel Model for Classic MOSES

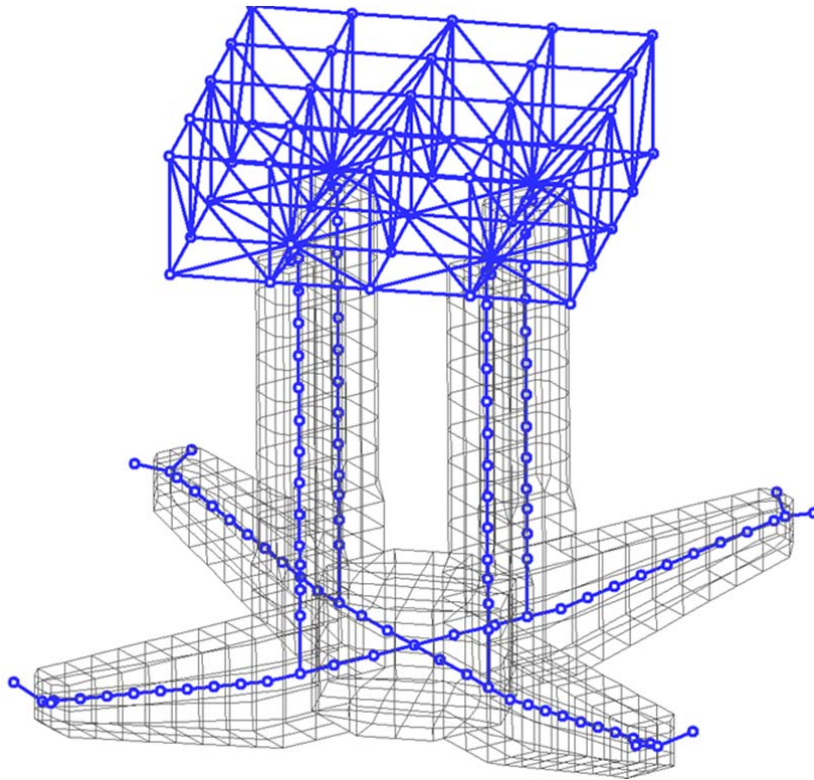


Figure 4-20 Structural Beam Model for Classic MOSES

5 Methodology - Hydrodynamic Calculation

In this section, hydrodynamic calculation method is explained and the calculation result of the program is compared with commercial software for verification. Explanation of the hydrodynamic calculation is based on the reference [5-1][5-2][5-3][5-4].

5.1 Flow Field around a Floating Body

Flow field surrounded by the floating body which oscillates in the wave is described in this section. Water depth is assumed to be infinity.

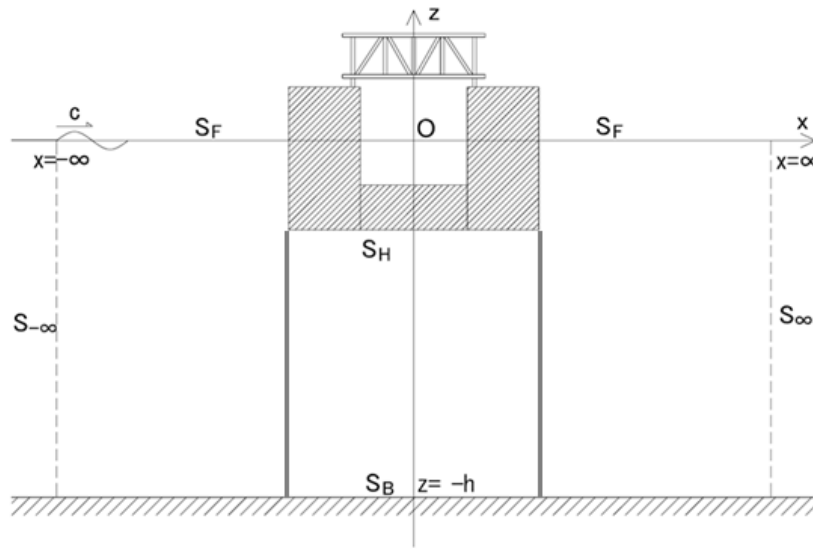


Figure 5-1 Flow Field around a Floating Body [5-1]

Fluid field is surrounded by, wetted surface of floating body S_H , free-surface S_F , sea bottom S_B , control surface at infinity S_∞ . Assuming these boundary conditions are all linear and adopting potential theory, the governing equation is expressed as follows:

$$[L] \quad \nabla^2 \Phi = 0 \quad z < 0 \quad (\text{Eq. 5-1})$$

$$[SF] \quad \frac{\partial^2 \Phi}{\partial t^2} + g \frac{\partial \Phi}{\partial z} = 0 \quad z = 0 \quad (\text{Eq. 5-2})$$

$$[SB] \quad \frac{\partial \Phi}{\partial z} = 0 \quad z = -h \quad (\text{Eq. 5-3})$$

$$[\text{SH}] \quad \frac{\partial \Phi}{\partial n} = \mathbf{V} \cdot \mathbf{n} \quad \text{on } S_H \quad (\text{Eq. 5-4})$$

$$[\text{A}] \quad \frac{\partial \Phi}{\partial t} = 0, \Phi = 0 \quad \text{at } t = 0 \quad (\text{Eq. 5-5})$$

Incident wave is assumed coming from the β direction (β radians counter-clockwise from x-axis). The amplitude of incident wave is defined as ζ . Assuming the flow field is periodically varying at the angular frequency ω driven by incident wave as external force, the velocity potential which meet (5-6) - (5-7) is expressed as follows:

$$\Phi = \text{Re}[\phi(x, y, z)e^{i\omega t}] \quad (\text{Eq. 5-6})$$

$$\phi(x, y, z) = \frac{g\zeta}{i\omega} \{ \phi_0(x, y, z) + \phi_7(x, y, z) \} + \sum_{j=1}^6 i\omega X_j \phi_j(x, y, z) \quad (\text{Eq. 5-7})$$

ϕ_0 is the velocity potential of incident wave and if the water depth can be assumed as infinity, ϕ_0 is as follows. ($K=\omega^2/g$);

$$\phi_0 = e^{-Kz+iK(x\cos\beta+y\sin\beta)} \quad (\text{Eq. 5-8})$$

ϕ_7 is the scattering potential. ϕ_j ($j=1-6$) are the radiation potential caused by the j-mode motion ($j=1$; Surge, $j=2$; Sway, $j=3$; Heave, $j=4$; Roll, $j=5$; Pitch, $j=6$; Yaw) of floating body. X_j is the complex j-mode motion amplitude of floating body. These velocity potential satisfy the following equation:

$$[\text{L}] \quad \nabla^2 \phi_j = 0 \quad z < 0 \quad (\text{Eq. 5-9})$$

$$[\text{F}] \quad \frac{\partial^2 \phi_j}{\partial t^2} + g \frac{\partial \phi_j}{\partial z} = 0 \quad z = 0 \quad (\text{Eq. 5-10})$$

$$[\text{B}] \quad \frac{\partial \phi_j}{\partial z} = 0 \quad z = -h \quad (\text{Eq. 5-11})$$

$$[\text{A}] \quad \frac{\partial \phi_j}{\partial n} = n_j \quad \text{on } S_H \quad (\text{Eq. 5-12})$$

$$\frac{\partial}{\partial n}(\phi_0 + \phi_7) = 0 \quad (\text{Eq. 5-13})$$

n_j is the j component of the normal vector and positive direction is from surface to fluid internal.

$$(n_1, n_2, n_3) = \mathbf{n} \quad (\text{Eq. 5-14})$$

$$(n_4, n_5, n_6) = \mathbf{r} \times \mathbf{n}$$

5.2 Integral Equation for the velocity potential

By applying Green's integral law, the velocity potential takes the following form. G is the Green function. P is the point on surface of floating body and Q is the arbitrary point.

$$\phi_j(P) = \iint_S \left\{ \frac{\partial \phi_j(Q)}{\partial n_Q} G(P; Q) + \phi_j(Q) \frac{\partial G(P; Q)}{\partial n_Q} \right\} dS(Q) \quad (\text{Eq. 5-15})$$

As the right hand of (4 15) is 0 on any boundary except S_H , ϕ_j is expressed as follows:

$$\begin{aligned} \frac{1}{2} \phi_j(P) &= \iint_S \phi_j(Q) \frac{\partial G(P; Q)}{\partial n_Q} dS(Q) \\ &= \begin{cases} \iint_S n_j(Q) G(P; Q) dS(Q) & j = 1 \sim 6 \\ \phi_0(P) & j = D \end{cases} \end{aligned} \quad (\text{Eq. 5-16})$$

Assuming water depth is large, the free-surface Green function takes the following form.

$$G(P; Q) = \frac{1}{4\pi} \left[-\left(\frac{1}{r} + \frac{1}{r_1} \right) + G_w(X, Y) \right] \quad (\text{Eq. 5-17})$$

$$r = \sqrt{(x - \xi)^2 + (y - \eta)^2 + (z - \zeta)^2} \quad (\text{Eq. 5-18})$$

$$r = \sqrt{(x - \xi)^2 + (y - \eta)^2 + (z - \zeta)^2} \quad (\text{Eq. 5-19})$$

$$G_W(X, Y) = -2K\hat{G}(X, Y) \quad (\text{Eq. 5-20})$$

$$X = KR = K\sqrt{(x - \xi)^2 + (y - \eta)^2} \quad (\text{Eq. 5-21})$$

$$Y = K(z + \zeta) \quad (\text{Eq. 5-22})$$

5.3 Numerical solution of Integral equation

Boundary element method is adopted in this section. By modeling the surface of floating body as number N of panel, the integral equation can be discretized as follows.

$$\begin{aligned} & 2\pi\phi_j(P_m) + \sum_{n=1}^N \phi_j(Q_n) \left[-D_{mn} + \left\{ \frac{\partial}{\partial n_Q} G_W(P_m, Q_n) \right\} \Delta S_n \right] \\ & = \begin{cases} \sum_{n=1}^N n_j(Q_n) [-S_{mn} + G_W(P_m, Q_n) \Delta S_n] & m = 1 \sim N \\ 4\pi\phi_0(P_m) & \end{cases} \quad (\text{Eq. 5-23}) \end{aligned}$$

$$D_{mn} = \iint_{S_n} \frac{\partial}{\partial n_Q} \left(\frac{1}{r} + \frac{1}{r_1} \right) dS(Q) \quad (\text{Eq. 5-24})$$

$$S_{mn} = \iint_{S_n} \left(\frac{1}{r} + \frac{1}{r_1} \right) dS(Q) \quad (\text{Eq. 5-25})$$

Free-surface Green function is calculated as follows:

$$G_W(P; Q) = -K\hat{G}(X, Y) \quad (\text{Eq. 5-26})$$

$$\frac{\partial}{\partial n_Q} G_W(P; Q) = -2K^2 \left[\frac{n_x(\xi - x) + n_y(\eta - y)}{R} \frac{\partial \hat{G}}{\partial X} + n_z \frac{\partial \hat{G}}{\partial Y} \right] \quad (\text{Eq. 5-27})$$

$$G(X, Y) = R_0(X, Y) - i\pi e^{-Y} J_0(X) \quad (\text{Eq. 5-28})$$

$$\frac{\partial \hat{G}}{\partial X} = R_1(X, Y) + i\pi e^{-Y} J_1(X) \quad (\text{Eq. 5-29})$$

$$\frac{\partial \hat{G}}{\partial Y} = -\frac{1}{\sqrt{X^2 + Y^2}} - \hat{G}(X, Y) \quad (\text{Eq. 5-30})$$

For diffraction problem, ϕ_0 can be expressed as follows;

$$\phi_0(P) = \phi_0^Z + \phi_0^N + i(\phi_0^X + \phi_0^Y) \quad (\text{Eq. 5-31})$$

$$\phi_0^X = e^{-Kz} \sin(Kx \cos \beta) \cos(Ky \sin \beta) \quad (\text{Eq. 5-32})$$

$$\phi_0^Y = e^{-Kz} \cos(Kx \cos \beta) \sin(Ky \sin \beta) \quad (\text{Eq. 5-33})$$

$$\phi_0^Z = e^{-Kz} \cos(Kx \cos \beta) \cos(Ky \sin \beta) \quad (\text{Eq. 5-34})$$

$$\phi_0^N = e^{-Kz} \sin(Kx \cos \beta) \sin(Ky \sin \beta) \quad (\text{Eq. 5-35})$$

5.4 Free-Surface Green Function

Assuming the water depth is large, and flow field is varying at the angular frequency of ω the equations which free-surface green function has to satisfy is expressed as follows;

$$\nabla^2 G = \delta(x - \xi) \delta(y - \eta) \delta(z - \zeta) \quad (\text{Eq. 5-36})$$

$$\frac{\partial G}{\partial z} + (K - i\mu)G = 0 \quad (\text{Eq. 5-37})$$

$$\frac{\partial G}{\partial z} \rightarrow 0 \quad \text{as } z \rightarrow 0 \quad (\text{Eq. 5-38})$$

The numerical method to calculate the free-surface Green functions is as follows. Depending on the values of X and Y, calculation methods varies considering its precision and efficiency;

- (A) X=0
- (B) Y=0
- (C) Y > 1.7 X and Y < 7.5
- (D) 0.25 X < Y < 1.7 X and R < 14
- (E) Y < 0.25 X and R < 14
- (F) Others

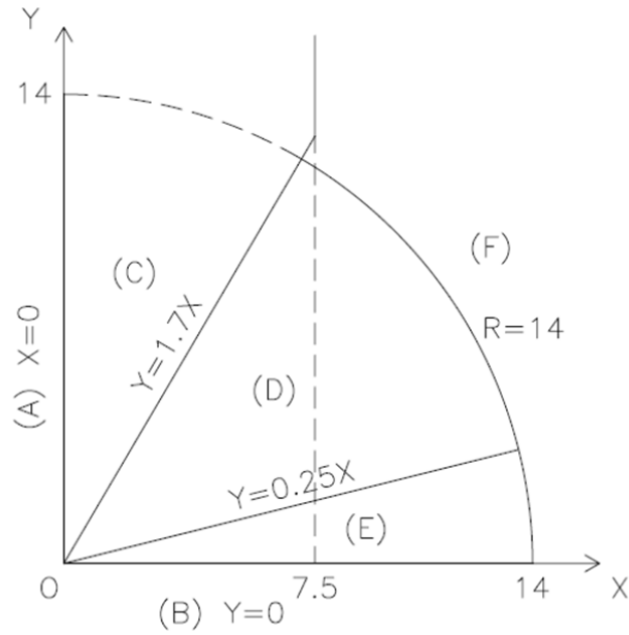


Figure 5-2 Method used for Green Function [5-1]

(A) $X=0$

$$R_0(0, Y) = e^{-Y} \text{Re}[E_1(-Y)] \quad (\text{Eq. 5-39})$$

$$R_1(0, Y) = 0 \quad (\text{Eq. 5-40})$$

(B) $Y=0$

$$R_0(X, 0) = -\frac{\pi}{2} \{H_0(X) + Y_0(X)\} \quad (\text{Eq. 5-41})$$

$$R_1(X, 0) = \frac{\pi}{2} \{H_1(X) + Y_1(X)\} - 1 \quad (\text{Eq. 5-42})$$

(C) $Y > 1.7 X$ and $Y < 7.5$

$$R_0(X, Y) = \sum_{n=0}^{\infty} \frac{\left(-\frac{X^2}{4}\right)^n}{(n!)^2} [F_n(Y) + e^{-Y} E_1(-Y)] \quad (\text{Eq. 5-43})$$

$$R_1(X, Y) = \frac{2}{X} \sum_{n=0}^{\infty} \frac{\left(-\frac{X^2}{4}\right)^n}{n!(n-1)!} [F_n(Y) + e^{-Y} E_1(-Y)] \quad (\text{Eq. 5-44})$$

$$F_n = F_{n-1} + \frac{(2n-2)!}{Y^{2n-1}} + \frac{(2n-1)}{Y^{2n}} \quad (n \geq 2) \quad (\text{Eq. 5-45})$$

$$F_0 = 0, F_1 = \frac{1}{Y} + \frac{1}{Y^2} \quad (\text{Eq. 5-46})$$

(D) $0.25 X < Y < 1.7 X$ and $R < 14$

$$R_0(X, Y) = -e^{-Y} f(X, Y) \quad (\text{Eq. 5-47})$$

$$f(X, Y) = \sum_{n=0}^{\infty} \frac{Y^n}{n!} I_n\left(\frac{X}{Y}\right) + \frac{\pi}{2} \{H_0(X) + Y_0(X)\} \quad (\text{Eq. 5-48})$$

$$R_1(X, Y) = -e^{-Y} f_X(X, Y) \quad (\text{Eq. 5-49})$$

$$f_X(X, Y) = \sum_{n=0}^{\infty} \frac{Y^{n-1}}{n!} I'_n\left(\frac{X}{Y}\right) - \frac{\pi}{2} \{H_1(X) + Y_1(X)\} + 1 \quad (\text{Eq. 5-50})$$

$$I_0(\xi) = \log\left(\frac{1 + \sqrt{\xi^2 + 1}}{\xi}\right) \quad (\text{Eq. 5-51})$$

$$I_1(\xi) = \sqrt{\xi^2 + 1} - \xi \quad (\text{Eq. 5-52})$$

$$nI_n(\xi) + \xi^2(n-1)I_{n-2}(\xi) = \sqrt{\xi^2 + 1} \quad n \geq 2 \quad (\text{Eq. 5-53})$$

$$I'_0(\xi) = -\frac{1}{\xi\sqrt{\xi^2 + 1}} \quad (\text{Eq. 5-54})$$

$$I'_1(\xi) = \frac{1}{\sqrt{\xi^2 + 1}} - 1 \quad (\text{Eq. 5-55})$$

$$nI'_n(\xi) + \xi(n-1)\{2I'_{n-2}(\xi) + \xi I'_{n-2}(\xi)\} = \frac{\xi}{\sqrt{\xi^2 + 1}} \quad n \geq 2 \quad (\text{Eq. 5-56})$$

(E) $Y < 0.25 X$ and $R < 14$

$$R_0(X, Y) = -e^{-Y} f(X, Y) \quad (\text{Eq. 5-57})$$

$$f(X, Y) = \frac{\pi}{2} Y_0(X) + J_0(X) \log\left(\frac{Y + r_1}{X}\right) - H_0(X) \frac{r_1}{X} + \sum_{n=0}^{\infty} \left\{ \frac{1}{(2n)!} U_{2n}(X, Y) + \frac{1}{(2n+1)!} U_{2n+1}(X, Y) \right\} \quad (\text{Eq. 5-58})$$

$$R_1(X, Y) = -e^{-Y} f_X(X, Y) \quad (\text{Eq. 5-59})$$

$$f_X(X, Y) = -\frac{\pi}{2} Y_1(X) - J_1(X) \log\left(\frac{Y + r_1}{X}\right) - J_0(X) \frac{Y}{X r_1} - \frac{\pi}{2} H_0(X) \frac{Y^2 r_1}{X^2} + \left\{ 1 - \frac{\pi}{2} H_1(X) \right\} \frac{r_1}{X} \quad (\text{Eq. 5-60})$$

$$+ \sum_{n=0}^{\infty} \left\{ \frac{1}{(2n)!} V_{2n}(X, Y) + \frac{1}{(2n+1)!} V_{2n+1}(X, Y) \right\} U_2(X, Y) = \frac{Y}{2} r_1 \quad (\text{Eq. 5-61})$$

$$U_{2n}(X, Y) = -\frac{2n-1}{2n} X^2 U_{2n-2}(X, Y) + \frac{Y^{2n-1}}{2n} r_1 \quad (\text{Eq. 5-62})$$

$$U_3(X, Y) = \frac{Y^2}{3} r_1 \quad (\text{Eq. 5-63})$$

$$U_{2n+1}(X, Y) = -\frac{2n}{2n+1} X^2 U_{2n-1}(X, Y) + \frac{Y^{2n}}{2n+1} r_1 \quad (\text{Eq. 5-64})$$

$$V_2(X, Y) = \frac{XY}{2r_1} \quad (\text{Eq. 5-65})$$

$$V_{2n}(X, Y) = -\frac{2n-1}{2n} \{X^2 V_{2n-2}(X, Y) + 2X U_{2n-2}(X, Y)\} + \frac{Y^{2n-1} X}{2n r_1} \quad (\text{Eq. 5-66})$$

$$V_3(X, Y) = \frac{XY^2}{3r_1} \quad (\text{Eq. 5-67})$$

$$V_{2n+1}(X, Y) = -\frac{2n}{2n+1} \{X^2 V_{2n-1}(X, Y) + 2X U_{2n-1}(X, Y)\} + \frac{Y^{2n} X}{2n+1 r_1} \quad (\text{Eq. 5-68})$$

(F) Others

$$R_0(X, Y) = - \sum_{n=1}^{\infty} \frac{1}{r_1^{n+1}} P_n \left(\frac{Y}{r_1} \right) - \pi e^{-Y} Y_0(X) \quad (\text{Eq. 5-69})$$

$$P_0(x) = 1, P_1(x) = x$$

$$P_n(x) = (2n - 1)xP_{n-1}(x) - (n - 1)^2 P_{n-2}(x) \quad (\text{Eq. 5-70})$$

$$R_1(X, Y) = X \sum_{n=1}^{\infty} \frac{1}{r_1^{n+3}} Q_n \left(\frac{Y}{r_1} \right) + \pi e^{-Y} Y_1(X) \quad (\text{Eq. 5-71})$$

$$Q_0(x) = 1, Q_1(x) = 3x$$

$$Q_n(x) = (2n + 1)xQ_{n-1}(x) - (n^2 - 1)Q_{n-2}(x) \quad (\text{Eq. 5-72})$$

5.5 Hydrodynamic force

Extracting the periodic-varying terms from linearized Bernoulli's pressure equation, the following equation is obtained.

$$p(x, y, z, t) = \text{Re}[\{p_D(x, y, z) + p_R(x, y, z) + p_S(x, y, z)\}e^{i\omega t}] \quad (\text{Eq. 5-73})$$

$$p_D(x, y, z) = -\rho g \zeta \phi_D(x, y, z) \quad (\text{Eq. 5-74})$$

$$p_R(x, y, z) = -\rho i \omega \sum_{j=1}^6 i \omega X_j \phi_j(x, y, z) \quad (\text{Eq. 5-75})$$

$$p_S(x, y, z) = -\rho g (X_3 + yX_4 - xX_5) \quad (\text{Eq. 5-76})$$

For radiation problem, the i component of the fluid force is expressed as follows. A_{ij} is the added mass coefficient and B_{ij} is the potential damping coefficient induced by the i -mode motion.

$$\begin{aligned} F_i &= - \iint_{S_H} p(x, y, z) n_i dS \\ &= \rho (i\omega)^2 \sum_{j=1}^6 X_j \iint_{S_H} \phi_j n_j dS \end{aligned} \quad (\text{Eq. 5-77})$$

$$\begin{aligned} &= \sum_{j=1}^6 [-(i\omega)^2 A_{ij} - (i\omega) B_{ij}] X_j \\ A_{ij} &= -\rho \iint_{S_H} \text{Re}[\phi_j(x, y, z)] n_i dS \end{aligned} \quad (\text{Eq. 5-78})$$

$$B_{ij} = \rho\omega \iint_{S_H} \text{Im}[\phi_j(x, y, z)]n_i dS \quad (\text{Eq. 5-79})$$

For diffraction problem, the i component of the fluid force is expressed as follows. E_i is the wave exciting force acting along i direction.

$$\begin{aligned} E_i &= - \iint_{S_H} p_D(x, y, z)n_i dS \\ &= \rho g \zeta \iint_{S_H} \text{Re}[\phi_D(x, y, z)]n_i dS \end{aligned} \quad (\text{Eq. 5-80})$$

5.6 Kochin Function and Wave Drift Forces

Kochin function for each mode of the fluid motion is expressed as follows:

$$\begin{aligned} H_j(K, \theta) &= \iint_{S_H} \left(\frac{\partial \phi_j}{\partial n} - \phi_j \frac{\partial}{\partial n} \right) e^{-Kz + iK(\xi \cos\theta + \eta \sin\theta)} dS \\ &= \sum_{n=1}^N \left[(n_j \phi_0)_n - \left(\phi_j \frac{\partial \phi_0}{\partial n} \right)_n \right] \Delta S_n \quad j = 1 \sim 6 \end{aligned} \quad (\text{Eq. 5-81})$$

$$\begin{aligned} H_7(K, \theta) &= - \iint_{S_H} \phi_D \frac{\partial}{\partial n} e^{-Kz + iK(\xi \cos\theta + \eta \sin\theta)} dS \\ &= - \sum_{n=1}^N \left(\phi_D \frac{\partial \phi_0}{\partial n} \right)_n \Delta S_n \end{aligned} \quad (\text{Eq. 5-82})$$

Assuming the floating body is double (x - y) symmetrical, the ϕ_0 can be expressed as follows:

$$\phi_0 = \phi_0^Z + \phi_0^N + i\{\phi_0^X + \phi_0^Y\} \quad (\text{Eq. 5-83})$$

$$\begin{aligned} \frac{\partial \phi_0}{\partial n} &= iK[n_x \cos\theta \phi_0^Z + n_y \sin\theta \phi_0^N - n_z \phi_0^X] \\ &\quad + iK[n_x \cos\theta \phi_0^N + n_y \sin\theta \phi_0^Z - n_z \phi_0^Y] \\ &\quad - iK[n_x \cos\theta \phi_0^X + n_y \sin\theta \phi_0^Y + n_z \phi_0^Z] \\ &\quad - iK[n_x \cos\theta \phi_0^Y + n_y \sin\theta \phi_0^X + n_z \phi_0^N] \end{aligned} \quad (\text{Eq. 5-84})$$

This Kochin function has the following relation to the wave exciting force and potential damping coefficient.

$$E_j = \rho g \zeta H_j(K, \beta) \quad (\text{Eq. 5-85})$$

$$B_{ij} = \frac{\rho \omega K}{4\pi} \int_0^{2\pi} \text{Re}[H_i(K, \theta) H_j^*(K, \theta)] d\theta \quad (\text{Eq. 5-86})$$

Wave drift force and moment are expressed as follows by using Kochin function.

$$\frac{F_x}{\rho g \zeta^2 L} = -\frac{KL}{8\pi} \int_0^{2\pi} |H(K, \theta)|^2 (\cos\beta + \cos\theta) d\theta \quad (\text{Eq. 5-87})$$

$$\frac{F_y}{\rho g \zeta^2 L} = -\frac{KL}{8\pi} \int_0^{2\pi} |H(K, \theta)|^2 (\sin\beta + \sin\theta) d\theta \quad (\text{Eq. 5-88})$$

$$\begin{aligned} \frac{M_z}{\rho g \zeta^2 L^2} = & -\frac{1}{8\pi} \int_0^{2\pi} \text{Im}[H'(K, \theta) H^*(K, \theta)] d\theta \\ & + \frac{1}{2KL} \text{Re}[H'(K, \beta + \pi)] \end{aligned} \quad (\text{Eq. 5-89})$$

$$H(K, \theta) = H_7(K, \theta) - KL \sum_{j=1}^6 \frac{X_j \epsilon_j}{\zeta} H_j(K, \theta) \quad (\text{Eq. 5-90})$$

5.7 Motion Equation for TLP

5.7.1 Motion Equation for TLP

In addition to added mass coefficient, wave damping coefficient and wave exciting force (those are described in previous subsection), mass coefficient, viscous damping coefficient, hydrodynamic restoring coefficient and tendon-and-TTR restoring coefficient constitute the motion equation of TLP. The motion equation takes the form of linear simultaneous complex equation. This equation is usually converted to non-dimensional form and solved.

$$\{M_{ij} + A_{ij}(\omega)\} \ddot{\mathbf{x}} + \{B_{ij}(\omega) + C_{ij}\} \dot{\mathbf{x}} + (K_{ij} + S_{ij}) \mathbf{x} = \mathbf{E}(\omega) \quad (\text{Eq. 5-91})$$

In this section, each coefficient and external force matrix can be described. The hull geometry of TLP is assumed to be symmetrical about x- and y-axis.

- Mass Matrix
 - o Platform Mass Matrix
 - o Platform Added Mass Matrix
 - o Tendon and Riser Mass Matrix
- Damping Matrix
 - o Wave Damping Matrix
 - o Viscous Damping Matrix
- Restoring Matrix
 - o Hydrostatic Restoring Matrix
 - o Tendon Restoring Matrix
 - o TTR Restoring Matrix
 - o SCR Restoring Matrix
- External Force
 - o Wave Exciting Force

5.7.2 Mass matrix

Mass matrix consists of the following components:

Table 5-1 Nondimensionalization of Mass Matrix

	$j = 1\sim 3$	$j = 4\sim 6$
$i = 1\sim 3$	ρV	ρVL
$i = 4\sim 6$	ρVL	ρVL^2

Mass matrix consists of the following components:

$$M_{ij} = \begin{pmatrix} m & 0 & 0 & 0 & mz_G & -my_G \\ 0 & m & 0 & -mz_G & 0 & mx_G \\ 0 & 0 & m & my_G & -mx_G & 0 \\ 0 & -mz_G & my_G & I_{XX} & I_{XY} & I_{XZ} \\ mz_G & 0 & -mx_G & I_{XY} & I_{YY} & I_{YZ} \\ -my_G & mx_G & 0 & I_{XZ} & I_{YZ} & I_{ZZ} \end{pmatrix} \quad (\text{Eq. 5-92})$$

Added Mass Matrix consists of the following components:

$$A_{ij} = \begin{pmatrix} A_{11} & 0 & 0 & 0 & A_{15} & 0 \\ 0 & A_{22} & 0 & A_{24} & 0 & 0 \\ 0 & 0 & A_{33} & 0 & 0 & 0 \\ 0 & A_{42} & 0 & A_{44} & 0 & 0 \\ A_{51} & 0 & 0 & 0 & A_{55} & 0 \\ 0 & 0 & 0 & 0 & 0 & A_{66} \end{pmatrix} \quad (\text{Eq. 5-93})$$

5.7.3 Damping matrix

Damping matrix can be non-dimensionalized by the following parameters:

Table 5-2 Nondimensionalization of Damping Matrix

	$j = 1\sim3$	$j = 4\sim6$
$i = 1\sim3$	$\rho V \sqrt{g/L}$	$\rho V \sqrt{gL}$
$i = 4\sim6$	$\rho V \sqrt{gL}$	$\rho VL \sqrt{gL}$

Potential Damping Matrix consists of the following components:

$$B_{ij} = \begin{pmatrix} B_{11} & 0 & 0 & 0 & B_{15} & 0 \\ 0 & B_{22} & 0 & B_{24} & 0 & 0 \\ 0 & 0 & B_{33} & 0 & 0 & 0 \\ 0 & B_{42} & 0 & B_{44} & 0 & 0 \\ B_{51} & 0 & 0 & 0 & B_{55} & 0 \\ 0 & 0 & 0 & 0 & 0 & B_{66} \end{pmatrix} \quad (\text{Eq. 5-94})$$

Viscous Damping Matrix consists of the following components:

$$C_{ij} = \begin{pmatrix} 0 & 0 & 0 & 0 & 0 & 0 \\ 0 & 0 & 0 & 0 & 0 & 0 \\ 0 & 0 & C_{33} & 0 & 0 & 0 \\ 0 & 0 & 0 & C_{44} & 0 & 0 \\ 0 & 0 & 0 & 0 & C_{55} & 0 \\ 0 & 0 & 0 & 0 & 0 & 0 \end{pmatrix} \quad (\text{Eq. 5-95})$$

$$C_{ii} = 2\alpha_i \sqrt{(M_{ii} + A_{ii})K_{ii}} \quad i = 3\sim5 \quad (\text{Eq. 5-96})$$

5.7.4 Restoring Matrix

Restoring matrix can be non-dimensionalized by the following parameters:

Table 5-3 Nondimensionalization of Restoring Matrix

	$j = 1\sim3$	$j = 4\sim6$
$i = 1\sim3$	$\rho V g/L$	$\rho V g$
$i = 4\sim6$	$\rho V g$	$\rho V g L$

Hydrostatic Restoring Matrix consists of the following components:

$$S_{ij} = \begin{pmatrix} 0 & 0 & 0 & 0 & 0 & 0 \\ 0 & 0 & 0 & 0 & 0 & 0 \\ 0 & 0 & S_{33} & 0 & 0 & 0 \\ 0 & 0 & 0 & S_{44} & 0 & S_{46} \\ 0 & 0 & 0 & 0 & S_{55} & S_{56} \\ 0 & 0 & 0 & 0 & 0 & 0 \end{pmatrix} \quad (\text{Eq. 5-97})$$

$$S_{33} = \rho g A_w \quad (\text{Eq. 5-98})$$

$$S_{44} = \rho g (S_{XX} + Vz_B) - mgz_G \quad (\text{Eq. 5-99})$$

$$S_{55} = \rho g (S_{YY} + Vz_B) - mgz_G \quad (\text{Eq. 5-100})$$

$$S_{46} = mgx_G \quad (\text{Eq. 5-101})$$

$$S_{56} = mgy_G \quad (\text{Eq. 5-102})$$

Tendon and TTR Restoring Matrix consists of the following components [5-5]. T is static tendon tension, L is tendon length, and λ is tendon stiffness. Tx, Ty, Tz are x, y, z-component of static tendon tension. (x_1, y_1, z_1) is tendon connection point coordinate, and (x_2, y_2, z_2) is tendon bottom coordinate.

$$K_{ij} = \begin{pmatrix} k_{11} & k_{12} & k_{13} & k_{14} & k_{15} & k_{16} \\ k_{21} & k_{22} & k_{23} & k_{24} & k_{25} & k_{26} \\ k_{31} & k_{32} & k_{33} & k_{34} & k_{35} & k_{36} \\ k_{41} & k_{42} & k_{43} & k_{44} & k_{45} & k_{46} \\ k_{51} & k_{52} & k_{53} & k_{54} & k_{55} & k_{56} \\ k_{61} & k_{62} & k_{63} & k_{64} & k_{65} & k_{66} \end{pmatrix} \quad (\text{Eq. 5-103})$$

$$k_{11} = \lambda \cos^2 \alpha + \frac{T}{L} \sin^2 \alpha \quad (\text{Eq. 5-104})$$

$$k_{21} = \left(\lambda - \frac{T}{L} \right) \cos \alpha \cos \beta = k_{12} \quad (\text{Eq. 5-105})$$

$$k_{22} = \lambda \cos^2 \beta + \frac{T}{L} \sin^2 \beta \quad (\text{Eq. 5-106})$$

$$k_{31} = \left(\lambda - \frac{T}{L} \right) \cos \alpha \cos \gamma = k_{13} \quad (\text{Eq. 5-107})$$

$$k_{32} = \left(\lambda - \frac{T}{L} \right) \cos \beta \cos \gamma = k_{23} \quad (\text{Eq. 5-108})$$

$$k_{33} = \lambda \cos^2 \gamma + \frac{T}{L} \sin^2 \gamma \quad (\text{Eq. 5-109})$$

$$k_{41} = k_{31}y_2 - k_{21}z_2 = k_{14} \quad (\text{Eq. 5-110})$$

$$k_{51} = k_{11}z_2 - k_{31}x_2 = k_{15} \quad (\text{Eq. 5-111})$$

$$k_{61} = k_{21}x_2 - k_{11}y_2 = k_{16} \quad (\text{Eq. 5-112})$$

$$k_{42} = k_{32}y_2 - k_{22}z_2 = k_{24} \quad (\text{Eq. 5-113})$$

$$k_{52} = k_{21}z_2 - k_{32}x_2 = k_{25} \quad (\text{Eq. 5-114})$$

$$k_{62} = k_{22}x_2 - k_{21}y_2 = k_{26} \quad (\text{Eq. 5-115})$$

$$k_{44} = k_{33}y_2^2 - 2k_{32}y_2z_2 + k_{22}z_2^2 \quad (\text{Eq. 5-116})$$

$$k_{54} = k_{31}y_2z_2 - k_{21}z_2^2 - k_{33}y_2x_2 + k_{32}x_2z_2 - T_x y \quad (\text{Eq. 5-117})$$

$$k_{45} = k_{31}y_2z_2 - k_{21}z_2^2 - k_{33}y_2x_2 + k_{32}x_2z_2 - T_y x \quad (\text{Eq. 5-118})$$

$$k_{64} = k_{32}x_2y_2 - k_{31}y_2^2 - k_{22}x_2z_2 + k_{21}y_2z_2 - T_x z \quad (\text{Eq. 5-119})$$

$$k_{46} = k_{32}x_2y_2 - k_{31}y_2^2 - k_{22}x_2z_2 + k_{21}y_2z_2 - T_z x \quad (\text{Eq. 5-120})$$

$$k_{55} = k_{11}z_2^2 - 2k_{31}x_2z_2 + k_{33}x_2^2 + T_x x + T_z z \quad (\text{Eq. 5-121})$$

$$k_{65} = -k_{11}y_2z_2 + k_{21}x_2z_2 + k_{31}x_2y_2 - k_{32}x_2^2 - T_y z \quad (\text{Eq. 5-122})$$

$$k_{56} = -k_{11}y_2z_2 + k_{21}x_2z_2 + k_{31}x_2y_2 - k_{32}x_2^2 - T_z y \quad (\text{Eq. 5-123})$$

$$k_{66} = k_{11}y_2^2 - 2k_{21}x_2y_2 + k_{22}x_2^2 + T_y y + T_x x \quad (\text{Eq. 5-124})$$

$$\cos\alpha = \frac{x_2 - x_1}{L} \quad (\text{Eq. 5-125})$$

$$\cos\beta = \frac{y_2 - y_1}{L} \quad (\text{Eq. 5-126})$$

$$\cos\gamma = \frac{z_2 - z_1}{L} \quad (\text{Eq. 5-127})$$

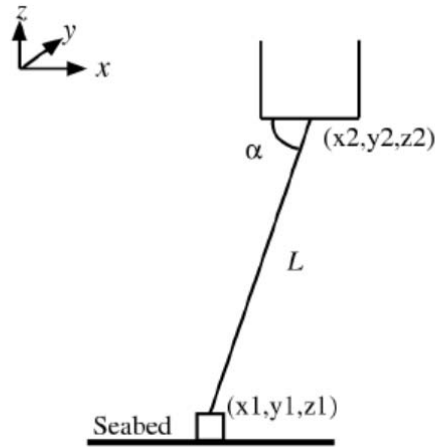


Figure 5-3 TLP element coordinate [5-5]

SCR Restoring Matrix consists of the following components [5-5]. S_h is horizontal spring constant, S_v is vertical spring constant, and α is horizontal angle of the line. P_x , P_y , P_z are x, y, z-component of pretension.

$$K_{ij} = \begin{pmatrix} k_{11} & k_{12} & 0 & k_{14} & k_{15} & k_{16} \\ k_{21} & k_{22} & 0 & k_{24} & k_{25} & k_{26} \\ 0 & 0 & k_{33} & k_{34} & k_{35} & k_{36} \\ k_{41} & k_{42} & k_{43} & k_{44} & k_{45} & k_{46} \\ k_{51} & k_{52} & k_{53} & k_{54} & k_{55} & k_{56} \\ k_{61} & k_{62} & k_{63} & k_{64} & k_{65} & k_{66} \end{pmatrix} \quad (\text{Eq. 5-128})$$

$$k_{11} = S_h \cos^2 \alpha_x \quad (\text{Eq. 5-129})$$

$$k_{21} = S_h \cos \alpha_x \cos \alpha_x = k_{12} \quad (\text{Eq. 5-130})$$

$$k_{22} = S_h \sin^2 \alpha_x \quad (\text{Eq. 5-131})$$

$$k_{33} = S_v \quad (\text{Eq. 5-132})$$

$$k_{41} = k_{31}y_2 - k_{21}z_2 = k_{14} \quad (\text{Eq. 5-133})$$

$$k_{51} = k_{11}z_2 - k_{31}x_2 = k_{15} \quad (\text{Eq. 5-134})$$

$$k_{61} = k_{21}x_2 - k_{11}y_2 = k_{16} \quad (\text{Eq. 5-135})$$

$$k_{42} = k_{32}y_2 - k_{22}z_2 = k_{24} \quad (\text{Eq. 5-136})$$

$$k_{52} = k_{21}z_2 - k_{32}x_2 = k_{25} \quad (\text{Eq. 5-137})$$

$$k_{62} = k_{22}x_2 - k_{21}y_2 = k_{26} \quad (\text{Eq. 5-138})$$

$$k_{43} = k_{33}y_2 - k_{32}z_2 = k_{34} \quad (\text{Eq. 5-139})$$

$$k_{53} = k_{31}z_2 - k_{33}x_2 = k_{35} \quad (\text{Eq. 5-140})$$

$$k_{63} = k_{32}x_2 - k_{31}y_2 = k_{36} \quad (\text{Eq. 5-141})$$

$$k_{44} = k_{43}y_2 - k_{42}z_2 + P_z z_2 + P_y y_2 \quad (\text{Eq. 5-142})$$

$$k_{54} = k_{14}z_2 - k_{43}x_2 - P_x y_2 \quad (\text{Eq. 5-143})$$

$$k_{45} = k_{14}z_2 - k_{43}x_2 - P_y x_2 \quad (\text{Eq. 5-144})$$

$$k_{64} = k_{24}x_2 - k_{41}y_2 - P_x z_2 \quad (\text{Eq. 5-145})$$

$$k_{46} = k_{24}x_2 - k_{41}y_2 - P_z x_2 \quad (\text{Eq. 5-146})$$

$$k_{55} = k_{51}z_2 - k_{53}x_2 + P_x x_2 + P_z z_2 \quad (\text{Eq. 5-147})$$

$$k_{65} = k_{52}x_2 - k_{43}y_2 - P_y z_2 \quad (\text{Eq. 5-148})$$

$$k_{56} = k_{52}x_2 - k_{43}y_2 - P_z y_2 \quad (\text{Eq. 5-149})$$

$$k_{66} = k_{62}x_2 - k_{61}y_2 + P_y y_2 + P_x x_2 \quad (\text{Eq. 5-150})$$

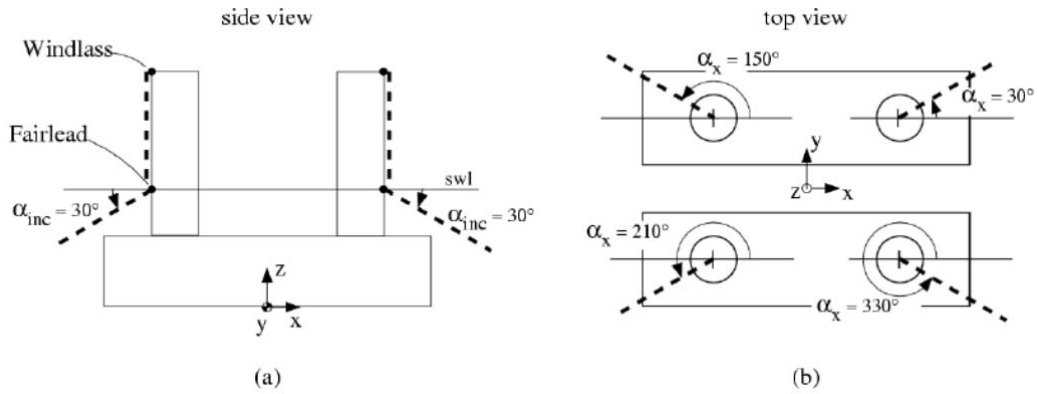


Figure 5-4 Catenary line coordinate [5-5]

5.7.5 External force

Wave exciting forces can be non-dimensionalized by the following parameters;

Table 5-4 Nondimensionalization of External Force

$i = 1\sim3$	$\rho Vg/L$
$i = 4\sim6$	ρVg

Wave exciting consists of the following components;

$$E_i = \begin{pmatrix} E_1 \\ E_2 \\ E_3 \\ E_4 \\ E_5 \\ E_6 \end{pmatrix} \quad (\text{Eq. 5-151})$$

5.8 Maximum Response Calculation

Motion, velocity, and accelerate response at point (x, y, z) are calculated from RAO by using the following equations.

Point Motion

$$X = X_1 + zX_5 - yX_6 \quad (\text{Eq. 5-152})$$

$$Y = X_2 + xX_6 - zX_4 \quad (\text{Eq. 5-153})$$

$$Z = X_3 + yX_4 - xX_5 \quad (\text{Eq. 5-154})$$

Velocity

$$U_x = i\omega(X_1 + zX_5 - yX_6) \quad (\text{Eq. 5-155})$$

$$U_y = i\omega(X_2 + xX_6 - zX_4) \quad (\text{Eq. 5-156})$$

$$U_z = i\omega(X_3 + yX_4 - xX_5) \quad (\text{Eq. 5-157})$$

Acceleration

$$A_x = -\omega^2(X_1 + zX_5 - yX_6) \quad (\text{Eq. 5-158})$$

$$A_y = -\omega^2(X_2 + xX_6 - zX_4) \quad (\text{Eq. 5-159})$$

$$A_z = -\omega^2(X_3 + yX_4 - xX_5) \quad (\text{Eq. 5-160})$$

Tendon tension response is calculated by the following equation. X_T is motion response at tendon connection point.

$$T = \lambda \vec{n} \cdot \vec{X}_T \quad (\text{Eq. 5-161})$$

$$\vec{n} = \frac{1}{L} (x_2 - x_1, \quad y_2 - y_1, \quad z_2 - z_1) \quad (\text{Eq. 5-162})$$

Standard deviation σ_x of a response $X(\omega)$ is calculated by the following equation.

$$\sigma_x^2 = \int X(\omega)^2 S(\omega) d\omega \quad (\text{Eq. 5-163})$$

$S(\omega)$ is irregular wave spectrum. In this study, the following JONSWAP spectrum is used as irregular wave model;

$$S(\omega) = \frac{\alpha g^2}{\omega^5} \exp\left\{-\beta\left(\frac{\omega_p}{\omega}\right)^4\right\} \gamma^{\exp\left\{\frac{(\omega/\omega_p-1)^2}{2\sigma^2}\right\}} \quad (\text{Eq. 5-164})$$

$$\alpha = \left(\frac{Hs\omega_p^2}{4g}\right)^2 \frac{1}{0.065\gamma^{0.803} + 0.135} \quad (\text{Eq. 5-165})$$

$$\sigma = \begin{cases} 0.07 & \text{for } \omega < \omega_p \\ 0.09 & \text{for } \omega > \omega_p \end{cases} \quad (\text{Eq. 5-166})$$

$$\omega_p = \frac{2\pi}{T_p} \quad (\text{Eq. 5-167})$$

$$\beta = 1.25 \quad (\text{Eq. 5-168})$$

The maximum response at short term sea states are calculated as follows.

$$X_{\max} = \sqrt{2 \ln N} \sigma_x \quad (\text{Eq. 5-169})$$

N=1000 is used for short term maximum response calculation.

5.9 Program Verification

For verification, the result of this hydrodynamic calculation module was compared with commercial software. As commercial software, Wadam in DNV Sesam Software Package was used. The calculation condition is as follows:

Hull Type	Conventional TLP
Main Dimension	
Column Diameter	20 m
Column Distance	60 m
Pontoon Width	10 m
Pontoon Height	10 m
Draft	30 m
Mass Properties	
Mass	36000 MT
VCG	15 m-WL
Tendon Properties	
Pretension	13,000 kN each
Axial Stiffness	19,800 kN/m each
Length	1,000m
TTR Properties	
Pretension	1,000 kN each
Axial Stiffness	1,000 kN/m each
Length	1,050 m
Offset/Setdown	(-71m, -71m, -5m)

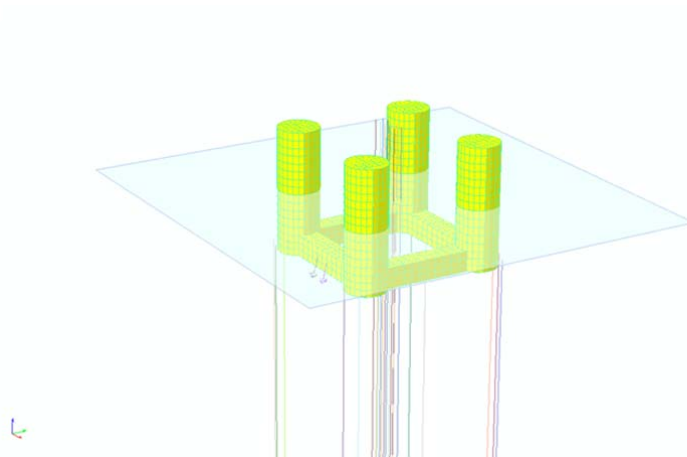


Figure 5-5 Wadam Calculation model

The calculated Response Amplitude Operators (RAOs) are in the Figure 5-4 – 5-27.

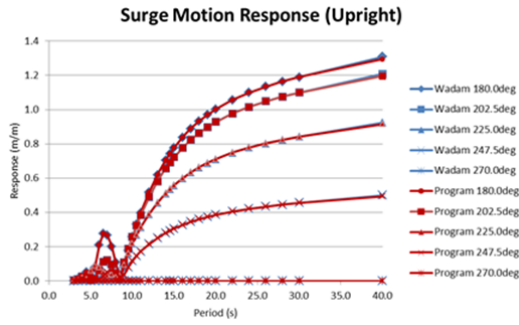


Figure 5-6 Surge motion RAO (Upright)

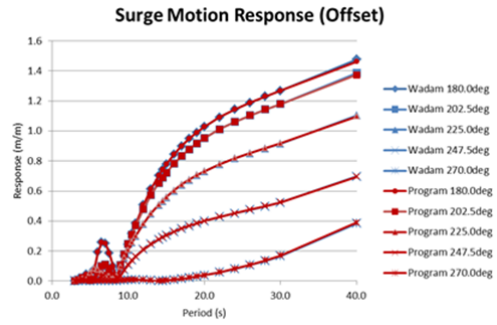


Figure 5-7 Surge motion RAO (Offset)

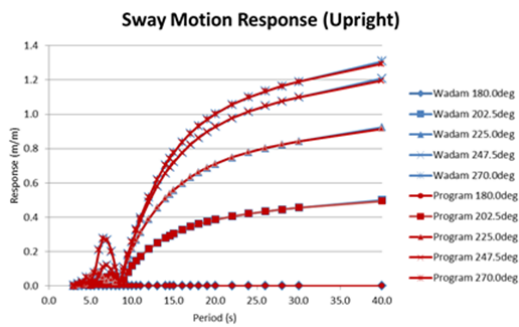


Figure 5-8 Sway motion RAO (Upright)

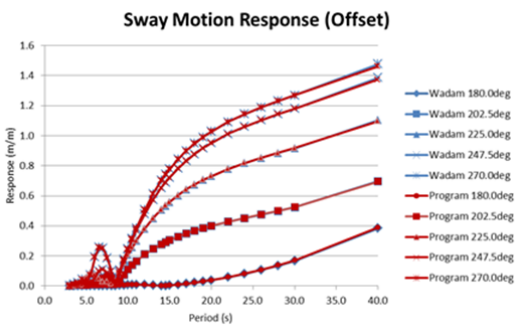


Figure 5-9 Sway motion RAO (Offset)

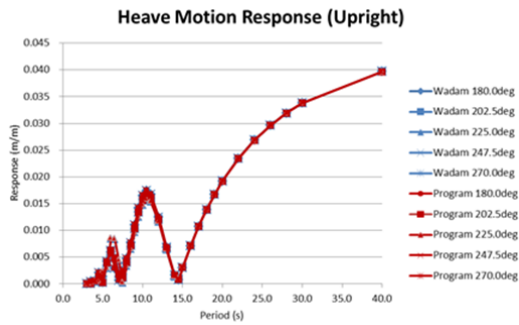


Figure 5-10 Heave motion RAO (Upright)

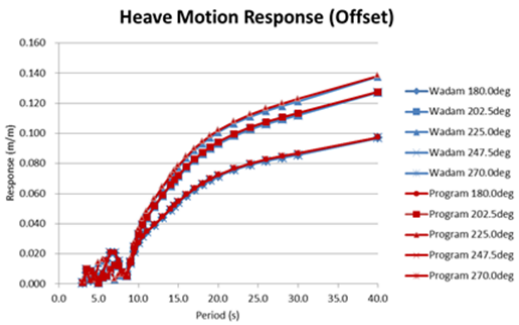


Figure 5-11 Heave motion RAO (Offset)

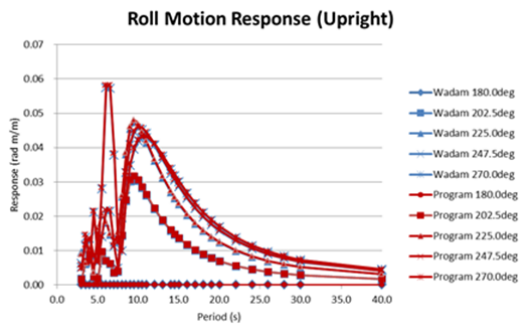


Figure 5-12 Roll motion RAO (Upright)

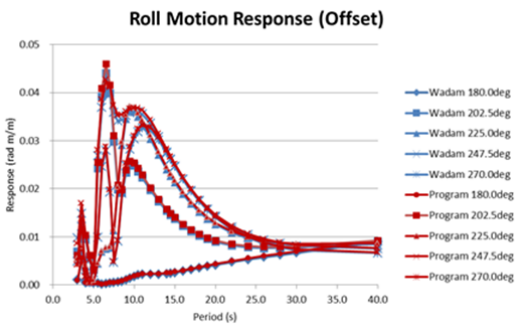


Figure 5-13 Roll motion RAO (Offset)

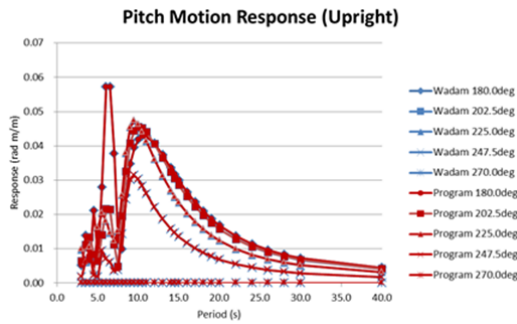


Figure 5-14 Pitch motion RAO (Upright)

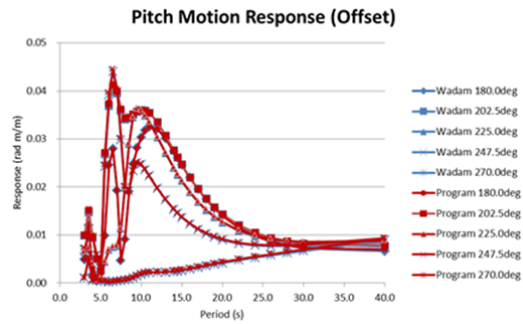


Figure 5-15 Pitch motion RAO (Offset)

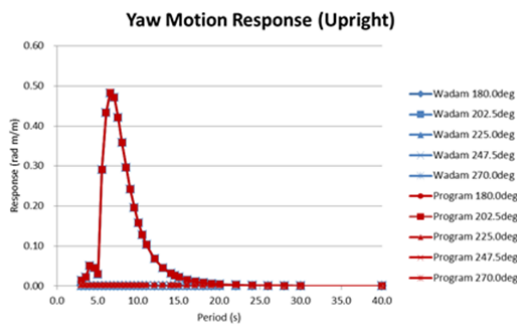


Figure 5-16 Yaw motion RAO (Upright)

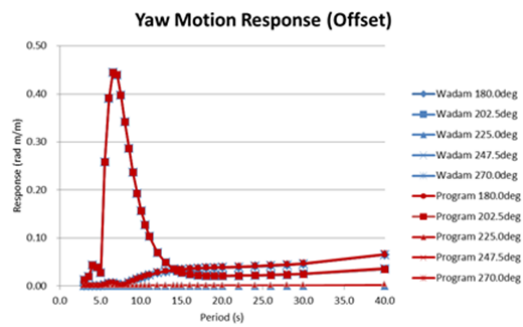


Figure 5-17 Yaw motion RAO (Offset)

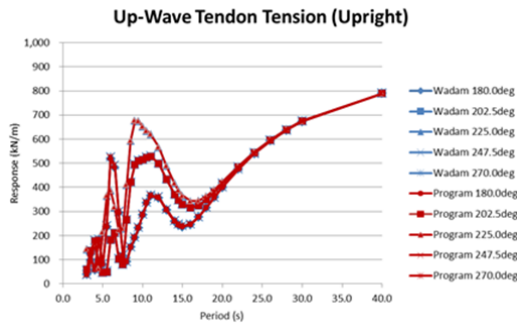


Figure 5-18 Tendon tension RAO (Upright)

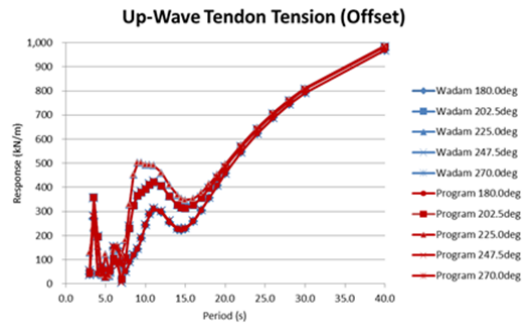


Figure 5-19 Tendon tension RAO (Offset)

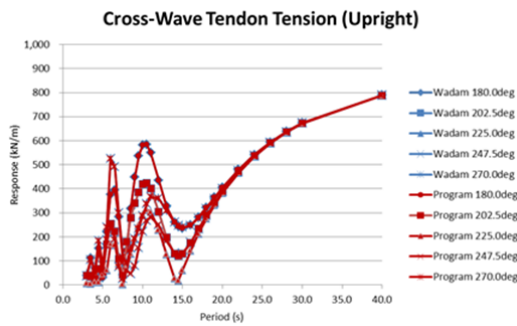


Figure 5-20 Tendon tension RAO (Upright)

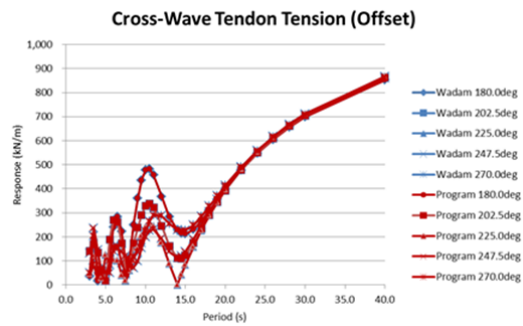


Figure 5-21 Tendon tension RAO (Offset)

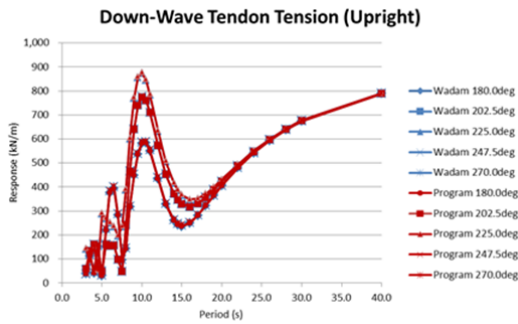


Figure 5-22 Tendon tension RAO (Upright)

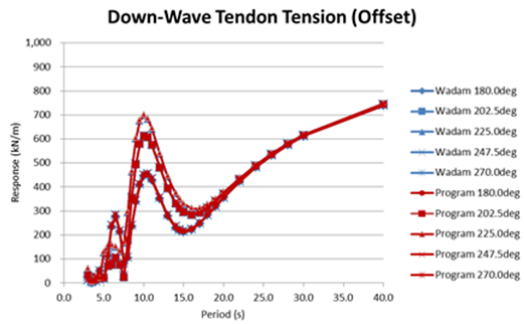


Figure 5-23 Tendon tension RAO (Offset)

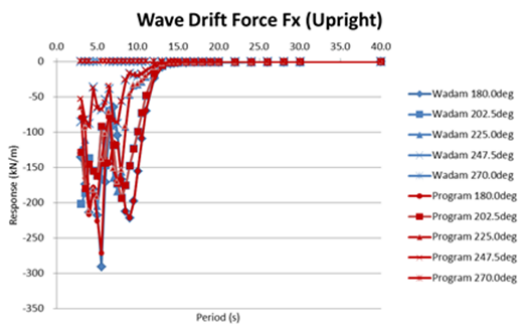


Figure 5-24 Wave drift force Fx (Upright)

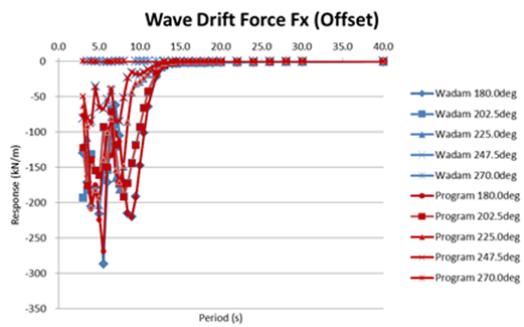


Figure 5-25 Wave drift force Fx (Offset)

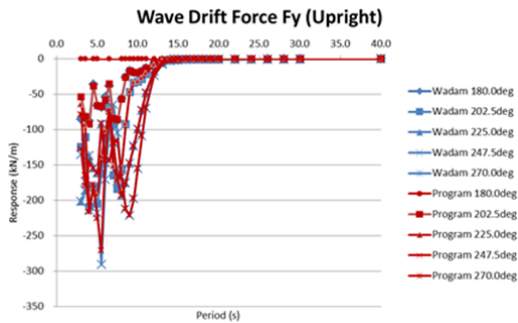


Figure 5-26 Wave drift force Fy (Upright)

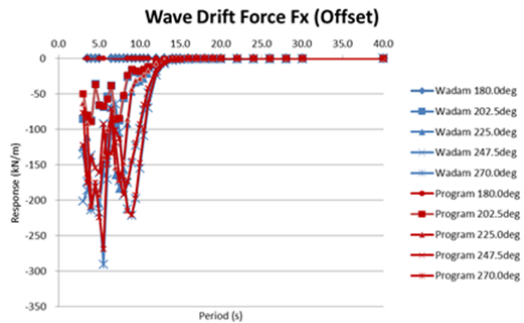


Figure 5-27 Wave drift force Fy (Offset)

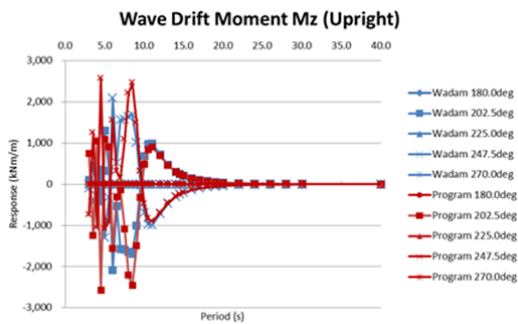


Figure 5-28 Wave drift force Mz (Upright)

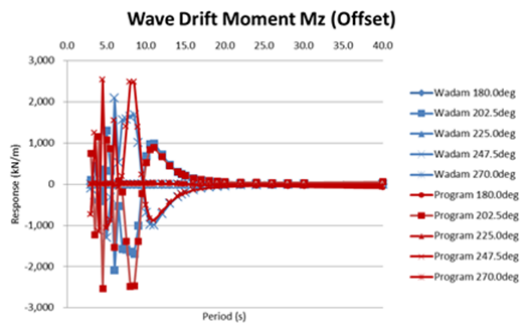


Figure 5-29 Wave drift force Mz (Offset)

6 Methodology - Global Performance Calculation

6.1 Global Parameters

The main purpose of the global performance calculation is to calculate the following key global performance parameters [6-1][6-2]:

- Maximum Offset
- Maximum Setdown
- Maximum Tendon Tension
- Minimum Tendon Tension
- Maximum Tendon Bottom Angle
- Minimum Airgap
- Maximum Acceleration

The frequency domain calculation is used to calculate the above parameters. The frequency domain calculation has the following frequency range.

- Mean Condition (Constant)
- Low Frequency (Over 30 sec. period)
- Wave Frequency (From 4 sec. to 30 sec. period)
- High Frequency (Less than 4 sec. period)

The following environmental effects are considered in this calculation:

- Wave
- Wind
- Current
- Tide, Storm Surge and Subsidence

The conditions considered in this analysis are as follows:

- Intact Condition
- Tendon Damaged Condition
- Tendon Flooded Condition
- Compartment Damaged Condition

6.2 Mean Condition Calculation

The mean condition is calculated by the balance of forces and moments. The following restoring forces and their derivations are to be calculated;

- Hydrostatic Force
- Tendon Restoring Force
- TTR Restoring Force
- SCR Restoring Force

The following mean environmental forces are counted as external forces;

- Wind Force
- Current Force
- Wave Drift Forces
- Viscous Drift Force
- Tide, Storm Surge and Subsidence

The 6-DOF of force and moment balance is described as follows. f^r is restoring forces and f^e is external forces.

$$K_{ij}\mathbf{x} = \mathbf{F} \quad (\text{Eq. 6-1})$$

$$F_x(x, y, z, \theta, \phi, \varphi) = f_x^r(x, y, z, \theta, \phi, \varphi) - f_x^e = 0 \quad (\text{Eq. 6-2})$$

$$F_y(x, y, z, \theta, \phi, \varphi) = f_y^r(x, y, z, \theta, \phi, \varphi) - f_y^e = 0 \quad (\text{Eq. 6-3})$$

$$F_z(x, y, z, \theta, \phi, \varphi) = f_z^r(x, y, z, \theta, \phi, \varphi) - f_z^e = 0 \quad (\text{Eq. 6-4})$$

$$M_x(x, y, z, \theta, \phi, \varphi) = m_x^r(x, y, z, \theta, \phi, \varphi) - m_x^e = 0 \quad (\text{Eq. 6-5})$$

$$M_y(x, y, z, \theta, \phi, \varphi) = m_y^r(x, y, z, \theta, \phi, \varphi) - m_y^e = 0 \quad (\text{Eq. 6-6})$$

$$M_z(x, y, z, \theta, \phi, \varphi) = m_z^r(x, y, z, \theta, \phi, \varphi) - m_z^e = 0 \quad (\text{Eq. 6-7})$$

The linear iteration method is used to solve the force balance equation and obtain the six degree of hull position;

$$x_{i+1} = x_i - \frac{F_{xi}}{F'_{xi}} \quad (\text{Eq. 6-8})$$

$$y_{i+1} = y_i - \frac{F_{yi}}{F'_{yi}} \quad (\text{Eq. 6-9})$$

$$z_{i+1} = z_i - \frac{F_{zi}}{F'_{zi}} \quad (\text{Eq. 6-10})$$

$$\theta_{i+1} = \theta_i - \frac{M_{xi}}{M'_{xi}} \quad (\text{Eq. 6-11})$$

$$\phi_{i+1} = \phi_i - \frac{M_{xi}}{M'_{xi}} \quad (\text{Eq. 6-12})$$

$$\varphi_{i+1} = \varphi_i - \frac{M_{xi}}{M'_{xi}} \quad (\text{Eq. 6-13})$$

6.2.1 Restoring Forces

6.2.1.1 Tendon and TTR Restoring Forces

Tendon and TTR tensions are described as follows. L_{0i} is initial length of the Tendon and TTR line and L is line length at the vessel position.

$$T_i = \lambda_i(L_i - L_{0i}) \quad (\text{Eq. 6-14})$$

$$L_i = \sqrt{(x'_{Fi} - x_{Bi})^2 + (y'_{Fi} - y_{Bi})^2 + (z'_{Fi} - z_{Bi})^2} \quad (\text{Eq. 6-15})$$

The fairlead positions in global coordinate system which the vessel position is taken into account are calculated as follows;

$$x'_{Fi} = x_{Fi} + x + z_{Fi}\phi - y_{Fi}\theta \quad (\text{Eq. 6-16})$$

$$y'_{Fi} = y_{Fi} + y + x_{Fi}\varphi - z_{Fi}\theta \quad (\text{Eq. 6-17})$$

$$z'_{Fi} = z_{Fi} + z + y_{Fi}\theta - x_{Fi}\phi \quad (\text{Eq. 6-18})$$

6-DOF of forces working on the vessel are described as follows;

$$F_{xi} = -\frac{x'_{Fi} - x_{Bi}}{L_i} T_i \quad (\text{Eq. 6-19})$$

$$F_{yi} = -\frac{y'_{Fi} - y_{Bi}}{L_i} T_i \quad (\text{Eq. 6-20})$$

$$F_{zi} = -\frac{z'_{Fi} - z_{Bi}}{L_i} T_i \quad (\text{Eq. 6-21})$$

$$M_{xi} = F_{zi}y_{Fi} - F_{yi}z_{Fi} \quad (\text{Eq. 6-22})$$

$$M_{yi} = F_{xi}z_{Fi} - F_{zi}x_{Fi} \quad (\text{Eq. 6-23})$$

$$M_{zi} = F_{yi}x_{Fi} - F_{xi}y_{Fi} \quad (\text{Eq. 6-24})$$

The derivations of those forces are to be calculated as follows;

$$\frac{\partial F_{xi}}{\partial x} = -\lambda_i \left\{ 1 - \frac{L_{0i}}{L_i} + \frac{(x'_{Fi} - x_{Bi})^2 L_{0i}}{L_i^3} \right\} \quad (\text{Eq. 6-25})$$

$$\frac{\partial F_{yi}}{\partial y} = -\lambda_i \left\{ 1 - \frac{L_{0i}}{L_i} + \frac{(y'_{Fi} - y_{Bi})^2 L_{0i}}{L_i^3} \right\} \quad (\text{Eq. 6-26})$$

$$\frac{\partial F_{zi}}{\partial z} = -\lambda_i \left\{ 1 - \frac{L_{0i}}{L_i} + \frac{(z'_{Fi} - z_{Bi})^2 L_{0i}}{L_i^3} \right\} \quad (\text{Eq. 6-27})$$

$$\frac{\partial M_{xi}}{\partial \theta} = -\lambda_i \left\{ (y_{Fi}^2 + z_{Fi}^2) \left(1 - \frac{L_{0i}}{L} \right) + \{ y_{Fi}(z_{Fi} - z_{Bi}) + z_{Fi}(y_{Fi} - y_{Bi}) \} \frac{L_{0i}}{L_i^3} \right\} \quad (\text{Eq. 6-28})$$

$$\frac{\partial M_{yi}}{\partial \phi} = -\lambda_i \left\{ (z_{Fi}^2 + x_{Fi}^2) \left(1 - \frac{L_{0i}}{L_i} \right) + \{ z_{Fi}(x_{Fi} - x_{Bi}) + x_{Fi}(z_{Fi} - z_{Bi}) \} \frac{L_{0i}}{L_i^3} \right\} \quad (\text{Eq. 6-29})$$

$$\frac{\partial M_{zi}}{\partial \varphi} = -\lambda_i \left\{ (x_{Fi}^2 + y_{Fi}^2) \left(1 - \frac{L_{0i}}{L_i} \right) + \{ x_{Fi}(y_{Fi} - y_{Bi}) + y_{Fi}(x_{Fi} - x_{Bi}) \} \frac{L_{0i}}{L_i^3} \right\} \quad (\text{Eq. 6-30})$$

6.2.1.2 SCR Restoring Forces

SCRs (Steel Catenary Risers) are to be calculated by using catenary line theory. The axial and bending stiffness and deformation are neglected and unit weight per line length is assumed to be uniform.

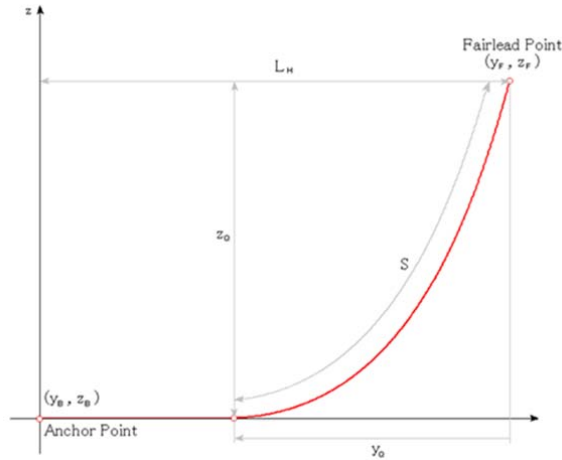


Figure 6-1 Schematic of Catenary Line Shape

The vertical force T_{vi} and horizontal force T_{hi} of catenary line i are described as follows;

$$T_{vi} = w_i s_i \quad (\text{Eq. 6-31})$$

$$T_{hi} = w_i a_i \quad (\text{Eq. 6-32})$$

The unit weight per line length is expressed as w_i , length of the catenary line is expressed as s_i and a_i is catenary parameter. The line length s_i and horizontal separation y_Q are calculated by using the following equations;

$$s_i = \sqrt{z_{Qi}(z_{Qi} + 2a_i)} \quad (\text{Eq. 6-33})$$

$$y_{Qi} = a_i \cosh^{-1} \left(\frac{s_i}{a_i} + 1 \right) \quad (\text{Eq. 6-34})$$

The total length of the line (from anchor point to fairlead point) is calculated by the following equation;

$$L_{Si} = \sqrt{z_{Qi}(z_{Qi} + 2a_i)} - a_i \cos^{-1} \left(\frac{s_i}{a_i} + 1 \right) + L_{Hi} \quad (\text{Eq. 6-35})$$

This total length must be constant. By using this condition, the catenary parameter a is calculated by Newton method (suffix i is not presented);

$$f_j = \sqrt{z_Q(z_Q + 2a_j)} - a_j \cos^{-1} \left(\frac{z_Q}{a_j} + 1 \right) + L_H - L_{S0} = 0 \quad (\text{Eq. 6-36})$$

$$f'_j = \frac{2z_Q}{\sqrt{z_Q(z_Q + 2a_j)}} - \cos^{-1} \left(\frac{z_Q}{a_j} + 1 \right) \quad (\text{Eq. 6-37})$$

$$a_{j+1} = a_j - \frac{f_j}{f'_j} \quad (\text{Eq. 6-38})$$

The forces and moment acting at the fairlead point are as follows;

$$F_x = -\frac{x'_F - x_B}{L_H} wa \quad (\text{Eq. 6-39})$$

$$F_y = -\frac{y'_F - y_B}{L_H} wa \quad (\text{Eq. 6-40})$$

$$F_z = -w \sqrt{z_Q(z_Q + 2a)} \quad (\text{Eq. 6-41})$$

$$M_x = F_z y - F_y z \quad (\text{Eq. 6-42})$$

$$M_y = F_x z - F_z x \quad (\text{Eq. 6-43})$$

$$M_z = F_y x - F_x y \quad (\text{Eq. 6-44})$$

The differential of those forces and moments are as follows;

$$\frac{\partial F_x}{\partial x} = -\frac{w(x_F - x_B) \partial a}{L_H \partial x} - \frac{wa}{L_H} + \frac{w(x_F - x_B)^2 a}{L_H^3} \quad (\text{Eq. 6-45})$$

$$\frac{\partial F_y}{\partial y} = -\frac{w(y_F - y_B) \partial a}{L_H \partial y} - \frac{wa}{L_H} + \frac{w(y_F - y_B)^2 a}{L_H^3} \quad (\text{Eq. 6-46})$$

$$\frac{\partial F_z}{\partial z} = -\frac{wz_Q}{\sqrt{z_Q(z_Q + 2a)}} \frac{\partial a}{\partial z} - \frac{w(z_Q + a)}{\sqrt{z_Q(z_Q + 2a)}} \quad (\text{Eq. 6-47})$$

$$\frac{\partial M_x}{\partial \theta} = -\frac{w(z_Q + a)y_F}{\sqrt{z_Q(z_Q + 2a)}} - \frac{wz_Q y_F}{\sqrt{z_Q(z_Q + 2a)}} \frac{\partial a}{\partial \theta} \quad (\text{Eq. 6-48})$$

$$\begin{aligned} & + \frac{w(y_F - y_B)z_F}{L_H} \frac{\partial a}{\partial \theta} - \frac{wz_F^2 a}{L_H} + \frac{wz_F^2 (y_F - y_B)^2 a}{L_H^3} \\ \frac{\partial M_y}{\partial \phi} & = -\frac{w(x_F - x_B)z_F}{L_H} \frac{\partial a}{\partial \phi} - \frac{wz_F^2 a}{L_H} - \frac{wz_F^2 (x_F - x_B)^2 a}{L_H^3} \\ & + \frac{w(z_Q + a)x_F}{\sqrt{z_Q(z_Q + 2a)}} + \frac{wz_Q x_F}{\sqrt{z_Q(z_Q + 2a)}} \frac{\partial a}{\partial \phi} \end{aligned} \quad (\text{Eq. 6-49})$$

$$\begin{aligned} \frac{\partial M_z}{\partial \varphi} & = -\frac{w(y_F - y_B)x_F}{L_H} \frac{\partial a}{\partial \varphi} - \frac{wx_F^2 a}{L_H} \\ & + \frac{wx_F \{x_F (y_F - y_B) - y_F (x_F - x_B)\} a}{L_H^3} \\ & + \frac{w(x_F - x_B)y_F}{L_H} \frac{\partial a}{\partial \varphi} - \frac{wy_F^2 a}{L_H} \\ & - \frac{wy_F \{x_F (y_F - y_B) - y_F (x_F - x_B)\} a}{L_H^3} \end{aligned} \quad (\text{Eq. 6-50})$$

6.2.1.3 Hydrostatic Forces

The hydrostatic restoring forces acting on the vessel are as follows;

$$F_z = \rho g A z \quad (\text{Eq. 6-51})$$

$$M_x = \{\rho g (I_{xx} + Vz_B) - mgz_G\} \theta \quad (\text{Eq. 6-52})$$

$$M_y = \{\rho g(I_{yy} + Vz_B) - mgz_G\}\phi \quad (\text{Eq. 6-53})$$

The differential of those components are expressed as follows;

$$\frac{\partial F_z}{\partial z} = \rho g A \quad (\text{Eq. 6-54})$$

$$\frac{\partial M_x}{\partial \theta} = \rho g(I_{xx} + Vz_B) - mgz_G \quad (\text{Eq. 6-55})$$

$$\frac{\partial M_y}{\partial \phi} = \rho g(I_{yy} + Vz_B) - mgz_G \quad (\text{Eq. 6-56})$$

6.2.2 Environmental Forces

The environmental forces considered in the mean environmental conditions are;

- Steady Wind
- Steady Current
- Mean Drift Forces
- Tide, Storm Surge and Subsidence

In this section, drag force coefficient calculation, wind and current force calculation and wave drift forces calculation are explained.

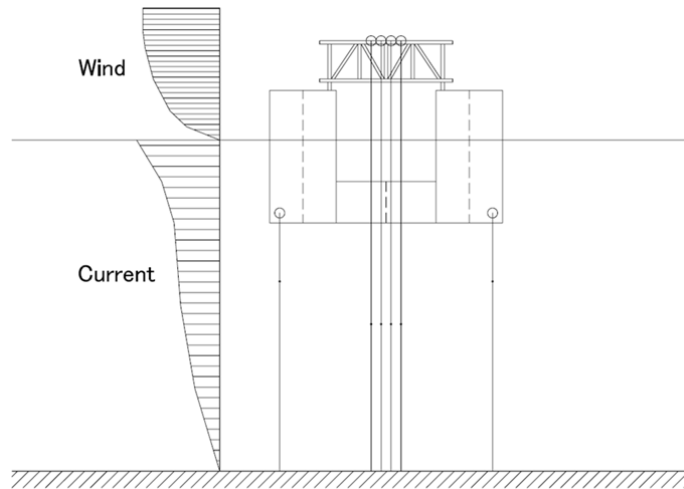


Figure 6-2 Wind and current loading on the platform

6.2.2.1 Drag Force Coefficient

According to DNV-RP-C205 [6-2], drag force is calculated by the following equation;

$$F_D = \frac{1}{2} \rho C S u^2 \sin \alpha \quad (\text{Eq. 6-57})$$

If the members are not solid (like truss structure), the drag force is calculated by the following equation. ϕ is the solidity ratio and C_e is the effective drag coefficient.

$$F_{De} = \frac{1}{2} \rho \phi C_e S u^2 \sin \alpha \quad (\text{Eq. 6-58})$$

If the member is a cylinder, the drag coefficient is calculated as follows. Δ is the roughness parameter.

$$C_d = \begin{cases} 0.65 & \Delta < 10^{-4} \text{ (smooth)} \\ \frac{29 + 4 \log_{10} \Delta}{20} & 10^{-4} < \Delta < 10^{-2} \\ 1.05 & \Delta > 10^{-2} \text{ (rough)} \end{cases} \quad (\text{Eq. 6-59})$$

If the member is a smooth rectangular, the drag coefficient is calculated as follows.

$$C_{d1} = 2K_R \sin \alpha \quad (\text{Eq. 6-60})$$

$$C_{d2} = \left(1 + \frac{b_2}{b_1}\right) K_R \cos \alpha \quad \text{for } b_2 \leq b_1 \leq 2b_2 \quad (\text{Eq. 6-61})$$

$$= 1.5K_R \cos \alpha \quad \text{for } b_1 > 2b_2 \quad (\text{Eq. 6-62})$$

$$K_R = 1.0 \quad \text{for } \frac{r}{b} \leq 0.10 \quad (\text{Eq. 6-63})$$

$$= \frac{1}{3} \left(4.3 - 13 \frac{r}{b}\right) \quad \text{for } 0.10 \leq \frac{r}{b} \leq 0.25 \quad (\text{Eq. 6-64})$$

$$= 0.35 \quad \text{for } \frac{r}{b} \geq 0.25 \quad (\text{Eq. 6-65})$$

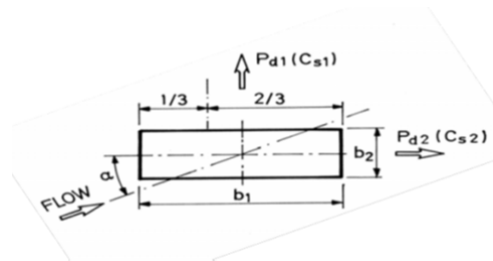


Figure 6-3 Drag force on rectangular cross section (DNV-RP-C205)

The following effective shape coefficient C_e is used in the calculation.

Table 6-1 Effective shape coefficient (DNV-RP-C205)

Solidity Ratio ϕ	Effective Shape Coefficient C_e		
	Flat-side members	Circular Sections	
		$Re < 4.2 \times 10^5$	$Re \geq 4.2 \times 10^5$
0.10	1.9	1.2	0.7
0.20	1.8	1.2	0.8
0.30	1.7	1.2	0.8
0.40	1.7	1.1	0.8
0.50	1.6	1.1	0.8
0.75	1.6	1.5	1.4
1.00	2.0	2.0	2.0

The effect of the finite length is considered in the calculation. The following reduction factors are applied in the drag force coefficient calculation.

Table 6-2 Reduction Factor for finite length (DNV-RP-C205)

A – Circular Cylinder – subcritical flow							
B – Circular Cylinder – Supercritical flow							
C – Flat plate perpendicular to flow							
l/d	2	5	10	20	40	50	100
A	0.58	0.62	0.68	0.74	0.82	0.87	0.98
B	0.80	0.80	0.82	0.90	0.98	0.99	1.00
C	0.62	0.66	0.69	0.81	0.87	0.90	0.95

6.2.2.2 Current Coefficient Calculation

The current speed distribution in vertical direction is considered. If the current speed data are available at certain positions in vertical direction, the current distributions are assumed to be linear among data points. Total force acting on a Morison member is as follows;

$$f = \frac{1}{2} \rho \int_{z_B}^{z_F} C_d \{u(z)\}^2 D dz \quad (\text{Eq. 6-66})$$

$$u(z) = \frac{u_{i+1} - u_i}{z_{i+1} - z_i} z + \frac{u_i z_{i+1} - u_{i+1} z_i}{z_{i+1} - z_i} \quad z_i \leq z < z_{i+1} \quad (\text{Eq. 6-67})$$

This equation is discretized as follows;

$$\begin{aligned}
f &= \sum_i \frac{1}{2} \rho \int_{z_i}^{z_{i+1}} C_d \{u(z)\}^2 D dz \\
&= \sum_i \left[\frac{1}{6} \rho C_d D \frac{z_{i+1} - z_i}{u_{i+1} - u_i} \left(\frac{u_{i+1} - u_i}{z_{i+1} - z_i} z + \frac{u_i z_{i+1} - u_{i+1} z_i}{z_{i+1} - z_i} \right)^3 \right]_{z_i}^{z_{i+1}} \\
&= \sum_i \frac{1}{6} \rho C_d D (z_{i+1} - z_i) (u_{i+1}^2 + u_{i+1} u_i + u_i^2)
\end{aligned} \tag{Eq. 6-68}$$

6.2.2.3 Wind Coefficient Calculation

Wind distribution is reproduced by using the model equation (2-63). Reference point of the data is normally located at 10m height from mean sea water level ($z_{10}=10\text{m}$). Total force acting on a Morison member is as follows;

$$f = \frac{1}{2} \rho \int_{z_B}^{z_F} C_d u^2 D dz \tag{Eq. 6-69}$$

$$u = u_{10} \left(\frac{z}{z_{10}} \right)^\alpha \tag{Eq. 6-70}$$

This equation is discretized as follows;

$$\begin{aligned}
f &= \sum_i \frac{1}{2} \rho \int_{z_i}^{z_{i+1}} C_d \{u(z)\}^2 D dz \\
&= \sum_i \left[\frac{1}{2} \rho C_d D \frac{1}{2\alpha + 1} \frac{u_{10}^2}{z_{10}^{2\alpha}} z^{2\alpha+1} \right]_{z_i}^{z_{i+1}} \\
&= \sum_i \frac{1}{2(2\alpha + 1)} \rho C_d D \frac{u_{10}^2}{z_{10}^{2\alpha}} (z_{i+1}^{2\alpha+1} - z_i^{2\alpha+1})
\end{aligned} \tag{Eq. 6-71}$$

6.3 Wave-frequency Motion Calculation

As mentioned in section 6, the wave-frequency motion is calculated by the following equation. For global performance calculation, the effect of the offset/setdown is considered in in each matrix.

$$\{M_{ij} + A_{ij}\} \ddot{x}_{wi} + \{B_{ij} + C_{ij}\} \dot{x}_{wi} + \{K_{ij} + S_{ij}\} x_{wi} = E_i \tag{Eq. 6-72}$$

6.4 Low-frequency Motion Calculation

6.4.1 Wind Induced Motion

For wind induced motion, the following motion equation is used for calculation.

$$\{M_{ij}+A_{ij}\}\ddot{x}_{ii} + B_{ij}\dot{x}_{ii} + \{K_{ij}+S_{ij}\}x_{ii} = 2CU \quad (\text{Eq. 6-73})$$

C is the wind coefficient and U is mean wind velocity.

6.4.2 Wind Spectrum

API wind spectrum [6-4] is expressed as follows. f is frequency and $U(z)$ is 1-hour mean wind speed at z meters above water line.

$$S(f) = \frac{\sigma^2(z)}{f} \frac{F}{(1+1.5F)^{5/3}} \quad (\text{Eq. 6-74})$$

$$\sigma(z) = \begin{cases} 0.15U(z) \left(\frac{z}{z_s}\right)^{-0.125} & \text{for } z \leq z_s \\ 0.15U(z) \left(\frac{z}{z_s}\right)^{-0.275} & \text{for } z > z_s \end{cases} \quad (\text{Eq. 6-75})$$

$$F = \frac{f}{f_p} \quad (\text{Eq. 6-76})$$

$$f_p = \frac{\beta U(z)}{z} \quad (\text{Eq. 6-77})$$

$$\beta = 0.025, z=10, z_s = 20 \quad (\text{Eq. 6-78})$$

ISO wind spectrum [6-5] is expressed as follows. f is frequency and U_0 is 1-hour mean wind speed at z meters above water line. z is height above water line.

$$S(f) = \frac{320 \left(\frac{U_0}{10}\right)^2 \left(\frac{z}{10}\right)^{0.45}}{\left(1 + f_m^n\right)^{5/n}} \quad (\text{Eq. 6-79})$$

$$f_m = 172 f \left(\frac{z}{10}\right)^{\frac{2}{3}} \left(\frac{U_0}{10}\right)^{-0.75} \quad (\text{Eq. 6-80})$$

$$n = 0.468 \quad (\text{Eq. 6-81})$$

6.4.3 Variable Wave Drift Force Induced Motion

For the low frequency motion due to variable wave drift force, the following motion equations are used.

$$\{M_{ij} + A_{ij}\} \ddot{x}_{dij} + \{B_{ij} + C_{ij}\} \dot{x}_{dij} + \{K_{ij} + S_{ij}\} x_{dij} = \frac{H_i + H_j}{2} \quad (\text{Eq. 6-82})$$

Newman's approximation [3-4] is used for the external force term. By solving this motion equation, quadratic transfer function is obtained.

6.5 Maximum/Minimum Value Calculation

Wave, wind, and variable wave drift force induced responses are multiplied with each external force spectrum. These response spectra are combined and filtered for each frequency ranges:

High Frequency Range: Period < 4 sec

Wave Frequency Range: 4 sec < Period < 30 sec

Low Frequency Range: 30 sec < Period

The standard deviation of the response is calculated as follows by using empirical calibration factors α , β , and γ .

$$\sigma = \sqrt{(\alpha\sigma_H)^2 + (\beta\sigma_W)^2 + (\gamma\sigma_L)^2} \quad (\text{Eq. 6-83})$$

Maximum and minimum value is calculated as follows. P_{\max} is peak factor for maximum response and P_{\min} is peak factor for minimum.

$$X_{\max} = X_{\text{mean}} + P_{\max} \sigma \quad (\text{Eq. 6-84})$$

$$X_{\min} = X_{\text{mean}} - P_{\min} \sigma \quad (\text{Eq. 6-85})$$

For maximum and minimum tendon tension calculation, the following margins are considered.

Pile misalignment margin	2 feet
Tendon weight margin	3%
Tendon buoyancy margin	3%

6.6 Program Verification

For verification, the result of this global performance calculation module was compared with commercial software. As commercial software, DeepC in DNV Sesam Software Package was used.

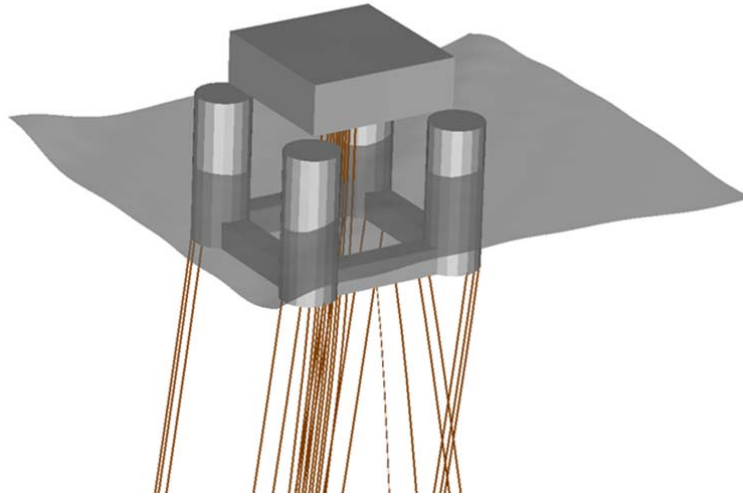


Figure 6-4 DeepC analysis model

Hull and Tendon/Riser conditions are the same as section 5. The environmental loading is as follows:

Significant Wave Height	19 m
Mean Wind Speed	55 m/s
Surface Current Speed	2.7 m/s
Sea Level	+0.8 m
Environmental Load Direction	Collinear toward SW (225deg)

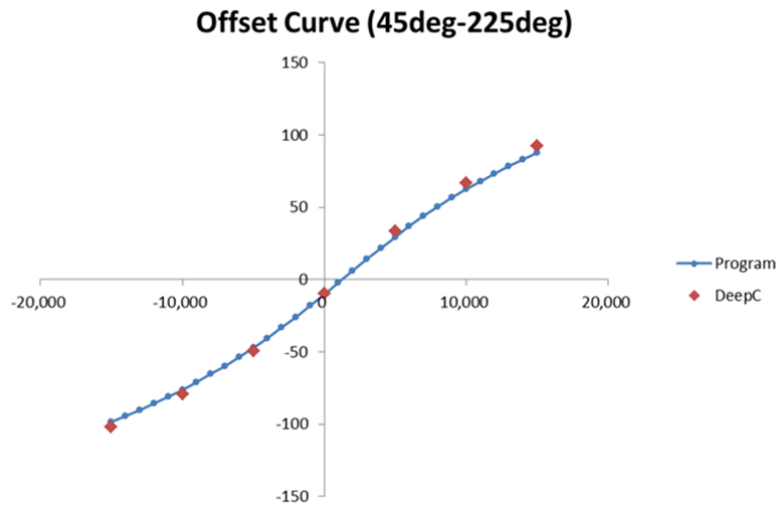


Figure 6-5 Offset value comparison

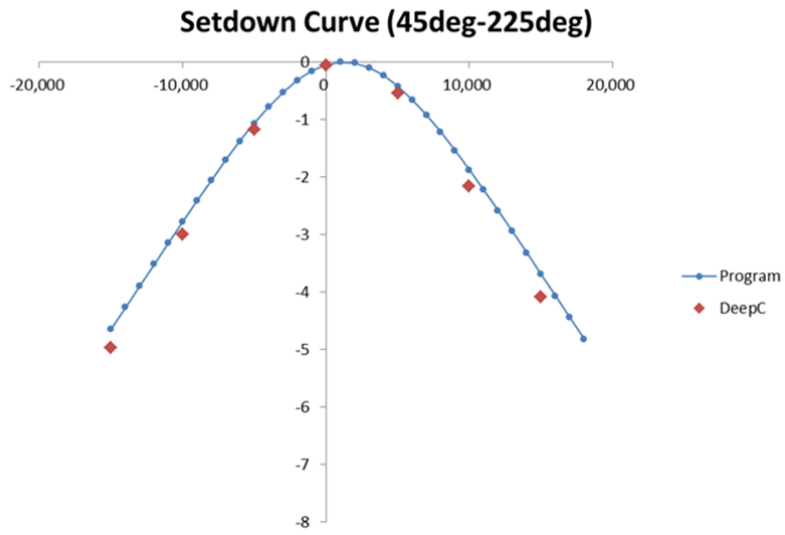


Figure 6-6 Setdown value comparison

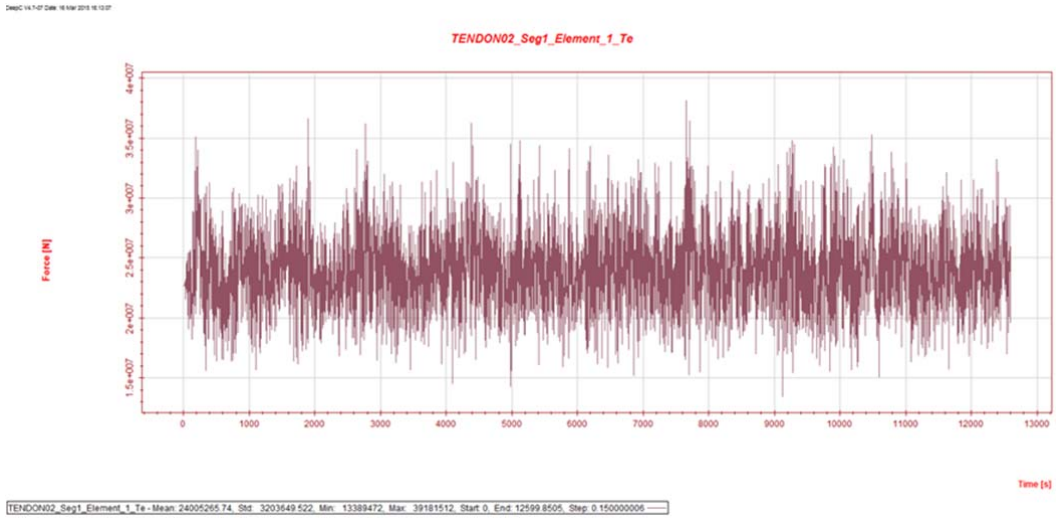


Figure 6-7 DeepC time history of up-wave tendon tension

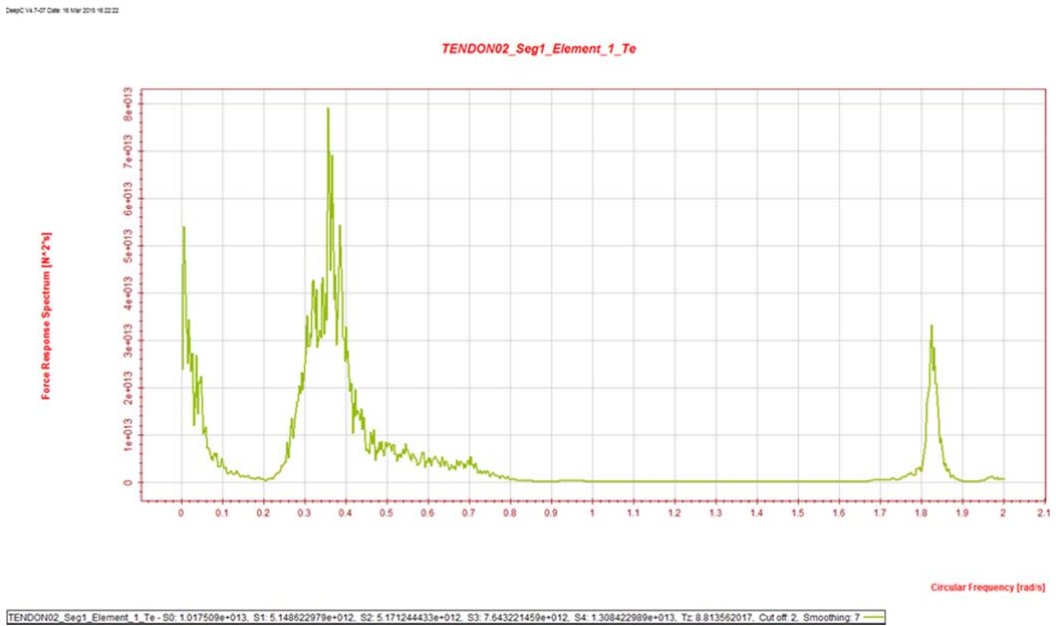


Figure 6-8 DeepC spectrum of up-wave tendon tension

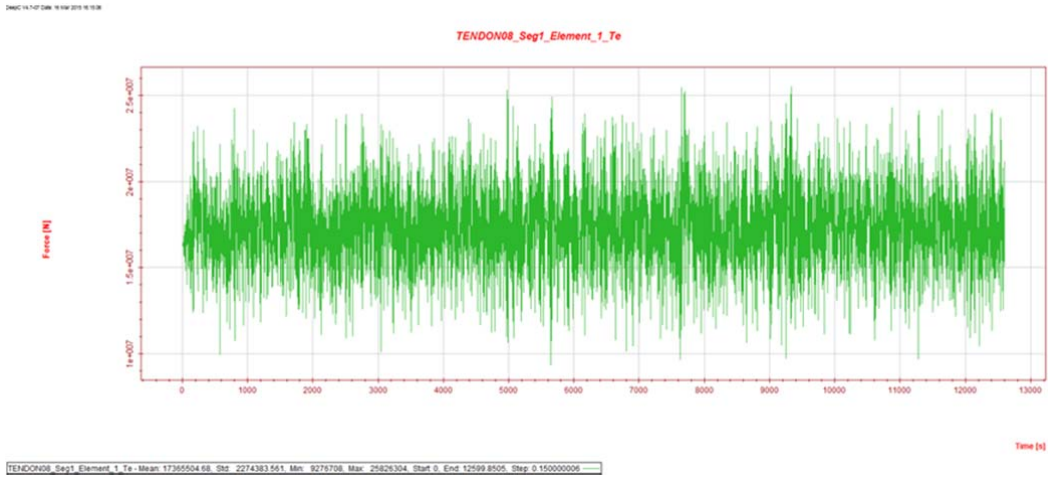


Figure 6-9 DeepC time history of down-wave tendon tension

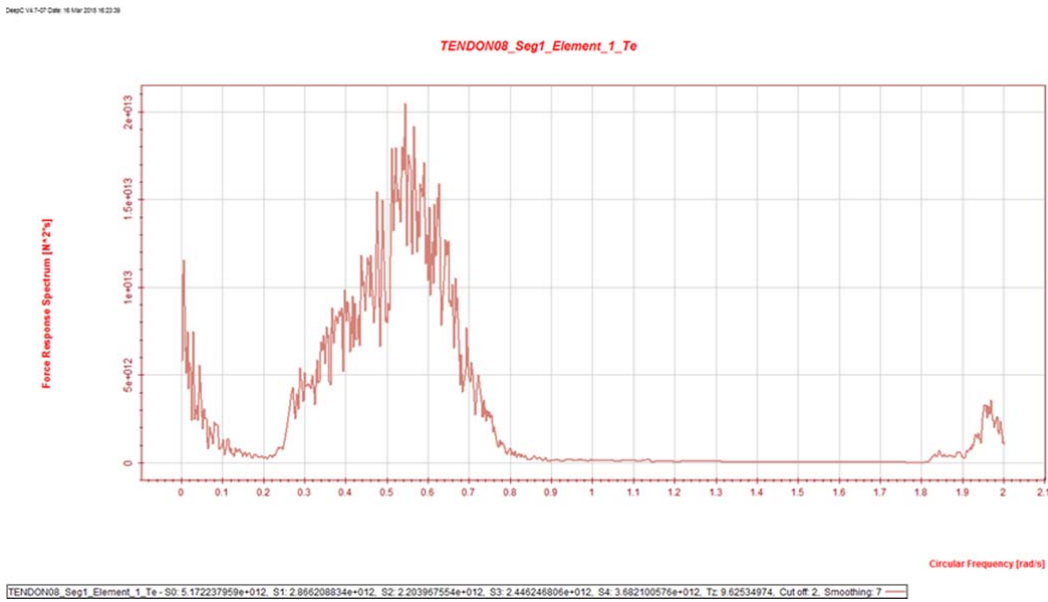


Figure 6-10 DeepC spectrum of down-wave tendon tension

[GP Comparison]

The following table shows calculated global performance result. Although, program is frequency domain calculation, and DeepC is time-domain calculation, the similar result was obtained.

Table 6-3 Global performance comparison

	Program	DeepC
Mean Offset	81m	79m
Max. Offset	102m	99m
Max. Tendon Tension	27,761 kN	28,562 kN
Min. Tendon Tension	8,652 kN	5,983kN

7 Methodology - Global Structure Calculation

In this analysis, the hull and topside members are modeled by beam elements. The benefits of this beam-model structural analysis are (1) simple and fast overview, (2) quick verification for shell element FEM analysis and (3) better understanding for physical phenomena by decomposing stress into each component. However, the effect such as local deformation, hoop stress, stress concentration, shear delay and so on are not included in the calculation result. These effects should be considered separately with another method.

To model the hull with beam element, the section properties of each hull girder member (such as Pontoon, Column and so on) are to be properly calculated. Correspondence between elements in panel model and beam elements in structural model is also necessary to transfer the hydrostatic and hydrodynamic pressure to the beam element.

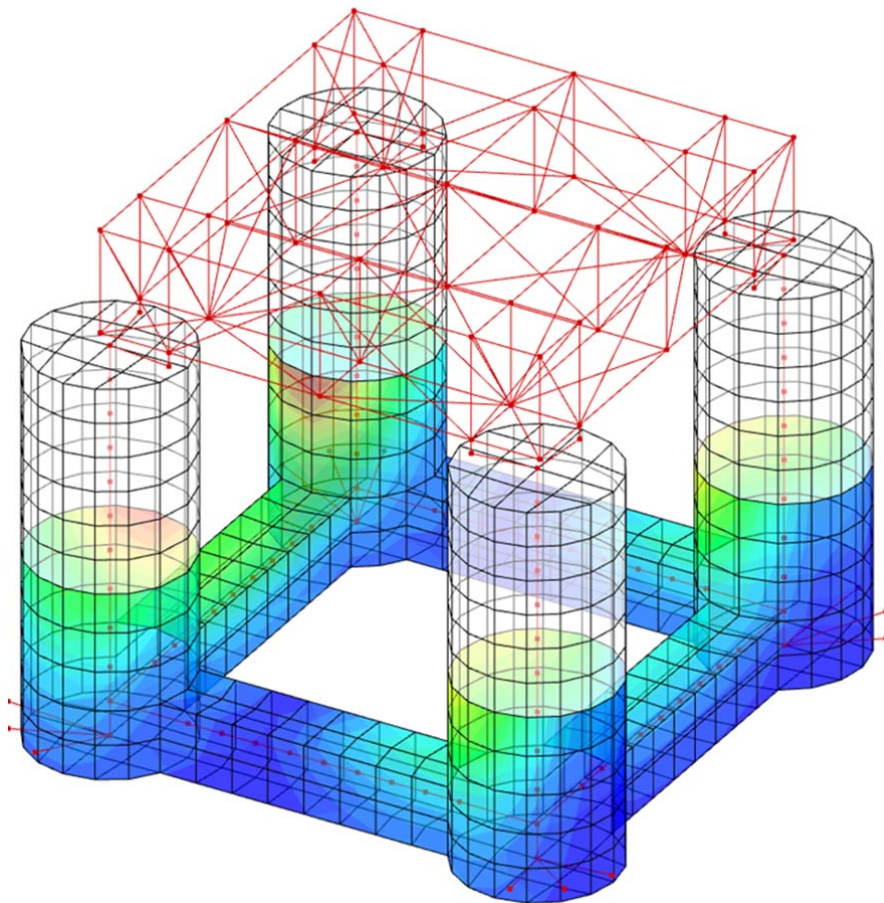


Figure 7-1 Beam Structural Model and Hydrodynamic Panel Model

7.1 Section Properties

In order to calculate the stiffness and stresses, section properties of the hull girder members are to be calculated correctly. Longitudinal members (shell plates, bulkheads and stiffeners) are counted in the section properties. Section area, moment of inertia, section modulus and shear area are required to be inputted.

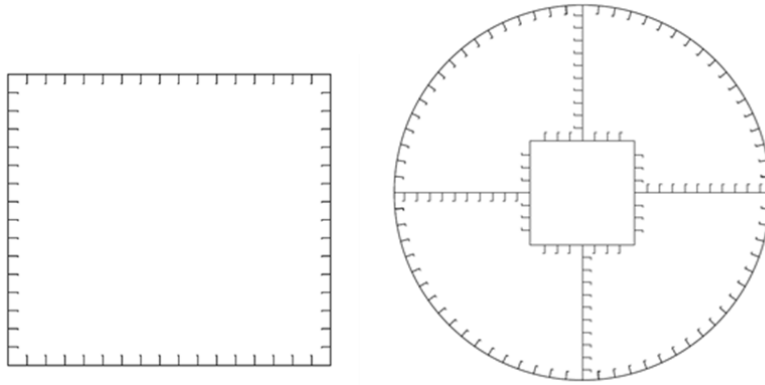


Figure 7-2 Section view of Pontoon and Column

Table 7-1 Section Properties

Symbol	Unit	Description
A	m ²	Section Area
I _{yy}	m ⁴	Second moment of area about y-axis
I _{zz}	m ⁴	Second moment of area about z-axis
I _{xx}	m ⁴	Torsional second moment of area
Z _{yy}	m ³	Section Modulus about y-axis
Z _{zz}	m ³	Section Modulus about z-axis
K	m ³	Torsional Section Modulus
A _y	m ²	Shear Area in y-direction
A _z	m ²	Shear Area in y-direction

7.2 Correspondence

Correspondence matrix is to be prepared to transfer the panel pressure loads to beam element. The panels which are surrounding the beam are hired as corresponding panels. There are “dummy rigid beams” which do not have the relation to the panels. These beams are defined to transfer the force from beam to beam.

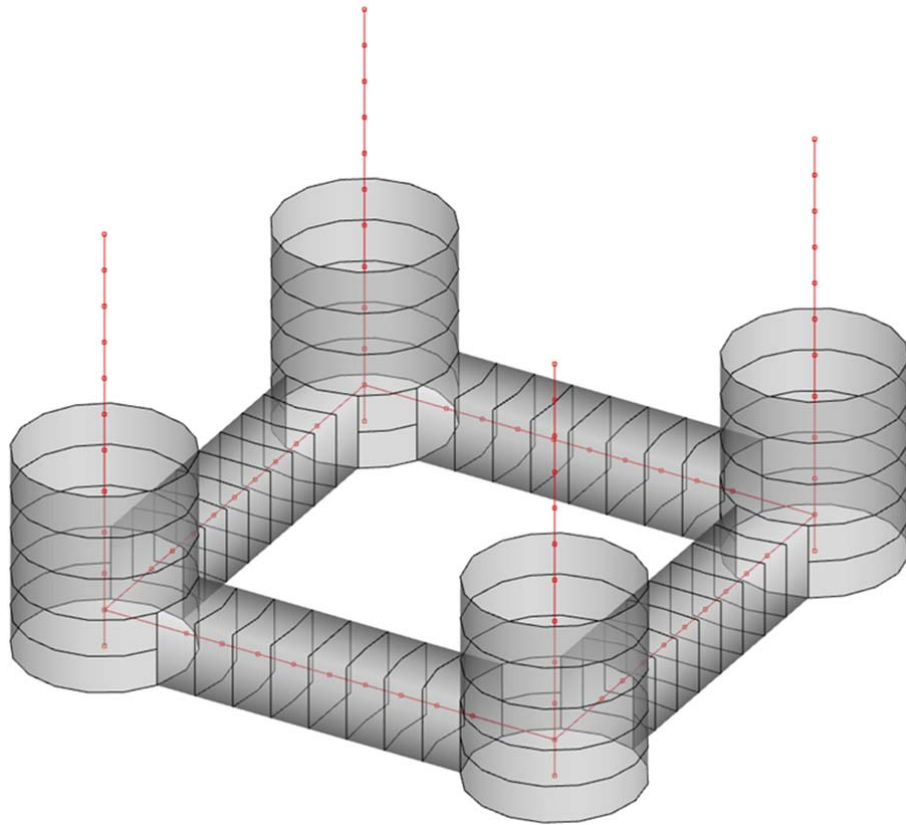


Figure 7-3 Correspondence between panels and beams

Table 7-2 Member ID definition

Section ID	Member
1	Dummy Rigid Beam
2	Column
3	Node
4	Pontoon

7.3 Spring Boundary corresponding Tendon stiffness

Spring boundary conditions which x -, y -, z -stiffness are same as tendons' stiffness are set on the tendon fairlead points. These boundary work as tendons, and help to avoid rigid-body motions.

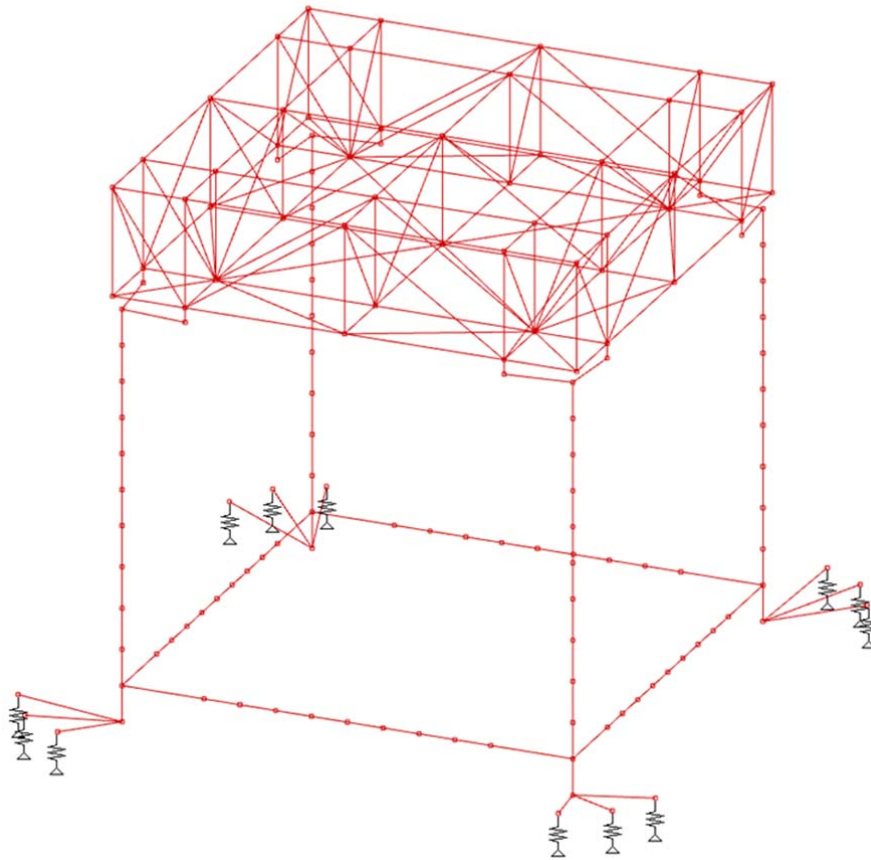


Figure 7-4 Spring Boundary corresponding to Tendons

7.4 Matrix Method

Matrix method [7-1] is used to calculate the force and moment in the grillage structure. This method is based on beam theory with small deformation and each element consists of 2 nodes.

Table 7-3 Symbols for matrix method formulation

Symbol	Unit	Description
E	Pa	Young's Modulus
G	Pa	Shear Modulus
A	m ²	Section Area of the element
I _y	m ⁴	Second moment of area about y-axis
I _z	m ⁴	Second moment of area about z-axis
K	m ⁴	St. Venant Torsional constant
l	m	Length of the element

P _{xi}	N	Axial Force at node i
Q _{yi}	N	Shear Force at node i
Q _{zi}	N	Shear Force at node i
M _{xi}	Nm	Moment about x at node i (torsion moment)
M _{yi}	Nm	Moment about y at node i
M _{zi}	Nm	Moment about z at node i
u _i	m	Displacement in x-direction at node i
v _i	m	Displacement in y-direction at node i
w _i	m	Displacement in z-direction at node i
θ _{xi}	rad	Angular displacement about x-axis at node i
θ _{yi}	rad	Angular displacement about y-axis at node i
θ _{zi}	rad	Angular displacement about z-axis at node i

7.4.1 Element Stiffness Matrix

The relation of stiffness and displacement in each mode is expressed as follows.

Axial Compression

$$\frac{EA}{l} \begin{pmatrix} 1 & -1 \\ -1 & 1 \end{pmatrix} \begin{pmatrix} u_i \\ u_j \end{pmatrix} = \begin{pmatrix} P_{xi} \\ P_{xj} \end{pmatrix} \quad (\text{Eq. 7-1})$$

Bending about z axis

$$\frac{EI_y}{l^3} \begin{pmatrix} 12 & & & \text{sym.} \\ 6l & 4l^2 & & \\ -12 & -6l & 12 & \\ 6l & 2l^2 & -6l & 4l^2 \end{pmatrix} \begin{pmatrix} v_i \\ \theta_{zi} \\ v_j \\ \theta_{zj} \end{pmatrix} = \begin{pmatrix} Q_{yi} \\ M_{zi} \\ Q_{yj} \\ M_{zj} \end{pmatrix} \quad (\text{Eq. 7-2})$$

Bending about y axis

$$\frac{EI_z}{l^3} \begin{pmatrix} 12 & & & \text{sym.} \\ 6l & 4l^2 & & \\ -12 & -6l & 12 & \\ 6l & 2l^2 & -6l & 4l^2 \end{pmatrix} \begin{pmatrix} w_i \\ \theta_{yi} \\ w_j \\ \theta_{yj} \end{pmatrix} = \begin{pmatrix} Q_{zi} \\ M_{yi} \\ Q_{zj} \\ M_{yj} \end{pmatrix} \quad (\text{Eq. 7-3})$$

Torsion

$$\frac{GK}{l} \begin{pmatrix} 1 & -1 \\ -1 & 1 \end{pmatrix} \begin{pmatrix} \theta_{xi} \\ \theta_{xj} \end{pmatrix} = \begin{pmatrix} M_{xi} \\ M_{xj} \end{pmatrix} \quad (\text{Eq. 7-4})$$

Element stiffness matrix takes the following form.

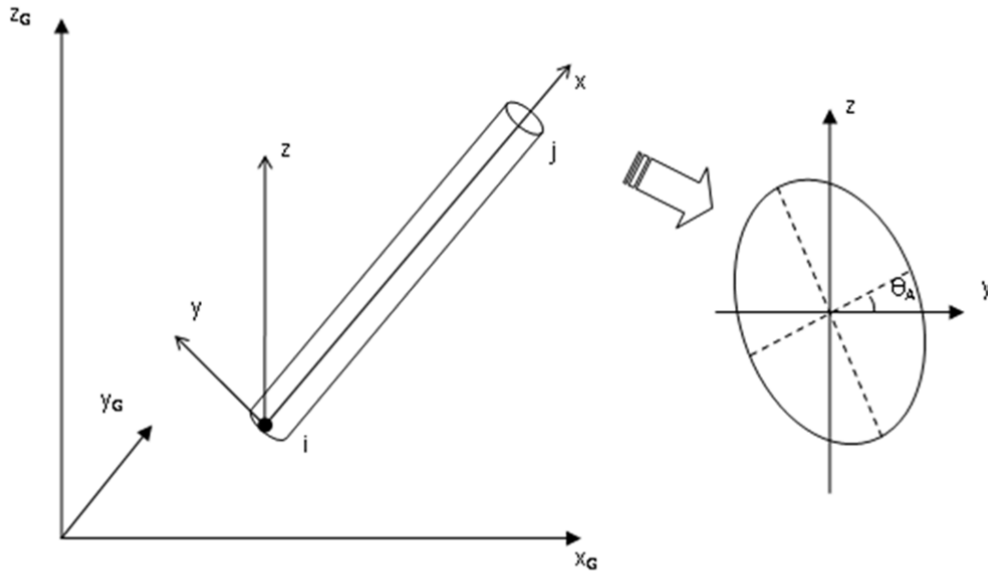


Figure 7-5 Coordinate Conversion [7-1]

$$T = \begin{pmatrix} l_x & l_y & l_z \\ m_x & m_y & m_z \\ n_x & n_y & n_z \end{pmatrix} \quad (\text{Eq. 7-6})$$

Each component is as follows:

$$\begin{pmatrix} l_x \\ m_x \\ n_x \end{pmatrix} = \begin{pmatrix} \frac{x_j^G - x_i^G}{l} \\ \frac{y_j^G - y_i^G}{l} \\ \frac{z_j^G - z_i^G}{l} \end{pmatrix} \quad (\text{Eq. 7-7})$$

$$l = \sqrt{(x_j^G - x_i^G)^2 + (y_j^G - y_i^G)^2 + (z_j^G - z_i^G)^2} \quad (\text{Eq. 7-8})$$

$$\lambda = \sqrt{l_x^2 + m_x^2} \quad (\text{Eq. 7-9})$$

If $\lambda \neq 0$ Then

$$\begin{pmatrix} l_y \\ m_y \\ n_y \end{pmatrix} = \frac{1}{\lambda} \begin{pmatrix} -m_x \cos \theta_A - n_x l_x \sin \theta_A \\ l_x \cos \theta_A - m_x n_x \sin \theta_A \\ \lambda^2 \sin \theta_A \end{pmatrix} \quad (\text{Eq. 7-10})$$

$$\begin{pmatrix} l_z \\ m_z \\ n_z \end{pmatrix} = \frac{1}{\lambda} \begin{pmatrix} m_x \sin \theta_A - n_x l_x \cos \theta_A \\ -l_x \sin \theta_A - m_x n_x \cos \theta_A \\ \lambda^2 \cos \theta_A \end{pmatrix} \quad (\text{Eq. 7-11})$$

Else if $\lambda = 0$ Then

$$\begin{pmatrix} l_y \\ m_y \\ n_y \end{pmatrix} = \begin{pmatrix} n_x \cos \theta_A \\ \sin \theta_A \\ 0 \end{pmatrix} \quad (\text{Eq. 7-12})$$

$$\begin{pmatrix} l_z \\ m_z \\ n_z \end{pmatrix} = \begin{pmatrix} -n_x \sin \theta_A \\ \cos \theta_A \\ 0 \end{pmatrix} \quad (\text{Eq. 7-13})$$

The global stiffness matrix is as follows;

$$k^G d^G = f^G \quad (\text{Eq. 7-14})$$

KG is calculated as follows;

$$k^G = T_d^t k T_d \quad (\text{Eq. 7-15})$$

$$T_d = \begin{pmatrix} T & & & \text{sym.} \\ O & T & & \\ O & O & T & \\ O & O & O & T \end{pmatrix} \quad (\text{Eq. 7-16})$$

7.4.3 Calculation of Section Forces

By solving the global stiffness matrix, displacements are obtained, and then section forces are calculated as follows;

$$P_{xi} = \frac{EA}{l}(u_i - u_j) \quad (\text{Eq. 7-17})$$

$$Q_{yi} = \frac{EI_z}{l^3}(12v_i + 6l\theta_{zi} - 12v_j + 6l\theta_{zj}) \quad (\text{Eq. 7-18})$$

$$Q_{zi} = \frac{EI_y}{l^3}(12w_i - 6l\theta_{yi} - 12w_j - 6l\theta_{yj}) \quad (\text{Eq. 7-19})$$

$$M_{xi} = \frac{GK}{l}(\theta_{xi} - \theta_{xj}) \quad (\text{Eq. 7-20})$$

$$M_{yi} = \frac{EI_y}{l^3}(-6lw_i + 4l^2\theta_{yi} + 6lw_j + 2l^2\theta_{yj}) \quad (\text{Eq. 7-21})$$

$$M_{zi} = \frac{EI_z}{l^3}(6lv_i + 4l^2\theta_{zi} - 6lv_j + 2l^2\theta_{zj}) \quad (\text{Eq. 7-22})$$

$$P_{xj} = \frac{EA}{l}(u_j - u_i) \quad (\text{Eq. 7-23})$$

$$Q_{yj} = -\frac{EI_z}{l^3}(12v_i + 6l\theta_{zi} - 12v_j + 6l\theta_{zj}) \quad (\text{Eq. 7-24})$$

$$Q_{zj} = -\frac{EI_y}{l^3}(12w_i - 6l\theta_{yi} - 12w_j - 6l\theta_{yj}) \quad (\text{Eq. 7-25})$$

$$M_{xj} = \frac{GK}{l}(\theta_{xj} - \theta_{xi}) \quad (\text{Eq. 7-26})$$

$$M_{yj} = \frac{EI_y}{l^3}(-6lw_i + 2l^2\theta_{yi} + 6lw_j + 4l^2\theta_{yj}) \quad (\text{Eq. 7-27})$$

$$M_{zj} = \frac{EI_z}{l^3}(6lv_i + 2l^2\theta_{zi} - 6lv_j + 4l^2\theta_{zj}) \quad (\text{Eq. 7-28})$$

7.4.4 Distributed Load

Distributed loads are applied as equivalent point load on the nodes. The equivalent point loads are calculated by the following equation;

$$P_{xi} = P'_{xi} + \frac{l}{6}(2w_{xi} + w_{xj}) \quad (\text{Eq. 7-29})$$

$$Q_{yi} = Q'_{yi} + \frac{l}{20}(7w_{yi} + 3w_{yj}) \quad (\text{Eq. 7-30})$$

$$Q_{zi} = Q'_{zi} + \frac{l}{20}(7w_{zi} + 3w_{zj}) \quad (\text{Eq. 7-31})$$

$$M_{xi} = M'_{xi} \quad (\text{Eq. 7-32})$$

$$M_{yi} = M'_{yi} - \frac{l^2}{60}(3w_{zi} + 2w_{zj}) \quad (\text{Eq. 7-33})$$

$$M_{zi} = M'_{zi} + \frac{l^2}{60}(3w_{yi} + 2w_{yj}) \quad (\text{Eq. 7-34})$$

$$P_{xj} = P'_{xj} + \frac{l}{6}(w_{xi} + 2w_{xj}) \quad (\text{Eq. 7-35})$$

$$Q_{yj} = Q'_{yj} + \frac{l}{20}(3w_{yi} + 7w_{yj}) \quad (\text{Eq. 7-36})$$

$$Q_{zj} = Q'_{zj} + \frac{l}{20}(3w_{zi} + 7w_{zj}) \quad (\text{Eq. 7-37})$$

$$M_{xj} = M'_{xj} \quad (\text{Eq. 7-38})$$

$$M_{yj} = M'_{yj} - \frac{l^2}{60}(2w_{zi} + 3w_{zj}) \quad (\text{Eq. 7-39})$$

$$M_{zj} = M'_{zj} + \frac{l^2}{60}(2w_{yi} + 3w_{yj}) \quad (\text{Eq. 7-40})$$

7.5 Load Cases

The following table summarizes the basic load cases applied on the model.

Table 7-4 Load Cases

ID	Name	
LC1	Static Loads	Hydrostatic Load
		Self Weight
LC2	Wave Loads	Hydrodynamic Load
		Inertia Load

7.5.1 Static Loads

Hydrostatic load is transferred to the beam element as distributed line load or point load. Self-weight of the hull is modeled as line load for each hull girder member. Topside self-weight is modeled as point load at Topside COG point with dummy beams connected each node to the COG point.

7.5.2 Wave Loads

Hydrodynamic load is transferred to the beam element as distributed line load or point load in complex number format (which means phase information is included). Inertia load of the hull is modeled as complex-number line load for each hull girder member. Topside inertia load is modeled as complex-number point load at Topside COG point with dummy beams connected each node to the COG point.

Steepness of design wave has a limitation according to DNV-RP-C103 Column-Stabilized Units [7-2]. Wave steepness is defined by;

$$S = \frac{2\pi H}{gT^2} \quad (\text{Eq. 7-41})$$

The combination of wave height and wave period that are considered should imply a value of steepness that is less than the following limit;

$$S = \begin{cases} \frac{1}{7} & \text{for } T \leq 6s \\ \frac{1}{7 + \frac{0.93}{H_{100}}(T^2 - 36)} & \text{for } T > 6s \end{cases} \quad (\text{Eq. 7-42})$$

The wave height and period combinations on the steepness limit are given by;

$$S = \begin{cases} 0.22T^2 & \text{for } T \leq 6s \\ \frac{T^2}{4.5 + \frac{0.6}{H_{100}}(T^2 - 36)} & \text{for } T > 6s \end{cases} \quad (\text{Eq. 7-43})$$

8 Methodology - Weight Calculation

In this section, scantling calculation and weight estimation method is described.

8.1 Scantling Calculation

8.1.1 Plating

For the designated permanent ballast tank boundary structures and external shell plating, the following expression (per paragraph 3-2-2/9.3 of ABS MODU2008 Rules [8-1]) governs:

$$t = \frac{sk\sqrt{qh}}{254} + 2.5 \text{ mm}$$
$$\geq \frac{s}{150} + 2.5 \text{ mm}$$

(Eq. 8-1)

- t = plate thickness (mm)
- s = spacing of stiffeners (mm)
- k = factor based on aspect ratio of panel
- = $(3.075\sqrt{\alpha} - 2.077)/(\alpha + 0.272)$
- = 1.0
- α = Aspect ratio of the panel (longer side/shorter side)
- q = $235/Y$
- Y = specified minimum yield strength of material (N/mm²)
- h = greatest of the following distances (m) from the lower edge of plate to:
- i. a point representing the design draft is used;
 - ii. a point located two-thirds of the distance from top of tank to the top of overflow;
 - iii. a point located 0.91 m above the top of the tank.

For areas subject to wave immersion, a minimum design head of 6.1 m is required. For all other subdivision boundary structures (such as internal watertight bulkheads and flats in void spaces), the following expression (per paragraph 3-2-2/7.3 of ABS MODU2008 Rules) is used:

$$t = \frac{sk\sqrt{qh}}{290} + 1.5 \text{ mm}$$
$$\geq \frac{s}{200} + 2.5 \text{ mm}$$

(Eq. 8-2)

8.1.2 Stiffener

For stiffeners on the designated permanent ballast tank boundary structures and external shells, the following expression (per paragraph 3-2-2/9.5 of ABS MODU2008 Rules [8-1]) for minimum scantling was used:

$$SM = fchsl^2 \text{ cm}^3 \quad (\text{Eq. 8-3})$$

f	=	7.8	
c	=	0.9	For stiffeners having clip attachments to deck or flat at to the ends or having such attachments at one end with the other end supported by girders.
	=	1.00	for stiffeners supported at both ends by girders
h	=	Greatest of the distances (m) from the middle of l to the same point to which h for plating is measured (1-1).	
s	=	spacing of stiffeners (m)	
l	=	length (m) between supports, where brackets are fitted at shell, deck or bulkhead supports, and the brackets are in accordance with 3-2-2/Table 2 of ABS MODU2008 Rules and have a slope of approximately 45 deg, the length l may be measured to a point on the bracket located at a distance from the toe equal to 25% of the length of the bracket.	

For stiffeners on all other subdivision boundary structures (such as column internal watertight bulkheads and flats in void spaces), the following expression (per paragraph 3-2-2/7.5 of ABS MODU2008 Rules) for minimum scantling were used:

$$SM = fchsl^2 \text{ cm}^3 \quad (\text{Eq. 8-4})$$

f	=	7.8	
c	=	0.56	For stiffeners having clip attachments to deck or flat at to the ends or having such attachments at one end with the other end supported by girders.
	=	0.60	for stiffeners supported at both ends by girders
h	=	Greatest of the distances (m) from the middle of l to the same point to which h for plating is measured (1-2). where the distance is less than 6.1 m, h is to be taken as 0.8 times the distance in m plus 1.22.	

Other parameters are defined similarly to those in previous expression

8.2 Weight estimation

The weight is estimated from the calculated scantling with applying factors for transverse and tertiary members.

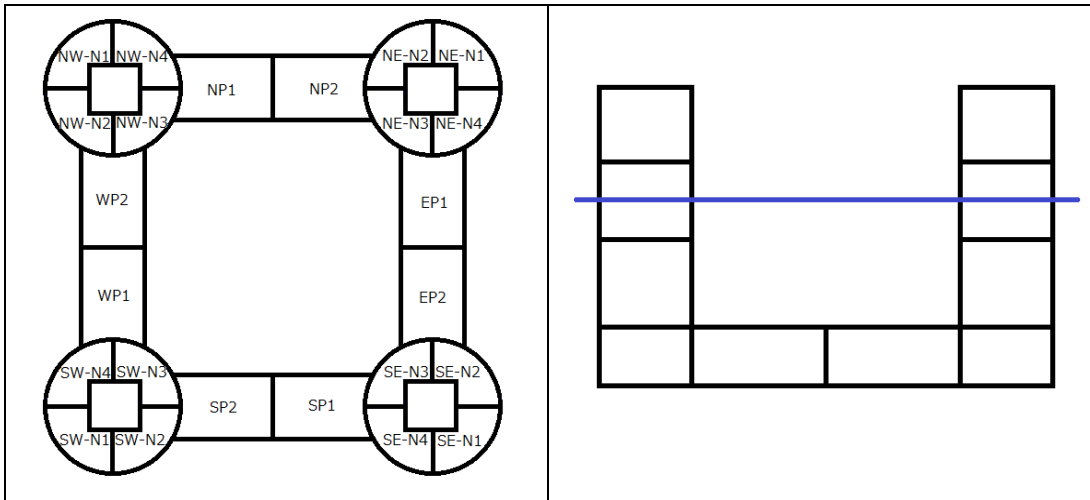


Figure 8-1 Compartment assumption for CTLP

Table 8-1 Structural Members for Conventional TLP

Structure		Member
Pontoon	Bottom	Plate/Stiffener/Transverse
	Inboard Shell	Plate/Stiffener/Transverse
	Outboard Shell	Plate/Stiffener/Transverse
	Top	Plate/Stiffener/Transverse
	Center Bulkhead	Plate/Stiffener/Transverse
Node	Bottom	Plate/Stiffener/Transverse
	Outer Shell	Plate/Stiffener/Transverse
	Inner Bulkhead	Plate/Stiffener/Transverse
	Access Shaft Bulkhead	Plate/Stiffener/Transverse
	Flat	Plate/Stiffener/Transverse
Column 1	Outer Shell	Plate/Stiffener/Transverse
	Inner Bulkhead	Plate/Stiffener/Transverse
	Access Shaft Bulkhead	Plate/Stiffener/Transverse
	Flat	Plate/Stiffener/Transverse
Column 2	Outer Shell	Plate/Stiffener/Transverse

	Inner Bulkhead	Plate/Stiffener/Transverse
	Access Shaft Bulkhead	Plate/Stiffener/Transverse
	Flat	Plate/Stiffener/Transverse
Column 3	Outer Shell	Plate/Stiffener/Transverse
	Inner Bulkhead	Plate/Stiffener/Transverse
	Access Shaft Bulkhead	Plate/Stiffener/Transverse
	Column Top	Plate/Stiffener/Transverse

On top of this structural weight, user-input outfitting, machinery, consumables, and weight margins are included in the total weight. Total weight, center of gravity and moment of inertia are calculated.

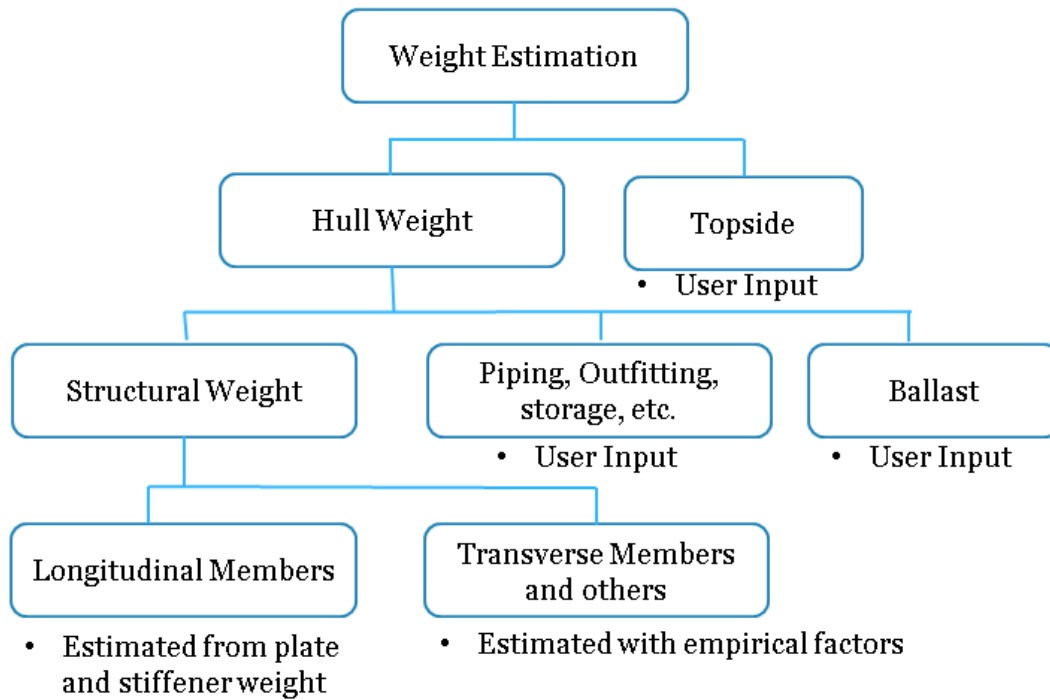


Figure 8-2 Weight Calculation Method

9 Calculation Result

9.1 Calculation Condition

The program is tested for the following environmental conditions. There are three environmental data:

- Gulf of Mexico metocean condition before the hurricane attack in 2005 (pre-2005)[9-1]
- Gulf of Mexico metocean condition after the hurricane attack in 2005 (post-2005) [9-2]
- A Southeast Asian environmental condition

These environmental data are summarized in Table 9-1. The total of hull outfitting, equipment and piping weights) is assumed to be 2,000MT. Topside and riser conditions are summarized in Table 9-2 and 9-3.

Table 9-1 Environmental Condition

	Case 1	Case 2			Case 3		
	GoM	GoM (Post-2005)			Southeast Asia		
Extreme	Extreme	Operating	Extreme	Survival	Operating	Extreme	Survival
Return Period	100yr	1yr	100yr	1000yr	1yr	100yr	1000yr
Wave height Hs	12.2m	10.0m	15.8m	19.8m	5.8m	7.6m	9.1m
Peak period Tp	14.2s	13.0s	15.4s	17.2s	12.5s	14.1s	15.4s
Wind Speed Vw	39.9m/s	33m/s	48m/s	60m/s	18.9m/s	22.6m/s	25.8m/s
Current Speed Vc	1.7m/s	1.7m/s	2.4m/s	3.0m/s	1.4m/s	1.8m/s	2.0m/s
Water level L	0.9m	0.4m	0.6m	0.8m	0.42m	0.55m	0.66m

The calculation condition for topside is as follows:

Table 9-2 Topside Condition

Topside weight	20,000MT
Topside vertical center of gravity	10 m from BOS
Footprint	65 m x 65 m
Total Height	20 m
Structure	See figure 9-1 Beam 1200x500x25x50 Pillar/Brace ϕ 1000x25

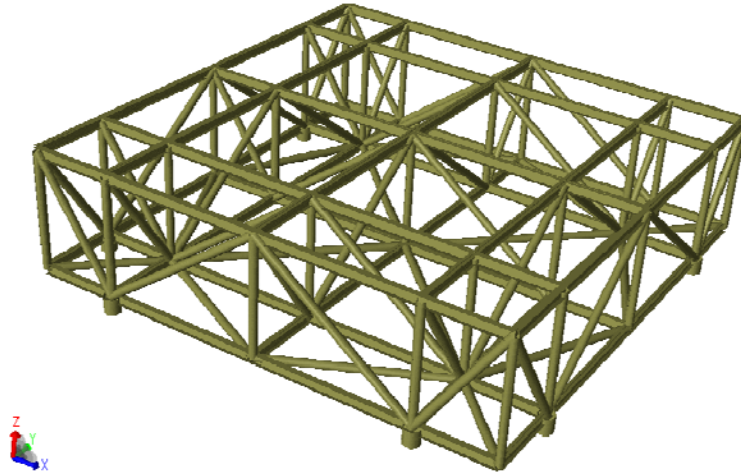


Figure 9-1 Topside Model

The followings are the riser properties:

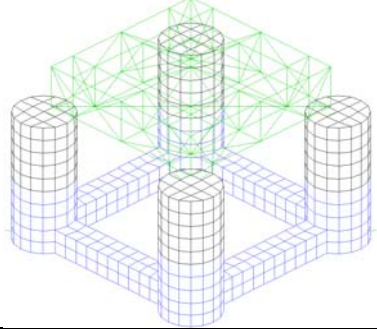
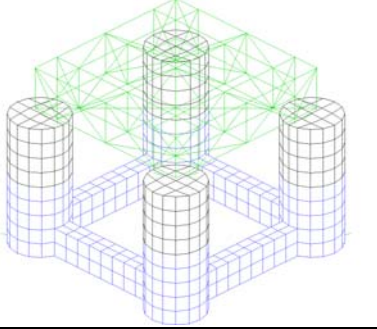
Table 9-3 Riser Condition

TTR	
Number	10
Pretension	1,000 kN for each
Stiffness	1,000 kN/m for each
Length	1050 m
SCR	
Number	4
Pretension	3,000 kN for each
Fairlead Angle	15 deg

9.2 GoM Pre-2005 condition (Case 1)

The calculation results of the GoM Pre-2005 by ASA and GA are summarized in the table below. Hull total weight was both about 14,000MT and tendon pretension was about 21%-22%. Optimization result of GA and ASA matched well.

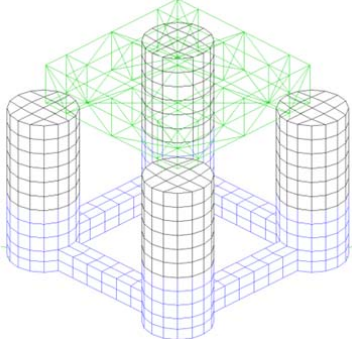
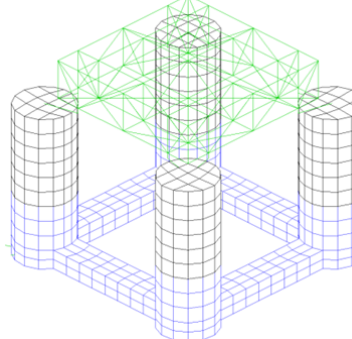
Table 9-4 Calculation result for GoM pre-2005 (Case1)

	ASA	GA
Hull Shape		
Column diameter	21.2 m	21.0 m
Column distance	67.2 m	61.8 m
Pontoon breadth	9.3 m	6.7 m
Pontoon height	8.7 m	10.3 m
Draft	23.5 m	26.3 m
Column height	47.3 m	48.0 m
Hull weight	14,153MT	13,920MT
Pretension Ratio	22%	21%

9.3 GoM Post-2005 condition (Case 2)

The calculation results of the GoM Post-2005 by ASA and GA are summarized in the table below. Hull total weight was both about 18,000MT and tendon pretension was about 37%. Column height was 58m for both.

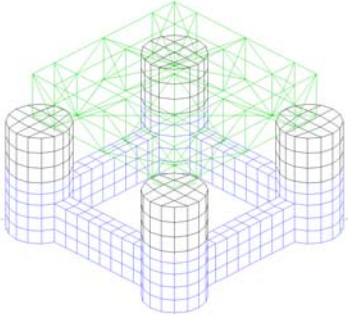
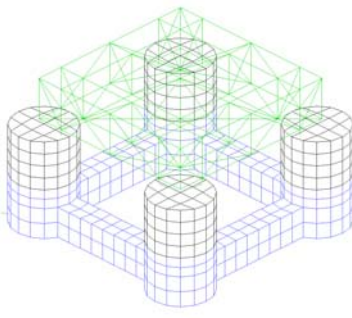
Table 9-5 Calculation result for GoM post-2005 (Case 2)

	ASA	GA
Hull Shape		
Column Diameter	24.7 m	23.2 m
Column Distance	65.2 m	70.5 m
Pontoon breadth	8.5 m	11.4 m
Pontoon height	8.2 m	7.4 m
Draft	24.4 m	25.0 m
Column height	57.8 m	59.8 m
Hull weight	17,425MT	17,903MT
Pretension Ratio	29%	29%

9.4 GoM Post-2005 condition (Case 3)

The calculation results of the Southwest Asian condition by ASA and GA are summarized in the table below. Hull total weight was both about 12,650MT and tendon pretension was about 20%. Column height was 36m-38m.

Table 9-6 Calculation Result for Southeast Asian Condition (Case 3)

	ASA	GA
Hull Shape		
Column Diameter	21.3 m	23.0 m
Column Distance	60.9 m	61.8 m
Pontoon breadth	6.6 m	8.7 m
Pontoon height	13.8 m	11.0 m
Draft	21.9 m	18.0 m
Column height	38.0 m	35.6 m
Hull weight	12,658MT	12,678MT
Pretension Ratio	21%	20%

10 Discussion

10.1 Comparison with an existing TLP hull shape

The followings are the comparison of case 1 with an existing TLP (Brutus TLP). Similar hull proportion was obtained. Hull weight of the calculation result was slightly smaller than Brutus TLP.

Table 10-1 Comparison with an existing TLP

	Brutus TLP	GoM pre-2005 (ASA)
Column Diameter	20 m	21.2 m
Column Distance	60 m	67.2 m
Pontoon Width	11 m	9.3 m
Pontoon Height	7 m	8.7 m
Draft	25 m	23.5 m
Column Length	51 m	47.3 m
Hull Steel Weight	12,900 MT	12,153MT
Hull Total Weight		14,153MT

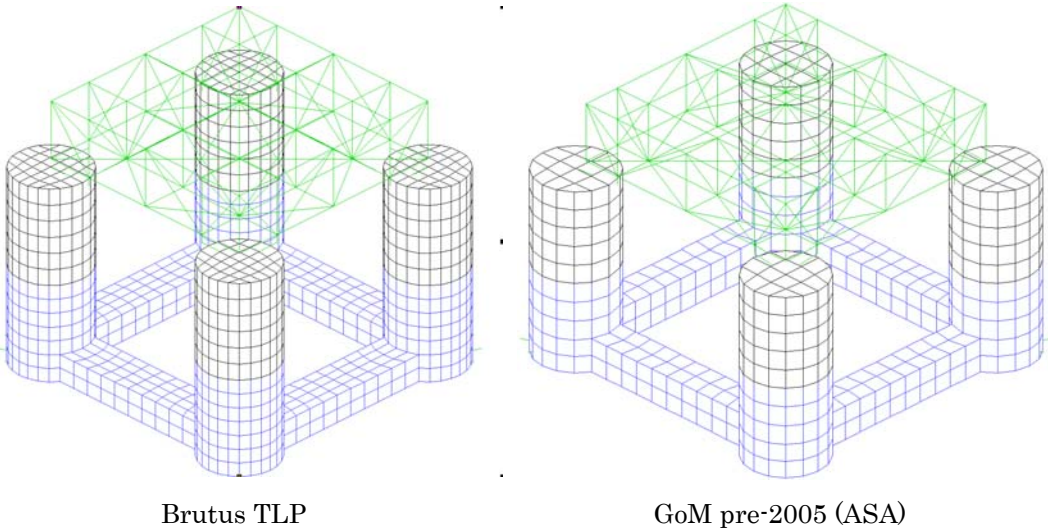


Figure 10-1 Comparison with an existing TLP

10.2 Pre v.s. Post Hurricane Condition

The following table and graph shows the comparison of pre- and post-Hurricane condition. Column height of post-Hurricane condition became much larger than pre-Hurricane condition. As a result, hull weight of post-Hurricane was 23% larger.

Table 10-2 Comparison between Pre- and Post-Hurricane Hull Shape

	GoM Pre-2005 (ASA)	GoM Post-2005 (ASA)
Column Diameter	21.2 m	24.7 m
Column Distance	67.2 m	65.2 m
Pontoon Width	9.3 m	8.5 m
Pontoon Height	8.7 m	8.2 m
Draft	23.5 m	24.4 m
Column Length	47.3 m	57.8 m
Hull Total Weight	14,153MT	17,425MT
Pretension Ratio	22%	29%

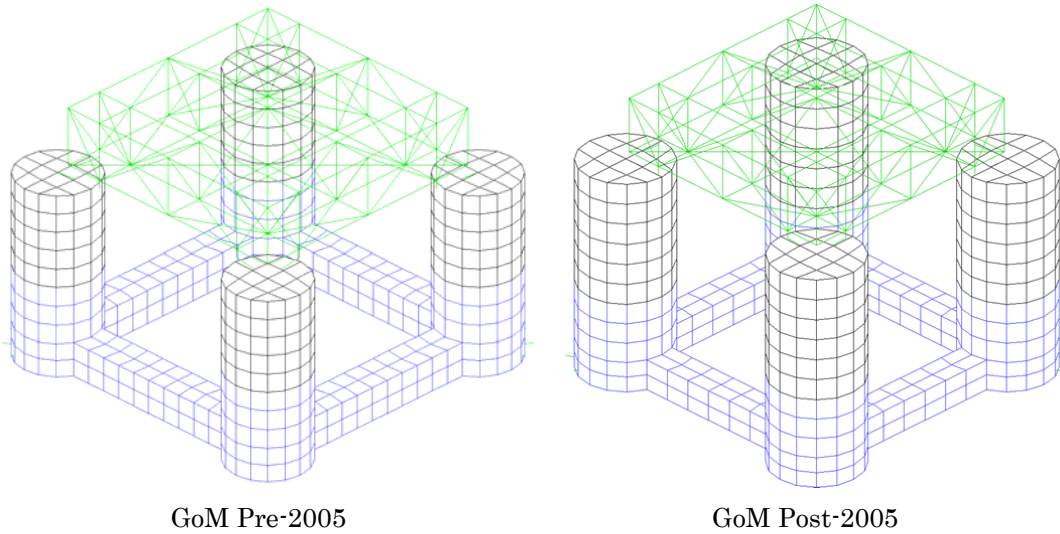


Figure 10-2 Comparison between Pre- and Post-Hurricane Hull Shape

10.3 Hash v.s. Mild Environment

This is the comparison between hash (GoM post-Hurricane) and mild (SE Asia) environment condition. The column became significantly shorter in mild condition. This is because of airgap criteria. The optimized hull weight has 38% difference between two conditions.

Table 10-3 Comparison between Pre- and Post-Hurricane Hull Shape

	GoM Post-2005 (ASA)	Southeast Asia (ASA)
Column Diameter	24.7 m	21.3 m
Column Distance	65.2 m	60.9 m
Pontoon Width	8.5 m	6.6 m
Pontoon Height	8.2 m	13.8 m
Draft	24.4 m	21.9 m
Column Length	57.8 m	38.0 m
Hull Weight	17,425MT	12,658MT
Tendon Pretension Ratio	29%	21%

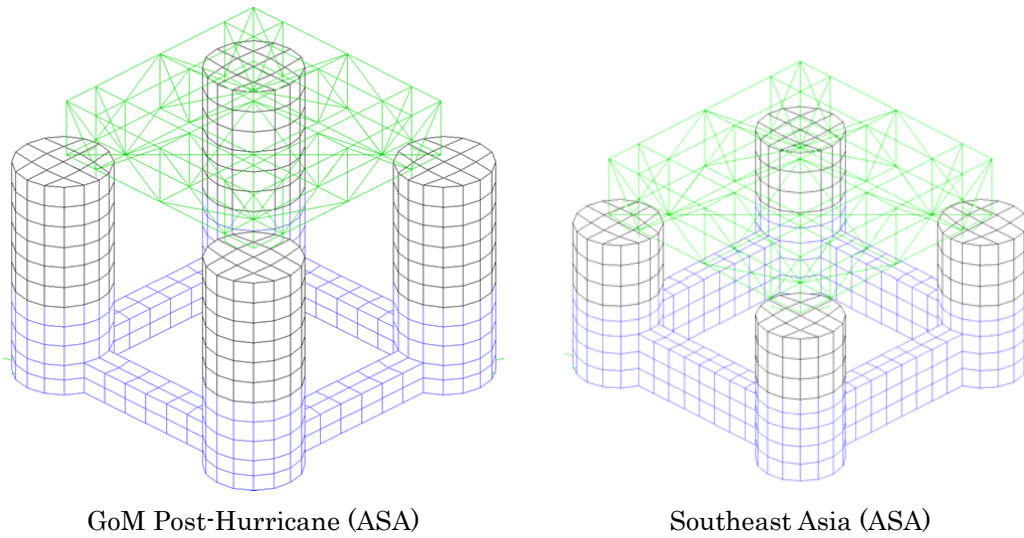


Figure 10-3 Comparison of Hull Shape for hash and mild environment

10.4 Comparison with hydrodynamic optimization result

This result shows the effect of selected objective function. Objective function was set to tendon tension RMS, and optimized hull shape was calculated by applying post-Hurricane condition. Initial criteria were considered into this calculation. As a result, pontoon height became significantly shallow and draft became significantly deep. The final hull weight was 23% larger.

Table 10-4 Comparison with hydrodynamic optimization result

	Weight Minimum	Response Minimum
Column Diameter	24.7 m	21.1 m
Column Distance	65.2 m	70.4 m
Pontoon Width	8.5 m	18.1 m
Pontoon Height	8.2 m	3.1 m
Draft	24.4 m	42.3 m
Column Length	57.8 m	69.3 m
Hull Weight	17,425MT	21,358 MT

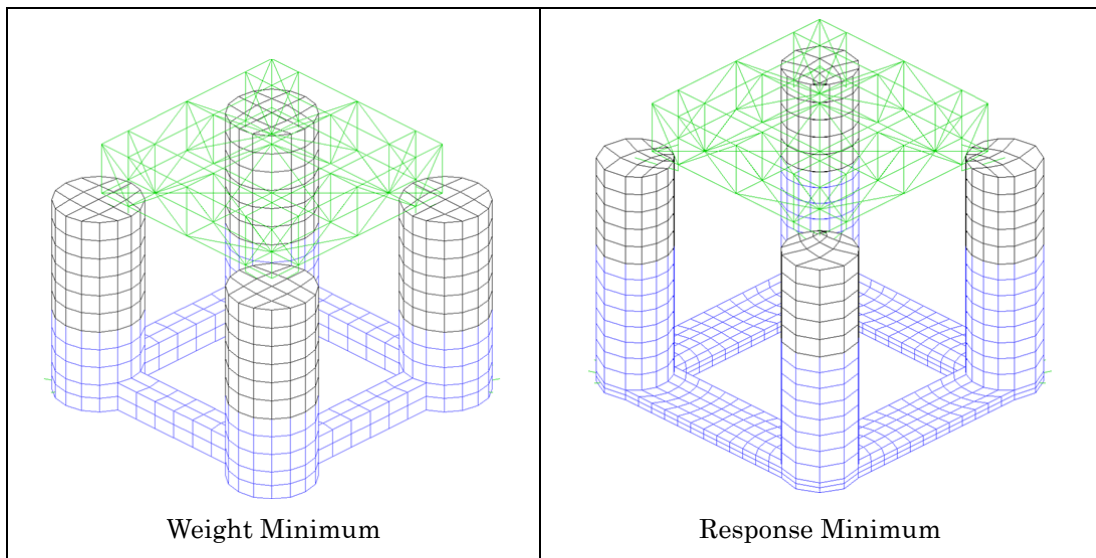


Figure 10-4 Comparison with hydrodynamic optimization result

10.5 Optimization process for GoM pre-2005

The following Figures show the process of optimization. The red and black lines show how the variables were optimized by each process for pre-2005 condition. The green dots represent the area constrained by criteria 1, as these dots are generated by uniform random numbers and screened by criteria 1. The light-blue dots show the area constrained by criteria 2. The blue points are also generated by random numbers and screened by criteria 3 to see the effect of each constraint condition. Hull dimensions of existing TLPs (Brutus TLP, Auger TLP) are also plotted in the same graph for comparison.

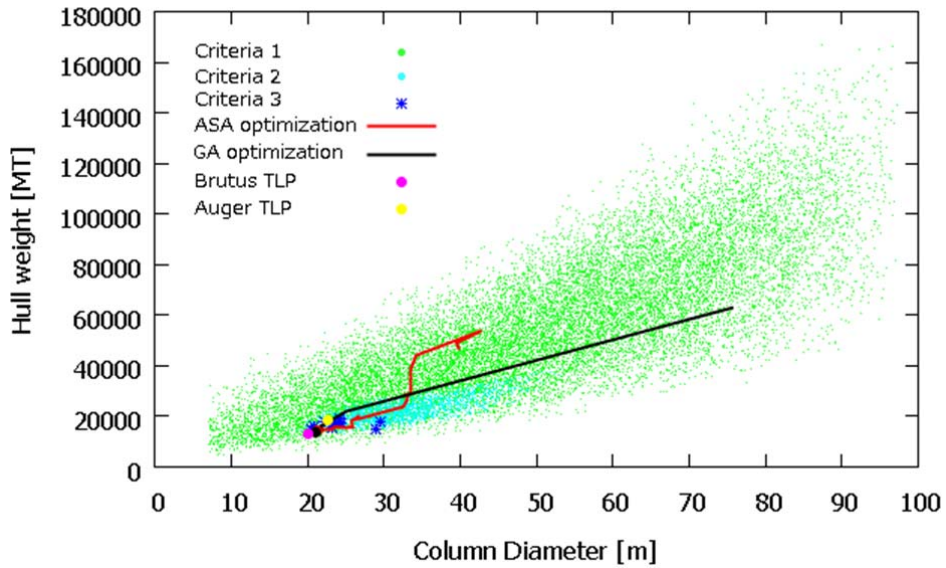


Figure 10-5 Column diameter v.s. Hull total weight (Case 1)

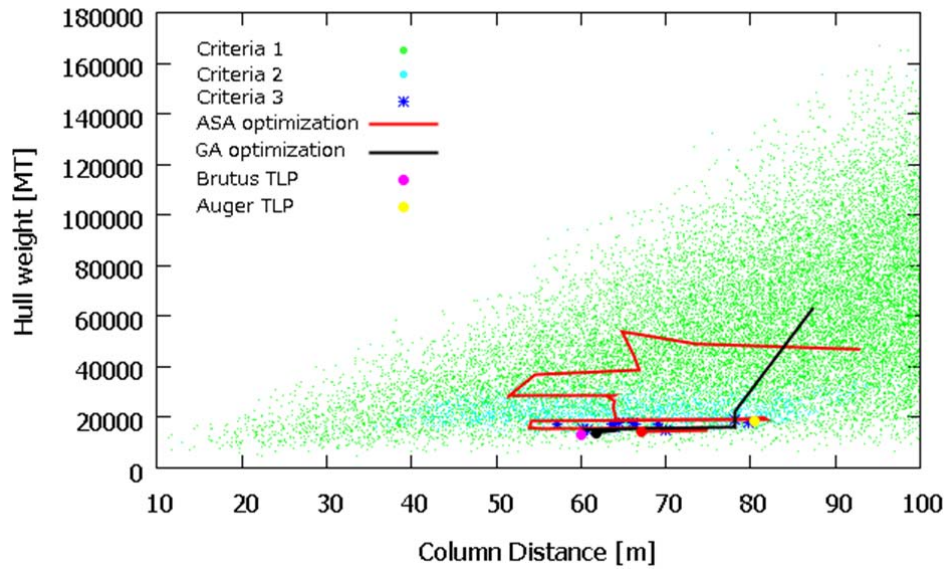


Figure 10-6 Column distance v.s. Hull total weight (Case 1)

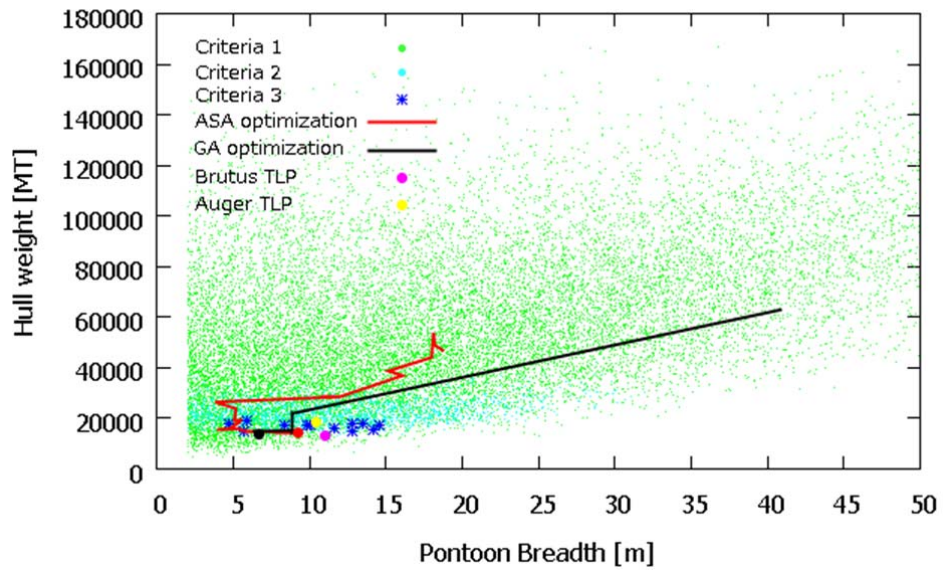


Figure 10-7 Pontoon breadth v.s. Hull weight (Case 1)

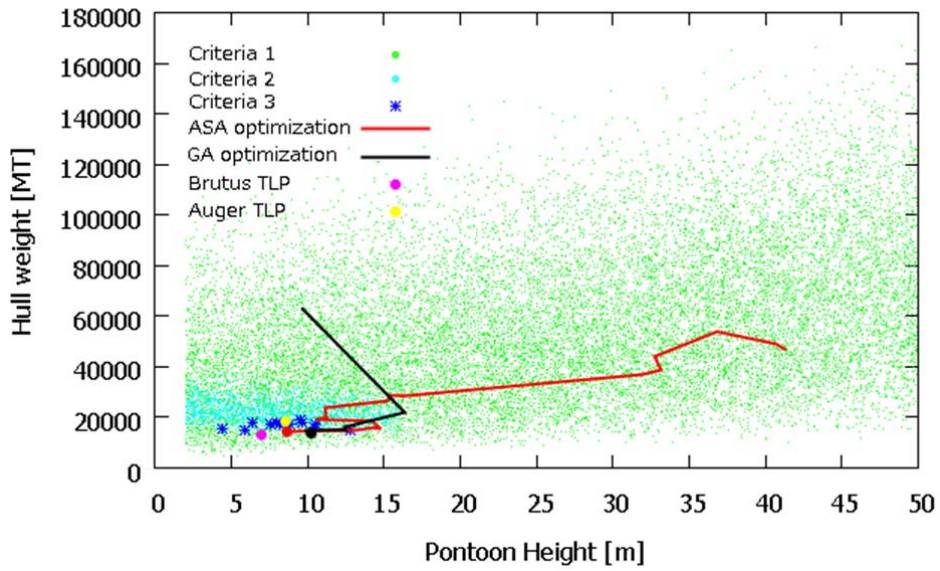


Figure 10-8 Pontoon height v.s. Hull weight (Case 1)

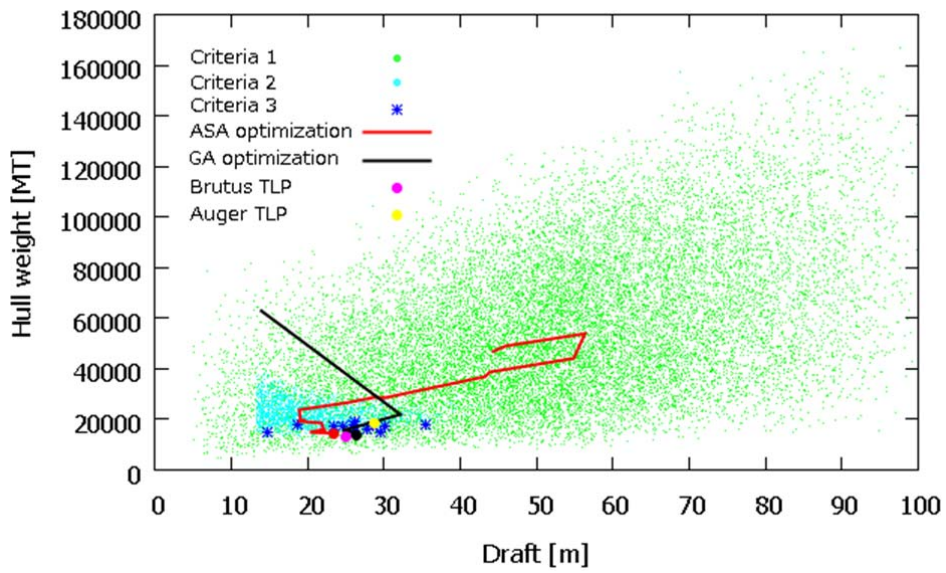


Figure 10-9 Draft v.s. Hull weigh (Case 1)

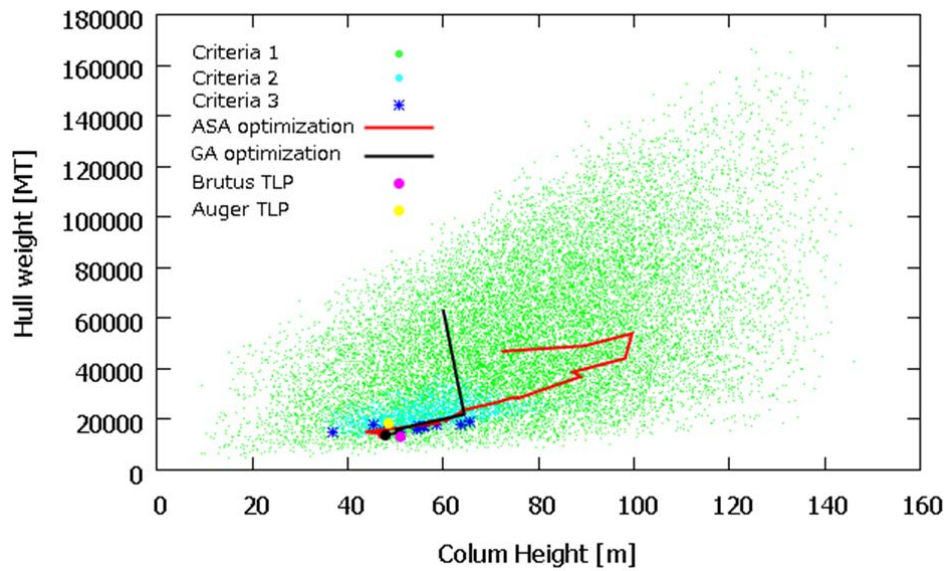


Figure 10-10 Column Height v.s. Hull weight (Case 1)

10.6 Optimization process for GoM post-2005

The following Figures show the process of optimization for post-2005 condition.

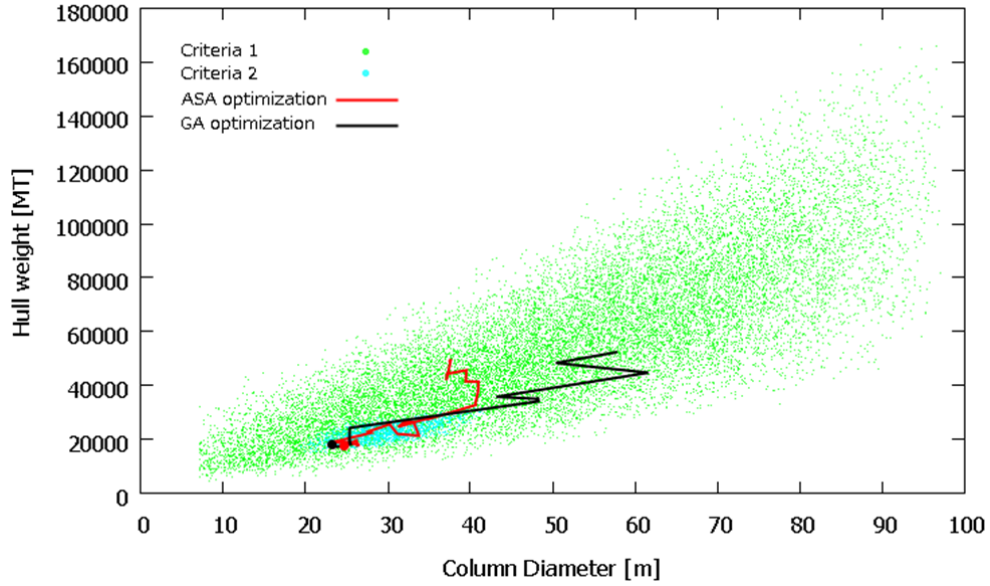


Figure 10-11 Column diameter v.s. Hull weight (Case 2)

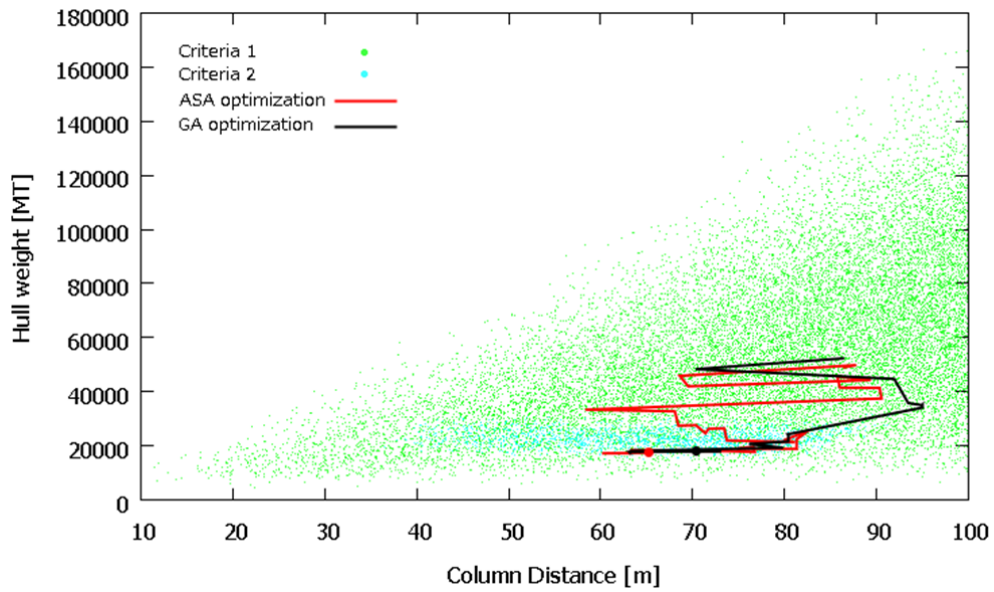


Figure 10-12 Column distance v.s. Hull weight (Case 2)

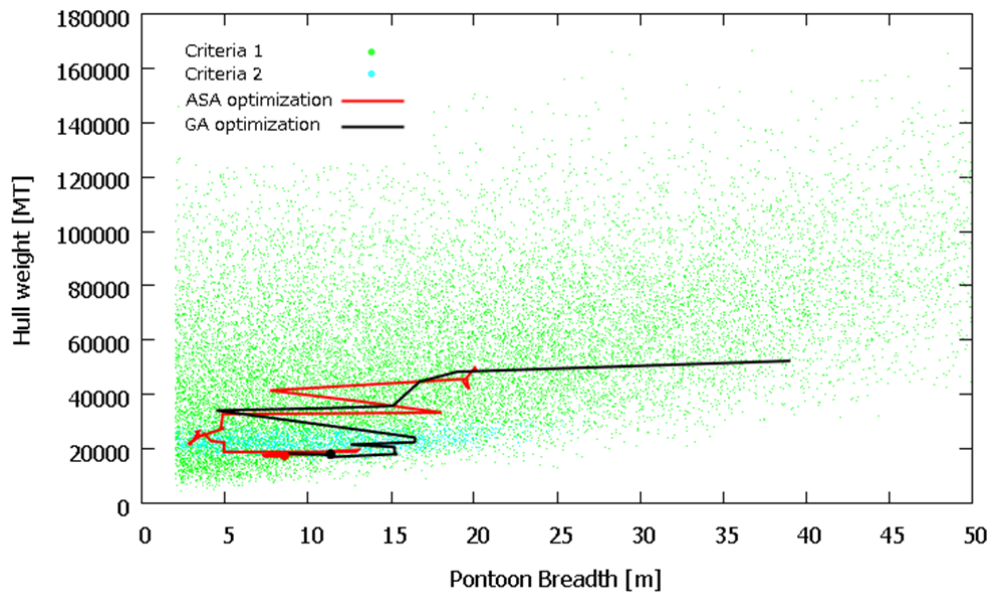


Figure 10-13 Pontoon width v.s. Hull weight (Case 2)

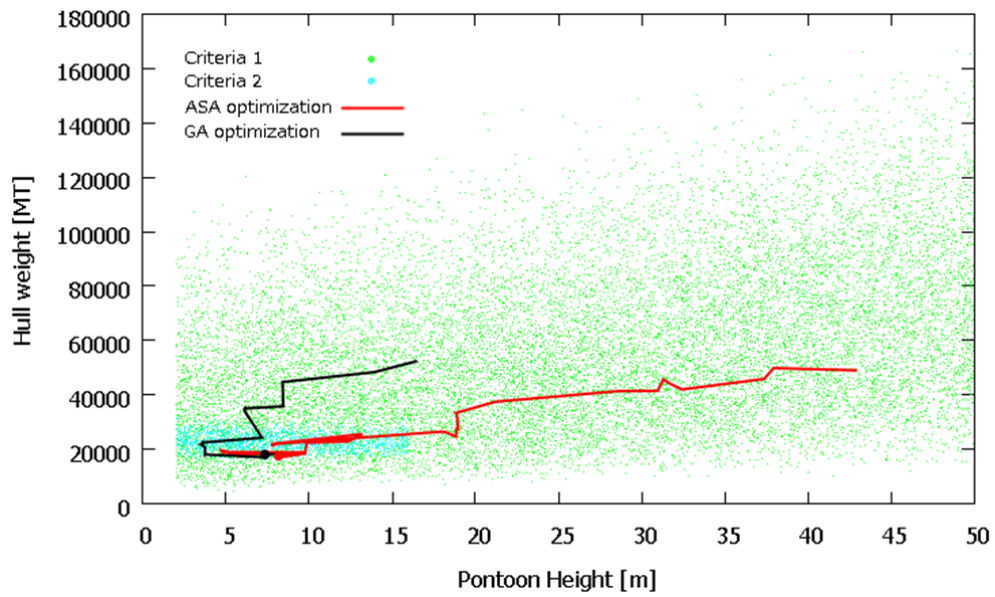


Figure 10-14 Pontoon Height v.s. Hull weight (Case 2)

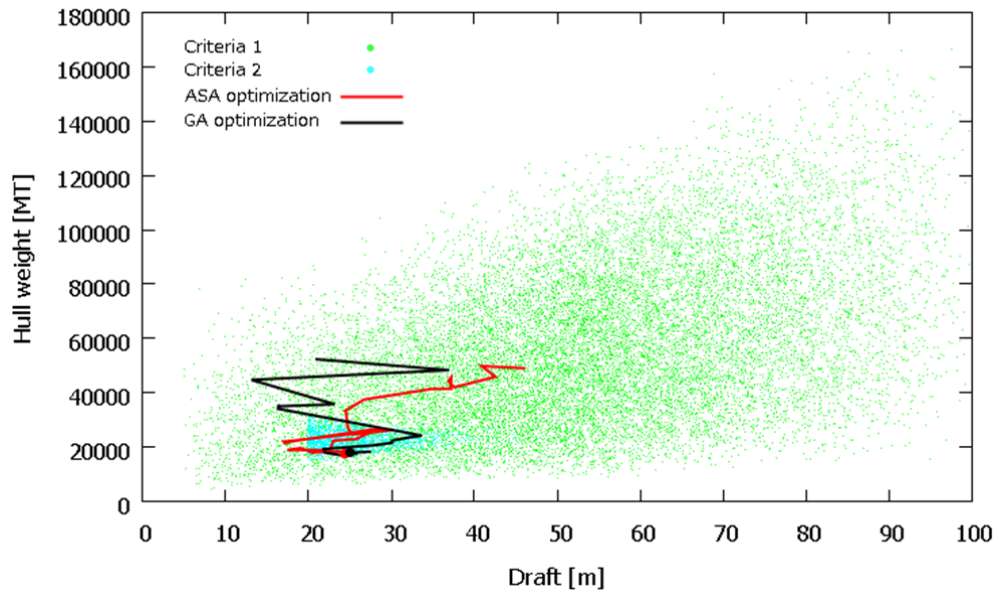


Figure 10-15 Draft v.s. Hull weight (Case 2)

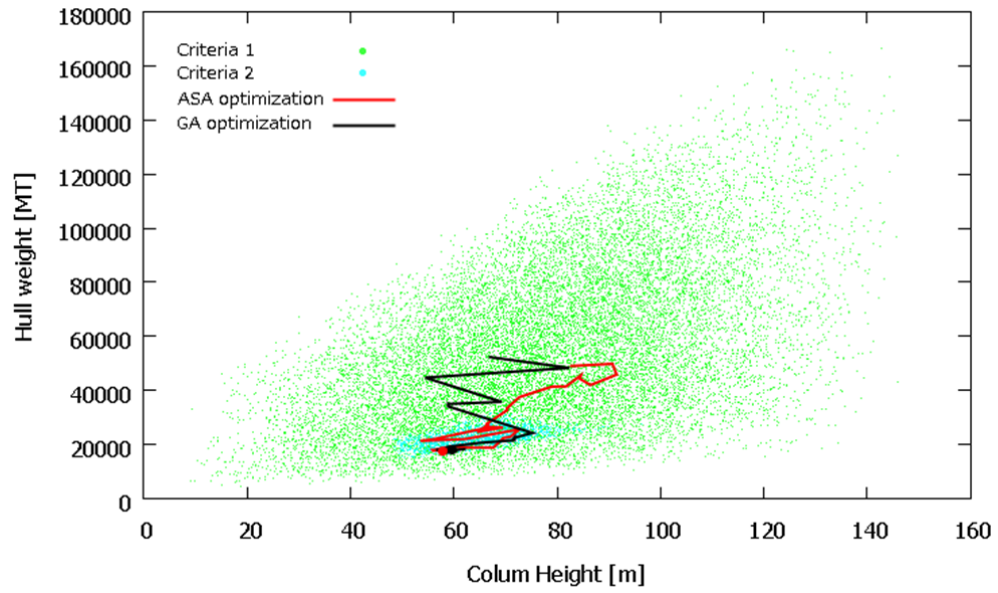


Figure 10-16 Column Height v.s. Hull weight (Case 2)

10.7 Optimization process for Southeast Asian Condition

The following Figures show the process of optimization for Southeast Asian condition.

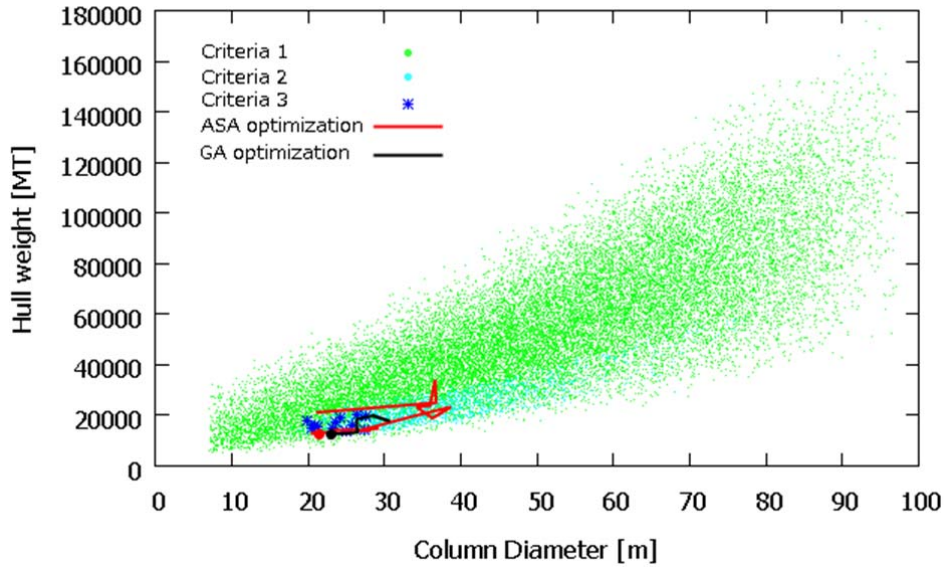


Figure 10-17 Column diameter v.s. Hull weight (Case 3)

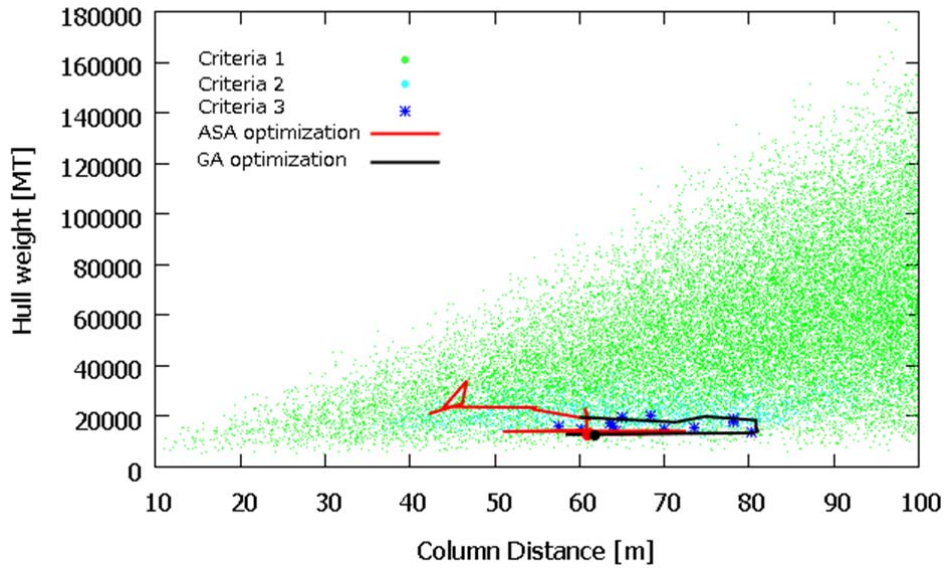


Figure 10-18 Column distance v.s. Hull weight (Case 3)

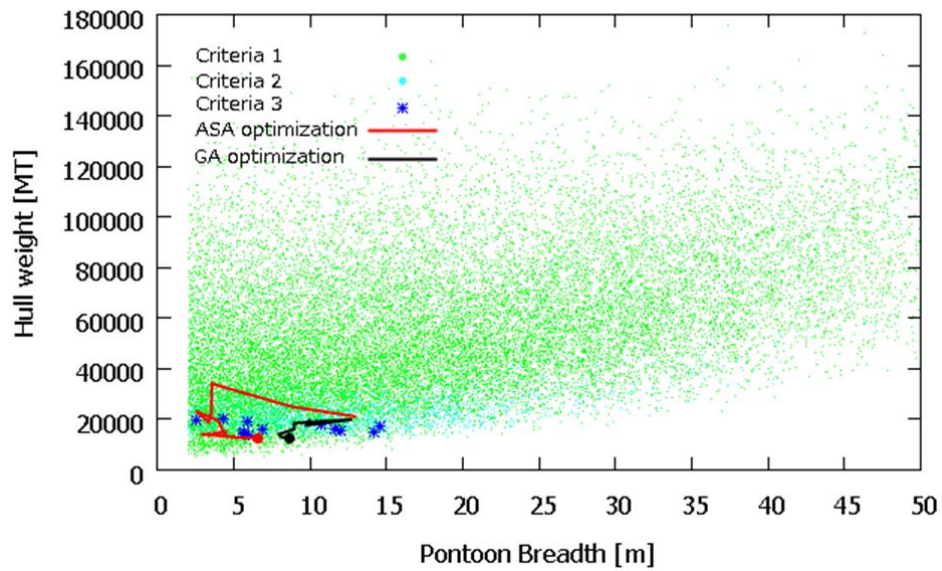


Figure 10-19 Pontoon width v.s. Hull weight (Case 3)

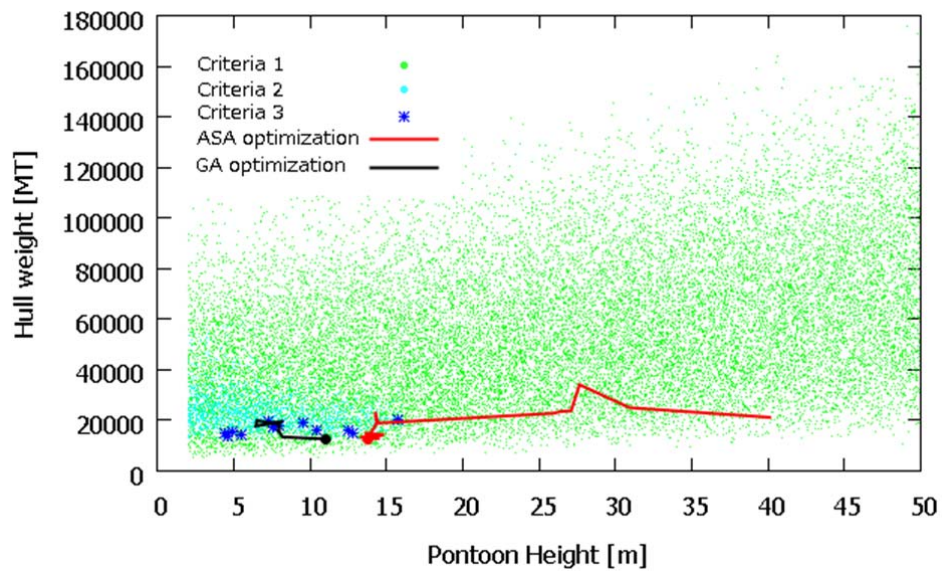


Figure 10-20 Pontoon Height v.s. Hull weight (Case 3)

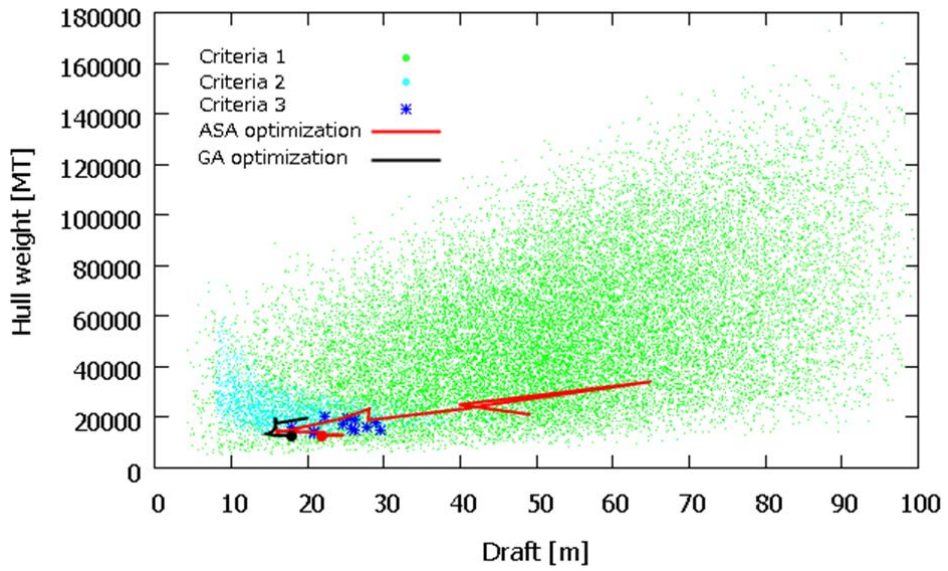


Figure 10-21 Draft v.s. Hull weight (Case 3)

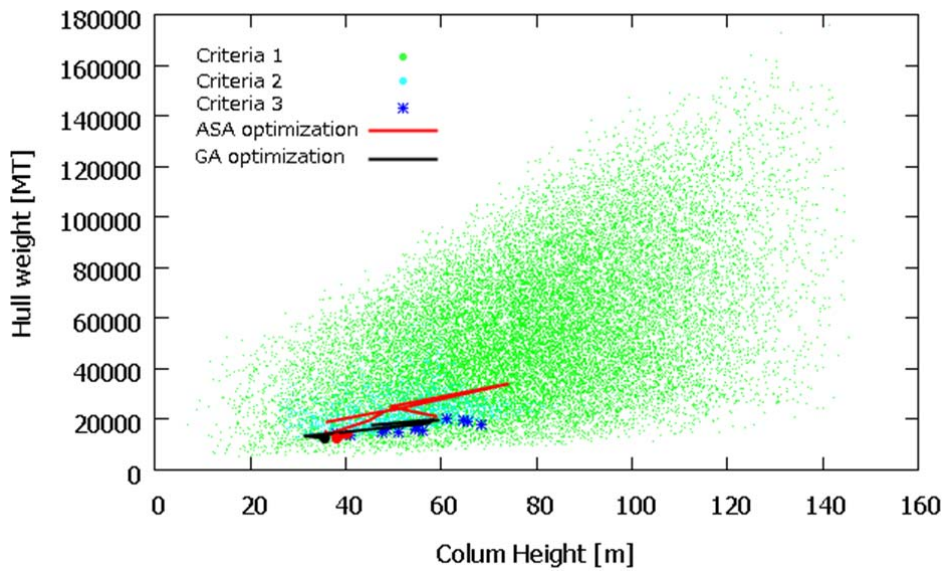


Figure 10-22 Column Height v.s. Hull weight (Case 3)

10.8 Study on Criteria – Pre-2005 condition

The following chart shows region governed by each criteria. The green, light blue and blue points are representing the territory to meet geometry criteria, hull sizing criteria and design criteria. This graph is plotted by generating random number and evaluating each criterion.

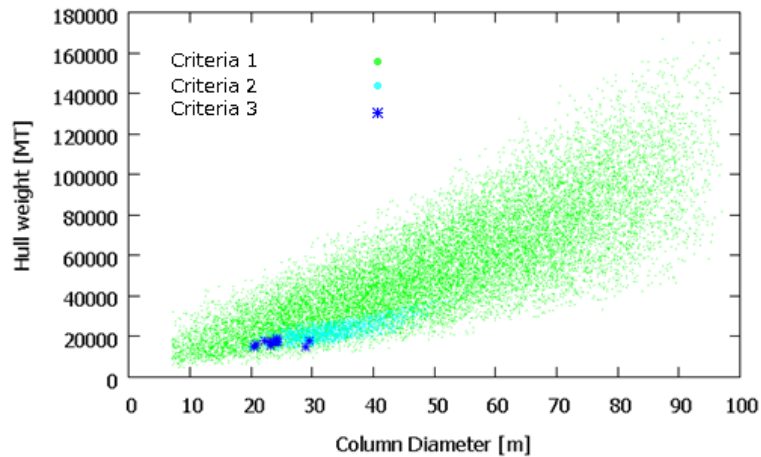


Figure 10-23 Criteria 1, 2, & 3 (Case 1)

The following plots show the territories of each hull sizing constraint condition. Intersection of these is the hull sizing criteria.

- Ballast amount (>5% of displacement)
- Installation stability ($GM > 2m$)
- Quayside stability ($GM > 2m$)
- Deck post location
- Airgap estimation
- Tendon pretension (5% -50% of displacement)

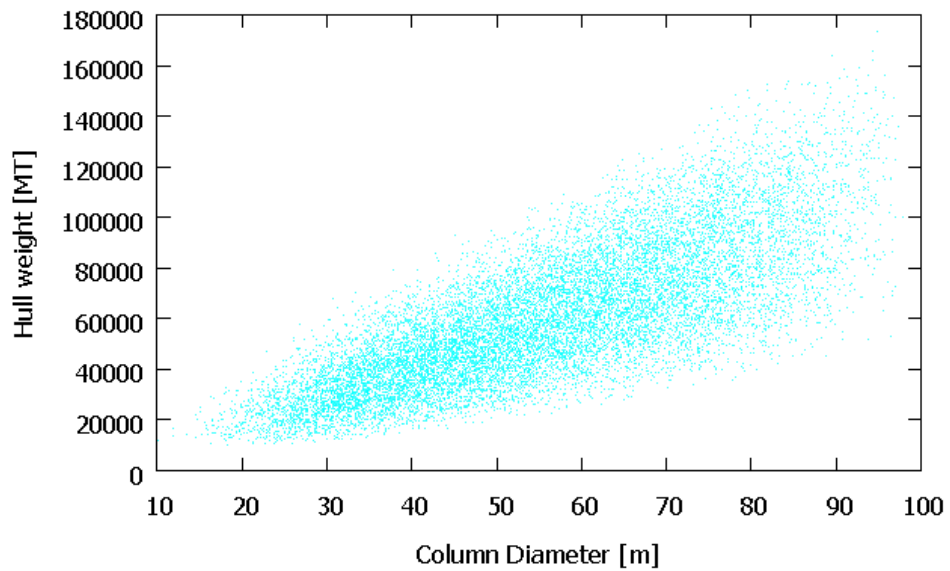


Figure 10-24 Ballast Amount Condition (Case 1)

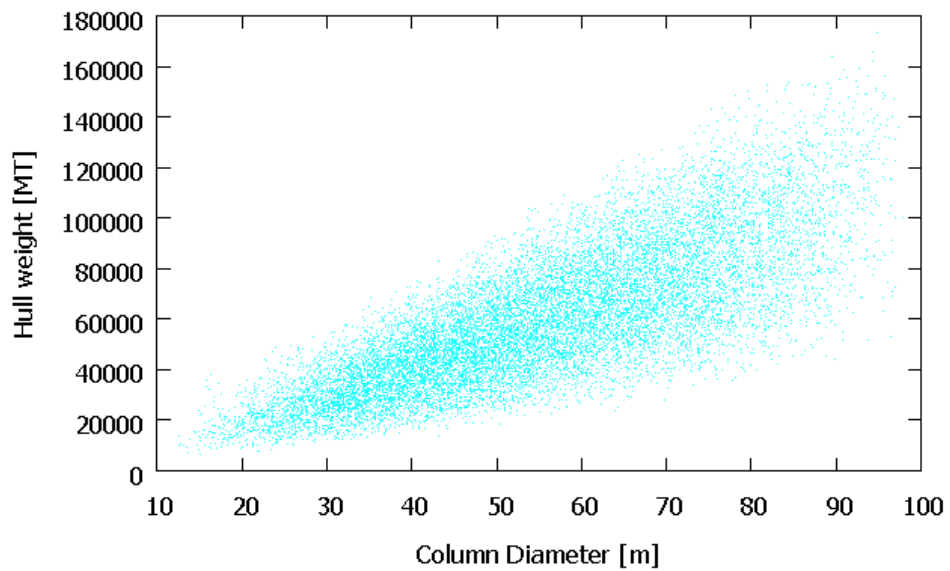


Figure 10-25 Installation Stability Condition (Case 1)

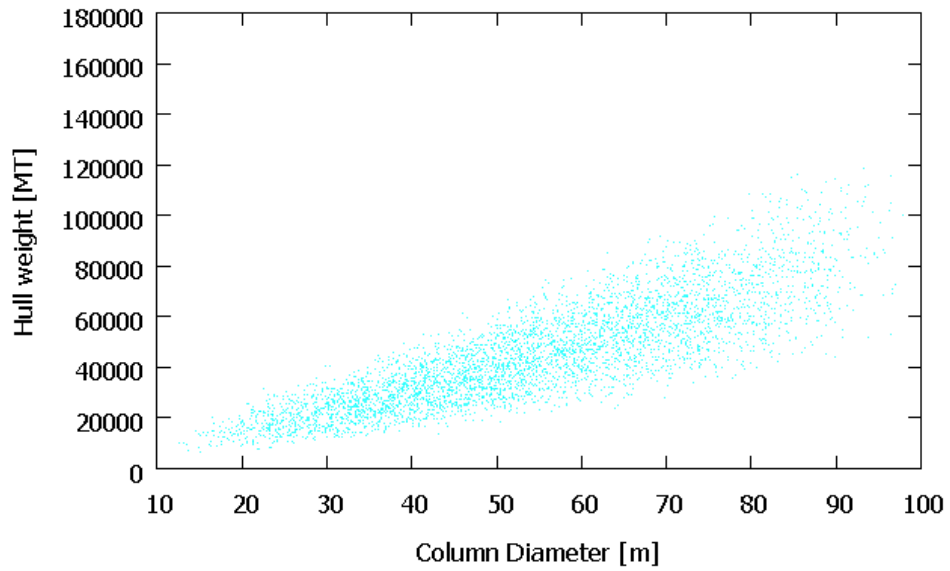


Figure 10-26 Quayside stability Condition (Case 1)

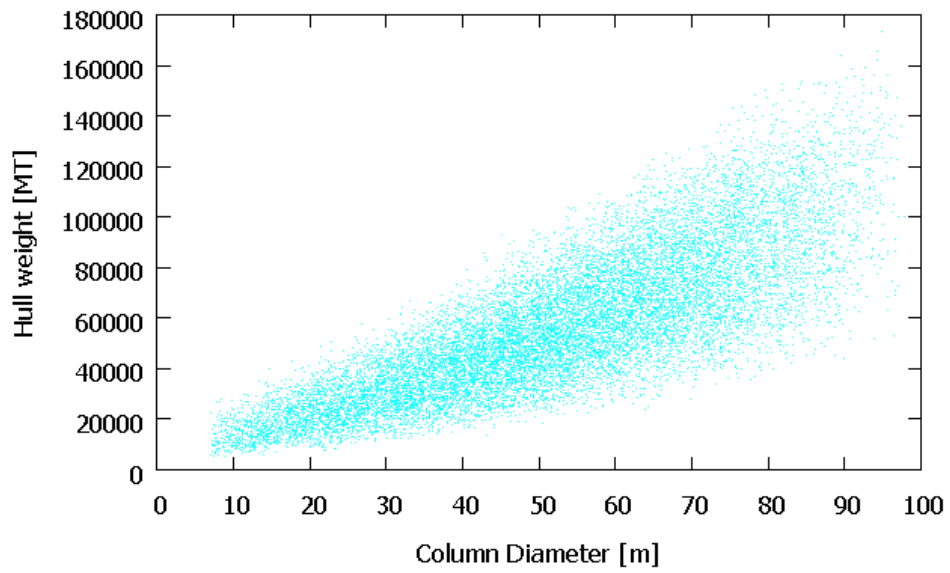


Figure 10-27 Deck post location Condition (Case 1)

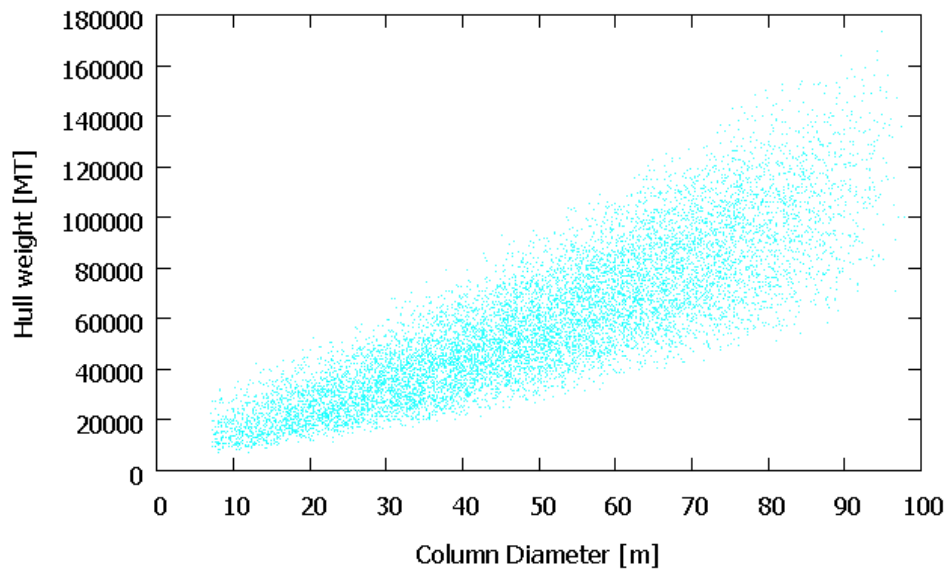


Figure 10-28 Airgap Condition (Case 1)

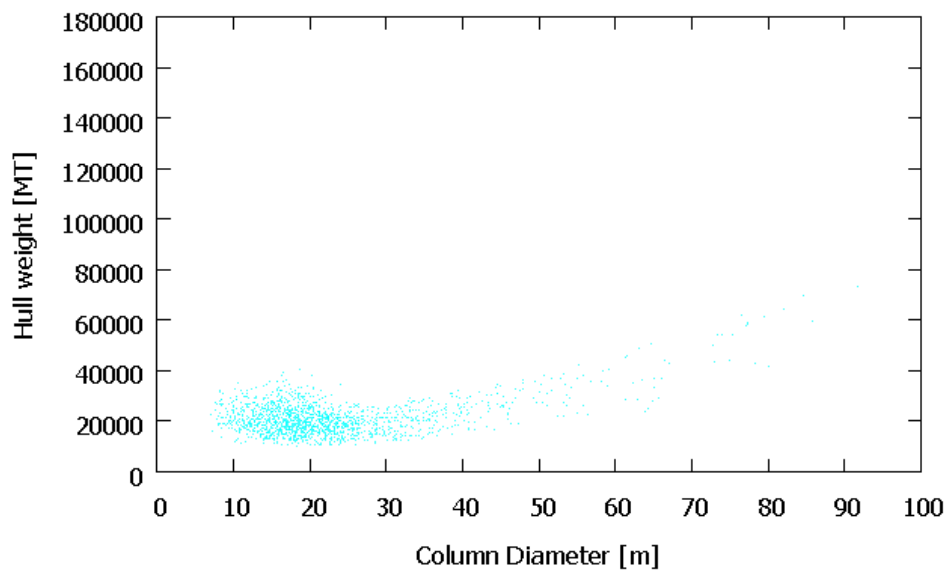


Figure 10-29 Tendon Pretension Condition (Case 1)

The following plots show the territories of each design constraint condition. Intersection of these is the design criteria.

- Natural period (<4.5s)
- Max offset (<10%-14% of water depth)
- Minimum Tendon Tension(>0)
- Airgap (>0)
- Tendon strength
- Hull strength

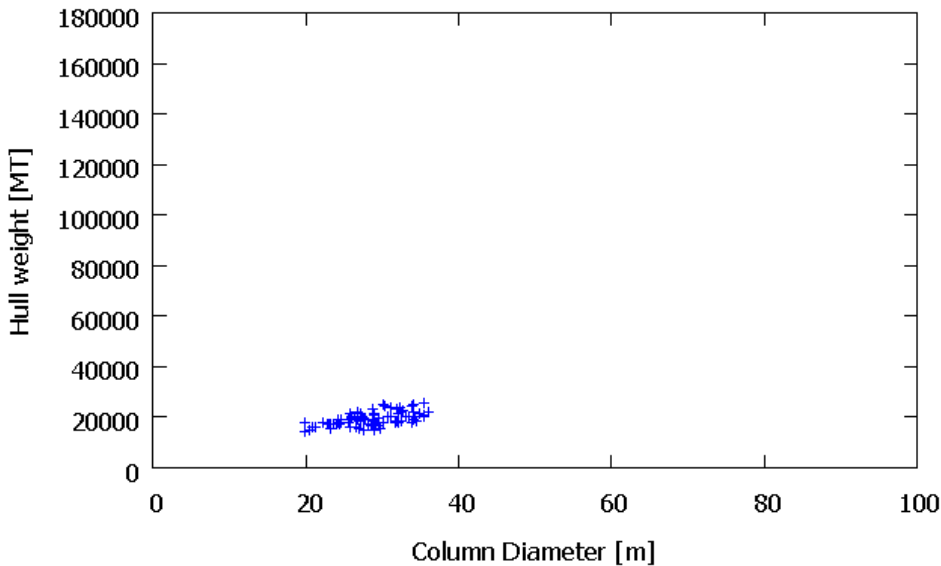


Figure 10-30 Natural Period Condition (Case 1)

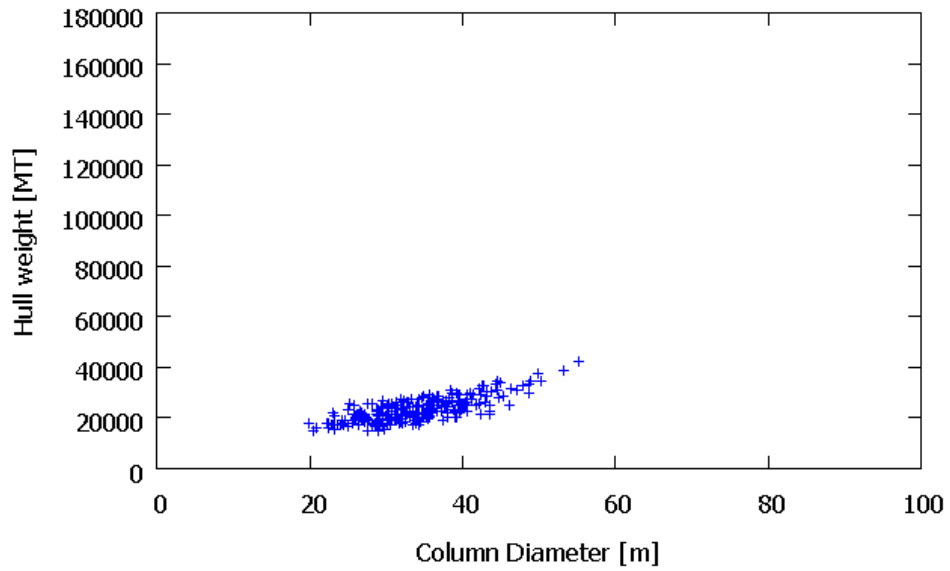


Figure 10-31 Max Offset Condition (Case 1)

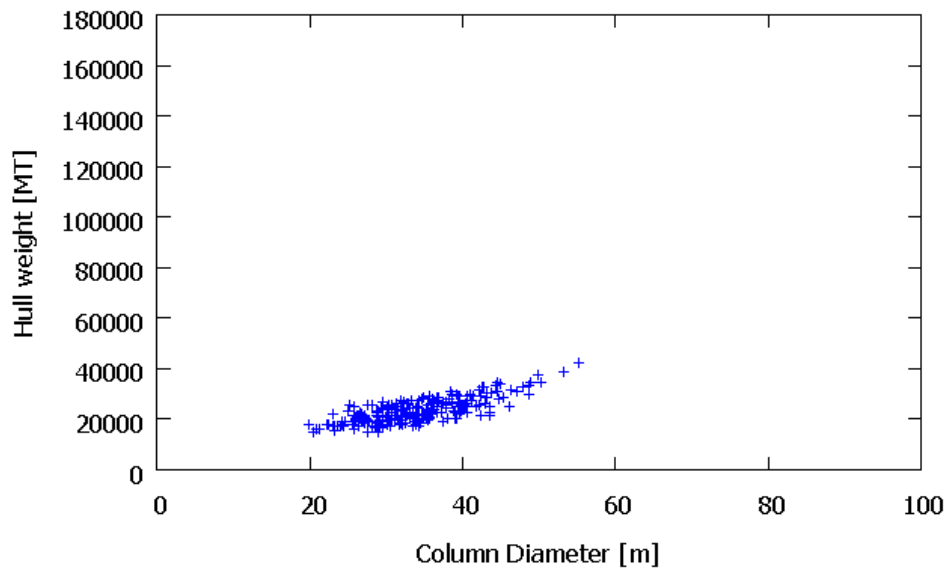


Figure 10-32 Minimum Tendon Tension Condition (Case 1)

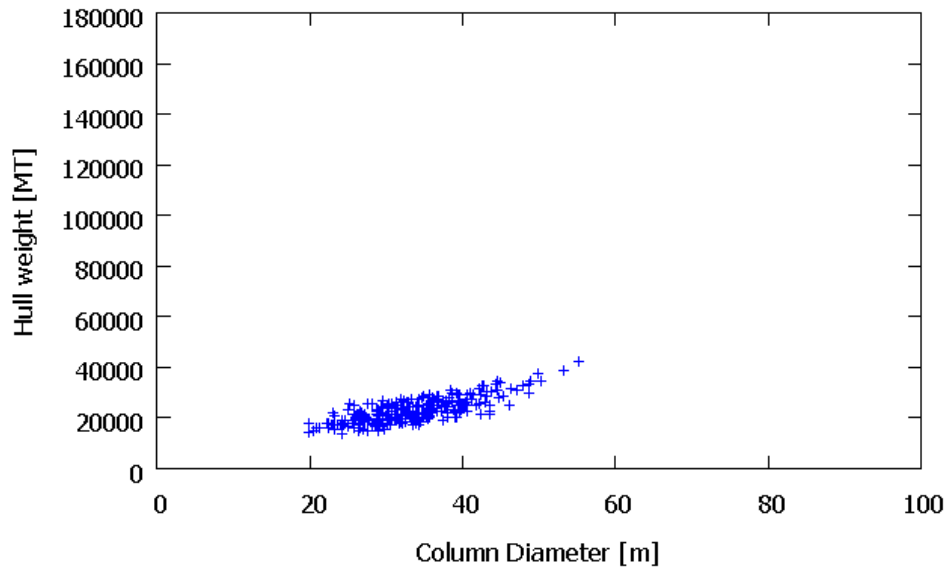


Figure 10-33 Airgap Condition (Case 1)

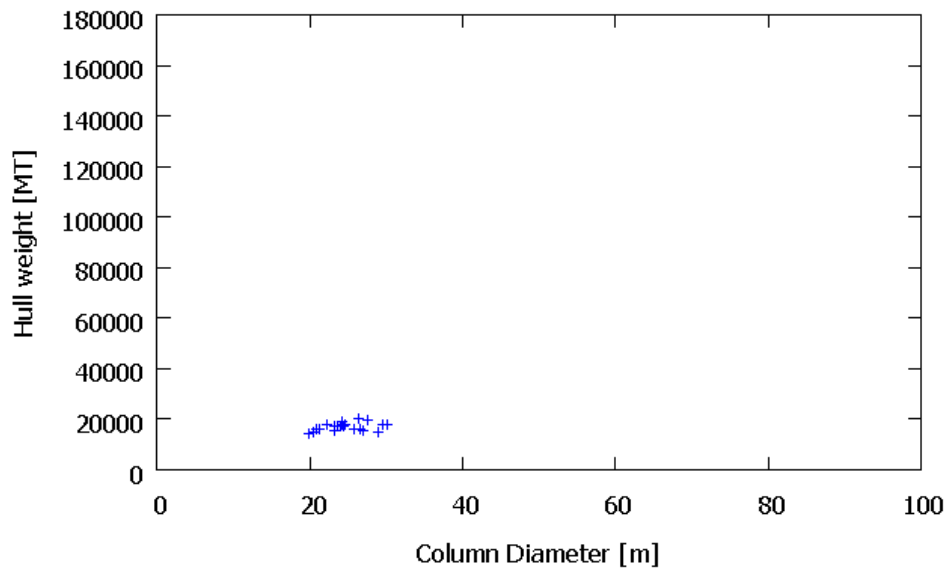


Figure 10-34 Tendon Strength Condition (Case 1)

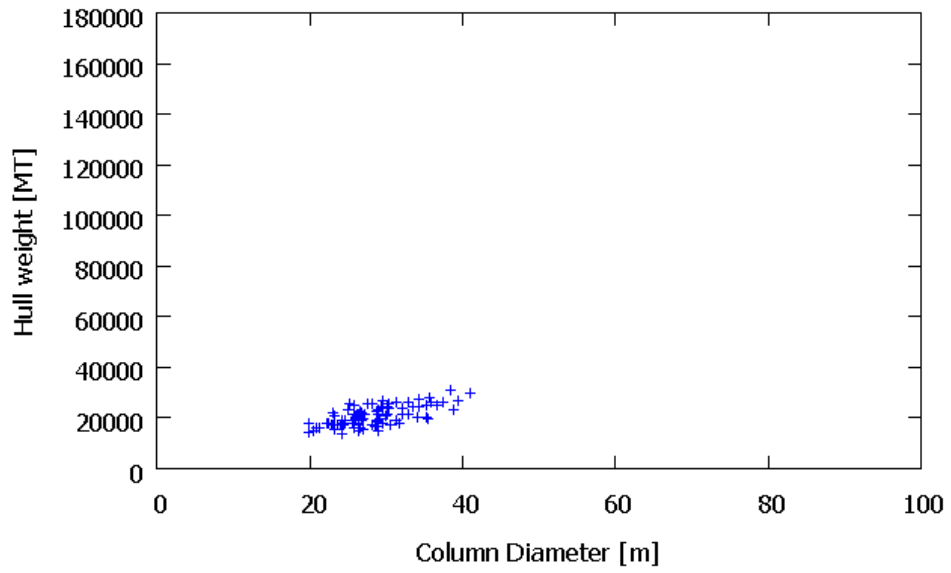


Figure 10-35 Hull strength Condition (Case 1)

11 Conclusion

TLP is an offshore platform which has very small motions due to the mooring by tendons. Recently TLPs are being installed on more global locations and TLPs are started to be subject to various type of environment condition. This trend causes lots of difficulty to design the optimized hull shape of TLPs, when we cannot utilize past experience for these new design condition.

In this study, optimization algorithm is utilized for hull shape optimization. Preceding works also utilize optimization algorithm, but they are not suitable for initial hull design. In section 2, the following goals are set.

- Develop hull optimization system that can find the optimized TLP hull shape. This system has more practical approach than preceding works: The platform weight and tendon weight are objective function to be minimized and design criteria are constraint condition.
- Compare the result with existing units for verification
- Compare with the result of hydrodynamic optimization
- Study application of TLPS to several environment condition

The hull sizing system developed in this study has the following characteristics:

- Objective function is hull and tendon weight, and constraint conditions are design criteria including global performance, strength, and initial screening criteria.
- This system can find optimized hull shape without using any empirical parameters or without input initial hull shape.
- This hull sizing system can find optimized hull shape in few hours, while it takes few weeks to carry out hull sizing with conventional method.

This system was tested for specific design conditions and the following points are found:

- Calculated hull shape was in line with existing TLP and the program is practically useful.
- Post hurricane condition requires larger tendon pretension and column height. As a result, the hull weight increased by 23%.
- For SE Asia, column length becomes significantly shorter, and weight can be reduced accordingly.
- Comparing between the weight and tension response for objective function, objective function of tension response gives significantly smaller pontoon height and deeper draft, and the hull weight also become larger. This means hydrodynamic optimization doesn't necessarily give the good solution.

12 Acknowledgement

I appreciate generous support and instruction from Professor Hideyuki Suzuki. I received continuous support from MODEC TLP group, so I'm deeply grateful to the group members.

Reference

Section 1

- [1-1] R. D'Souza, and Rajiv Aggarwal, The Tension Leg Platform Technology - Historical and Recent Developments, OTC-24512
- [1-2] E.F.H. Lim, and B.F. Ronalds, Evolution of the Production Semisubmersible, SPE Annual Technical Conference and Exhibition SPE-63036
- [1-3] Anil K. Sablok, and Steven Alexander Barras, Spar Technology- Developments in Deepwater spar installation, Offshore Technology Conference, 4-7 May, Houston, Texas, OTC-20234
- [1-4] MODEC Inc. website: <http://www.modec.com/index.html>
- [1-5] Tangvald, T.B., Goliat Field Development Circular Fpso in Harsh Environment, 2009-035 OMC Conference Paper – 2009
- [1-6] IMA, 2015 Jan FPS Outlook Report
- [1-7] Mustang and Offshore Magazine, Worldwide survey of TLPs, TLWPs, 2010
- [1-8] R. M. Rainey, Brutus Project Overview “Challenges and Results”, OTC-13990
- [1-9] Stephen B. Wetch, and Peter G. Wybro, West Seno: Facilities Approach, Innovations and Benchmarking, OTC-16521
- [1-10] Stephen E. Kibbee, and David C. Snell, New Directions in TLP Technology, OTC-14175
- [1-11] Stephen E. Kibbee et al., Morpeth SeaStar Mini-TLP, OTC-10855
- [1-12] Jun-Ho Song et al., Introduction of Hull Construction for Big Foot E-TLP, ISOPE-I-13-049
- [1-13] A.G. Grant, S. Sircar, and L. A. Nikodym, A systematic Procedure for Developing Optimum TLP Configuration, OTC-6570
- [1-14] R. D. Larrabee, S. B. Hodges, B. E. Cox, and R. Gonzalez, Concept Selection and Global Sizing of Mars TLP, OTC8369

Section 2

- [2-1] Clauss, G., and Birk, L., 1996, “Hydrodynamic shape optimization of large offshore structures”, Applied Ocean Research, 18(4), pp.157-171.
- [2-2] Birk, L., Clauss, G., and Lee, J.Y., 2004, “Practical application of global optimization to the design of offshore structures”, Proceedings of 23th International Conference on Offshore Mechanics and Arctic Engineering, Vancouver, British Columbia, Canada.
- [2-3] Lee, J.Y., and Lim, S.J., 2008, “Hull form optimization of a tensioned leg platform based on coupled analysis”, Proceedings of 18th International Offshore and Polar

Engineering Conference, Vancouver, British Columbia, Canada.

[2-4] Lee, J.Y., Koo, B.J., and Clauss, G., 2007, “Automated design of a tension leg platform with minimized tendon fatigue damage and its verification by a fully coupled analysis”, *Ship Technology Research*, Vol.54 No.1, pp. 11-27.

Section 3

[3-1] Fiacco, A.V., and McCormick, G. P., 1968, *Non-linear Programming, Sequential Unconstrained Minimization Technique*, John Wiley, New York.

[3-2] Ingber, L., 1993, “Simulated Annealing: Practice versus Theory”, *Mathematical and Computer Modeling*, 18, 11, pp.29-57.

[3-3] Hitoshi Iba, *Identeki Algorithm no kiso*, Ohmu-sha, Tokyo

[3-4] Hitoshi Iba, *Excel de Manabu Identeki Algorithm*, Ohmu-sha, Tokyo

[3-5] Hirokazu Anai, *Suri Saitekika no Jissen Guide*, Kodan-sha, Tokyo

[3-6] Keiji Kawamo, Hiroshi Hasegawa, and Masaaki Yokoyama, *Saitekika Riron no Kiso to Ouyou*, Korona-sha, Tokyo

Section 5

[5-1] Nihon Zosen Gakkai Kaiyoukougaku-Iinkai Seinou-bukai, 2003, *Futai no Ryuutai Rikigaku*, Seizando , Tokyo

[5-2] Matao Takagi and Shinichi Arai, *Senpaku Kaiyou-kouzoubutsu no Taiha Riron*, Seizan-do, Tokyo

[5-3] Masashi Kashiwagi, *Hydrodynamics of a Floating Body in Waves*, *Ouyou-suri* 11(3), 198-208, 2001-09-14

[5-4] Newman, J.N., 1977, *Marine Hydrodynamics*, The MIT Press, Cambridge, Massachusetts

[5-5] Det Norske Veritas, 2008, *SESAM user manual* Wadam.

Section 6

[6-1] American Petroleum Institute, 2010, *Recommended Practice for Planning, Designing and Constructing Tension Leg Platforms*, 3rd Edition (API RP 2T)

[6-2] American Petroleum Institute, 2008, *Design and Analysis of Stationkeeping Systems for Floating Structures*, 3rd Edition (API RP 2SK)

[6-3] Det Norske Veritas, 2007, *Environmental Conditions and Environmental Loads (DNV-RP-C205)*

[6-4] American Petroleum Institute, 2014, *Planning, Designing, and Constructing Fixed Offshore Platforms—Working Stress Design (API RP 2A-WSD)*

[6-5] ISO, 2005, Petroleum and natural gas industries -- Specific requirements for offshore structures - Part 1: Metocean design and operating considerations (ISO 19901-1).

Section 7

[7-1] Fujii, D., 2005, Excel de toku san-jigen kenchikukouzou kaiseiki, Maruzen, Tokyo

[7-2] Det Norske Veritas, 2012, Column-Stabilized Units (DNV-RP-C103)

Section 8

[8-1] American Bureau of Shipping, 2013, Rules for building and classing mobile offshore drilling unit

Section 9

[9-1] American Petroleum Institute, 2007, Interim Guidance on Hurricane Conditions in the Gulf of Mexico (API 2INT-MET)

[9-2] Richard D'Souza et al. A Comparison of Pre- and Post-2005 Sanctioned Gulf of Mexico Tension Leg, Semisubmersible, and Spar Floating Platforms, OTC-25442